CELECOXIB DELIVERY WITH EPIDERMAL GROWTH FACTOR RECEPTOR-TARGETED IMMUNOLIPOSOMES FOR CANCER THERAPY

A THESIS SUBMITTED TO
THE GRADUATE SCHOOL OF NATURAL AND APPLIED SCIENCES
OF
MIDDLE EAST TECHNICAL UNIVERSITY

BY

YANUAR DWI PUTRA LIMASALE

IN PARTIAL FULFILLMENT OF THE REQUIREMENTS
FOR
THE DEGREE OF MASTER OF SCIENCE
IN
BIOTECHNOLOGY

FEBRUARY 2015

Approval of the thesis:

CELECOXIB DELIVERY WITH EPIDERMAL GROWTH FACTOR RECEPTOR-TARGETED IMMUNOLIPOSOMES FOR CANCER THERAPY

Submitted by **YANUAR DWI PUTRA LIMASALE** in partial fulfillment of the requirements for the degree of **Master of Science in Biotechnology Department, Middle East Technical University** by,

Prof. Dr. Mevlüde Gülbin Dural Ünver _____
Dean, Graduate School of **Natural and Applied Sciences**

Prof. Dr. Filiz Bengü Dilek _____
Head of Department, **Biotechnology**

Assoc. Prof. Dr. Dilek Keskin _____
Supervisor, **Engineering Sciences Dept., METU**

Assoc. Prof. Dr. Sreeparna Banerjee _____
Co-Supervisor, **Biological Sciences Dept., METU**

Examining Committee Members:

Assoc. Prof. Dr. Mesut Muyan _____
Biological Sciences Dept., METU

Assoc. Prof. Dr. Dilek Keskin _____
Engineering Sciences Dept., METU

Assoc. Prof. Dr. Sreeparna Banerjee _____
Biological Sciences Dept., METU

Assoc. Prof. Dr. Ayşen Tezcaner _____
Engineering Sciences Dept., METU

Assist. Prof. Dr. İrem Erel Göktepe _____
Chemistry Dept., METU

Date: _____

I hereby declare that all information in this document has been obtained and presented in accordance with academic rules and ethical conduct. I also declare that, as required by these rules and conduct, I have fully cited and referenced all material and results that are not original to this work.

Name, Last Name : Yanuar Dwi Putra LIMASALE

Signature :

ABSTRACT

CELECOXIB DELIVERY WITH EPIDERMAL GROWTH FACTOR RECEPTOR-TARGETED IMMUNOLIPOSOMES FOR CANCER THERAPY

Limasale, Yanuar Dwi Putra

M.S., Department of Biotechnology

Supervisor: Assoc. Prof. Dr. Dilek Keskin

Co-Supervisor: Assoc. Prof. Dr. Sreeparna Banerjee

February 2015, 115 pages

Inhibition of the cyclooxygenase-2 (COX-2) pathway by a selective COX-2 inhibitor, Celecoxib (CLX), may be an alternative strategy for cancer prevention and therapy as COX-2 is highly expressed in wide range of cancer. One way to improve CLX's therapeutic efficacy while minimizing its adverse side effects is through its encapsulation within liposomes. Previous studies have reported the non-targeted long circulating liposomes formulations of CLX and its functional effect against colorectal cancer cell lines. However, to improve the CLX-loaded liposomes' selectivity and internalization, targeting ligands such as Cetuximab (anti-Epidermal Growth Factor Receptor (EGFR) monoclonal antibody) can be grafted on the surface of the liposomes to generate EGFR-targeted immunoliposomes. Cetuximab represents a promising targeting ligand since EGFR is highly expressed in a wide range of solid tumors. The aim of the thesis was to develop EGFR-targeted immunoliposomes for enhancing the delivery of CLX and to evaluate its functional effects in cancer cell lines. The immunoliposomes with size of approximately 120 nm and 40% of encapsulation of CLX were shown to have sustained release profile

of the drug. In addition, cell association studies demonstrated that the immunoliposome uptake was higher in EGFR-overexpressing cells compared to the non-targeted liposomes. The CLX-loaded-anti-EGFR immunoliposomes were also significantly more toxic compared to the non-targeted ones in cancer cells with EGFR-overexpression but not in the cells with low EGFR expression, regardless of their COX-2 expression status. Thus, selective targeting of CLX with anti-EGFR immunoliposomes appears to be a promising strategy to treat tumors with overexpression of EGFR.

Key words: Liposome, immunoliposomes, EGFR, cancer, Celecoxib

ÖZ

KANSER TEDAVİSİ İÇİN ANTİ-EPİDERMAL BÜYÜME FAKTÖR RESEPTÖR HEDEFLİ İMMÜNOLİPOZOMLAR İLE CELECOXIB SALINIMI

Yüksek Lisans, Biyoteknoloji Bölümü
Tez Yöneticisi: Doç. Dr. Dilek Keskin
Ortak Tez Yöneticisi: Doç. Dr. Sreeparna Banerjee
Şubat 2015, 115 sayfa

Siklooksijenaz-2 (COX-2) birçok farklı kanser türünde yüksek miktarda ifade edilmektedir. Bu nedenle seçici bir COX-2 inhibitörü ile COX-2 yolağının baskılanması kanserden korunma ve tedavi için alternatif bir strateji olabilir. Celecoxib (CLX), suda az çözünmektedir ve geniş bir doku distribüsyonuna sahiptir. Ayrıca, uzun süreli CLX kullanımı kardiyovasküler hastalıkların yüksek oranda görülmesi ile ilişkilidir. Lipozomal ilaç taşıma sistemleri, CLX'in yan etkilerini azaltmanın yanı sıra tedavi edici etkisini arttırmak amacı ile kullanılabilir. Önceki çalışmalar hedeflenmemiş uzun süreli dolaşan lipozamlarla kapsüllenen CLX'i ve onun kolorektal kanser hücre hatlarındaki fonksiyonel etkilerini göstermiştir. Bununla birlikte, CLX-yüklenmiş lipozomların seçiciliği ve internalizasyonları lipozomların yüzeyindeki ligandların aşılama ile hedeflenmesiyle daha fazla arttırılabilir. EGFR birçok katı tümör çeşidinde yüksek miktarda ifade edildiğinden, Cetuximab (anti- Epidermal Büyüme Faktör Reseptörü (EGFR) monoklonal antikoru) ümit vaat eden bir EGFR ligandıdır. Bu tezin amacı CLX taşınımını arttırmak için EGFR hedefli immünolipozomlar geliştirmek ve kanser hücre hatlarındaki fonksiyonel etkilerini değerlendirmektir. Hücre ilişkili çalışmalar

göstermektedir ki immünolipozomların alımı EGFR-aşırı ifadeli hücrelerde hedeflenmemiş lipozomlar ile karşılaştırıldığında daha fazladır. Ayrıca, CLX-yüklenmiş-anti-EGFR immünolipozomlar, hedeflenmemiş lipozomlar ile kanser hücrelerinde COX-2 ifadesine bakılmaksızın karşılaştırıldığında EGFR-aşırı ifadeli hücrelerde, fakat az EGFR ifadeli hücrelerde değil, önemli ölçüde daha toksiktir. Böylelikle anti-EGFR immünolipozomlar ile seçici hedeflenen CLX, EGFR aşırı ifadeli tümörlerin tedavisinde umut vaat eden bir yöntem olarak görülmektedir.

Anahtar kelimeler: Lipozom, immünolipozom, EGFR, kanser, Celecoxib.

To my country, Indonesia and my family who support me all the time

ACKNOWLEDGMENTS

I would like to express my gratitude to my advisor Assoc. Prof. Dr. Dilek Keskin for her guidance, patient, encouragement, and support throughout my thesis study. I would like to express special appreciation and thanks to my co-advisor Assoc. Prof. Dr. Sreeparna Banerjee for her continues support, advice and assistance throughout the whole of my thesis study. I would also like to express my special thanks to Assoc. Prof. Dr. Ayşen Tezcaner for her constructive and valuable input as well as her encouragement during my master study.

I would like to thank to my thesis committee members, Assoc. Prof. Dr. Mesut Muyan and Assist. Prof. Dr. İrem Erel Göktepe for their assistances and recommendations regarding the improvement of my thesis

My special thanks to:
Dr. Can Özen, İpek Durusu, and Fatma Gül, from METU Central lab for their assistance in using the confocal microscope
Dr. Asli Astarcı (Erdoğ), Şeyma Ceyhan, Richardas Rachkauskas, Dr. Aslı Sade Memişoğlu, Dr. Shabnam Enayat, Dr. Seda Tunçay, Doğukan Hazar Ülgen, Melis Çolakoğlu, Dr. İsmail Çimen, Dr. Erhan Astarcı, and Mümine Küçükdemir, from Lab.B-59,
Assoc.Prof. Mayda Gürsel, and her students from METU Biological Sciences Department, for teaching me how to use flow cytometry and the analysis,
Ayşegül Kavas, Zeynep Barcin, Sibel Ataol, and Merve Güldiken from METU Engineering Sciences Department for helping me doing HPLC and other important analysis for my thesis study
I would like to thank Assist. Prof. Dr. İrem Erel Göktepe Alyan and Muhammad Alyan Ahmed Khan, from METU, Chemistry Department for allowing and helping me to perform particle size and zeta potential analysis,

Assoc.Prof. İhsan Gürsel and Tamer Kahraman from Bilkent University Molecular Biology and Genetics Department.
I am grateful to my roommate and Indonesians friends who supported and helped me during the completion of my thesis,
Arham Achlak, Yosheph Yang, Amirul Fatta and Ridho Asiddiki

I would like to thank Turkish Government for the financial support through the Turkish Government Scholarship Program for Graduate Student
This thesis was funded by METU BAP-07-02-2014-004

TABLE OF CONTENTS

LIST OF TABLES

TABLES

LIST OF FIGURES

FIGURES

LIST OF ABBREVIATIONS

% EE	: Percentage encapsulation efficiency
2-MEA	: 2-mercaptoethylamine or cysteamine
AKT	: Protein kinase B
ATF	: cAMP-dependent transcription factor
ATP	: Adenosine triphosphate
AP-1	: Activator protein 1
APC	: Adenomatous polyposis coli
Bcl-2	: B-cell lymphoma 2
BRAF	: v-Raf murine sarcoma viral oncogene homolog B
BSA	: Bovine serum albumin
cAMP	: Cyclic adenosine monophosphate
CD19	: Cluster of differentiation 19
CD20	: Cluster of differentiation 20
C/EBP	: CCAAT-enhancer-binding proteins
Chol	: Cholesterol
CHOP	: C/EBP-homologous protein
CLX	: Celecoxib
COX	: Cyclooxygenase
COXIB	: Selective cox-2 inhibitor
CRC	: Colorectal carcinoma
DDS	: Drug delivery system
DNA	: Deoxyribonucleic acid
DiI	: 1,1′-dioctadecyl-3,3,3′,3′ tetramethylindodicarbocyanine
DiO	: 3,3’-dioctadecyloxacarbocyanine perchlorate
DMBA	: Dimethylbenzanthracene
DMSO	: Dimethyl sulfoxide
DOXIL	: Liposome-encapsulated doxorubicin

DSPC	: 18:0 PC; 1,2-Distearoyl-sn-glycero-3 phosphocholine
DSPE-PEG(2000)Maleimide	:1,2-distearoyl-sn-glycero-3-phosphoethanolamine-N-maleimide(polyethylene glycol)-2000
DTT	: 2-Dithiothreitol
DXR	: Doxorubicin
ECM	: Extracellular matrix
EDTA	: Ethylenediaminetetraacetic acid
EGF	: Epidermal growth factor
EGFR	: Epidermal growth factor receptor
EGFR vIII	: Epidermal growth factor receptor variant III
EPR	: Enhanced permeability and retention effect
FACS	: Fluorescence activated cell sorting
FAP	: Familial adenomatous polyposis
FCS	: Forward Scatter
FDA	: Food and Drug Association
HBS	: HEPES buffered saline
HDL	: High density lipoproteins
HEPES	: 4-(2-hydroxyethyl)-1-piperazineethanesulfonic acid
HER2	: Human epidermal receptor 2
HUVEC	: Human umbilical vein endothelial cell
i.v.	: intravenous
Ig	: Immunoglobulins
IL	: Immunoliposome
IκB kinase β	: Inhibitor of kappa B kinase β
KRAS	: Kirsten rat sarcoma viral oncogene homolog
LDL	: Low density lipoproteins
LOX	: Lipoxygenase
LPS	: Lipopolysaccharide
LSCM	: Laser scanning confocal microscopy
LUV	: Large unilamellar vesicles

mAbs	: monoclonal antibodies
MAPK	: Mitogen-activated protein kinase
Mcl-1	: Myeloid cell leukemia 1
Mean FL-1	: Mean Relative Fluorescence Intensity
MLV	: Multilamellar vesicles
MMP	: Matrix metalloprotease
mPEG(2000)-DSPE	:1,2-distearoyl-sn-glycero-3-phosphoethanolamine-N-methoxy(polyethylene glycol)-2000
MPS	: Mononuclear phagocyte system
mTOR	: Mammalian target of rapamycin
MTT	: 3-(4,5-Dimethylthiazol-2-yl)-2,5 diphenyltetrazolium bromide
MWCO	: Molecular weight cut-off
NCI	: National Cancer Institute
NF-κB	: Nuclear factor kappa B
NSAIDs	: Non-steroidal anti-inflammatory drugs
NSCLC	: Non-small cell lung cancer
P21	: Cyclin-dependent kinase inhibitor 1
PAGE	: Polyacrylamide Gel Electrophoresis
PBS	: Phosphate buffered saline
PC	: Polycarbonate
PdI	: Polydispersity index
PDK-1	: Phosphoinositide-dependent kinase 1
PEG	: Polyethylene glycol
PES	: Polyethersulfone
PG	: Prostaglandin
PI3K	: Phosphatidylinositol 3-kinase
PKB	: Protein kinase B
PMA	: Phorbol myristate acetate
PP	: Polypropylene

PPAR	: Peroxisome proliferator-activated receptor
RES	: Reticuloendothelial System
Rhodamine DHPE or Rh-PE	: Lissamine™ rhodamine B 1,2-dihexadecanoyl-sn-glycero-3-phosphoethanolamine, triethylammonium salt
S.E.M	: Standard error of the mean
SATA	: N-succinimidyl S- acetylthioacetate
SP	: Specifity proteins
SP-DiOC18(3)	: 3,3′-dioctadecyl-5,5′-di(4-sulfophenyl) oxacarbocyanine, sodium salt
SSC	: Side scatter
STAT	: Src tyrosine kinase
SUV	: Small unilamellar vesicles
TEM	: Transmission Electron Microscopy
TGFα	: Transforming growth factor α
TKI	: Tyrosine Kinsae Inhibitor
TX	: Thromboxane
VCAM-1	: Vascular cell adhesion molecule-1
VEGF	: Vascular endothelial growth factor
Z avg	: Average hydrodynamic diameter
β-ME	: β-mercaptoethanol

CHAPTER 1

INTRODUCTION

1.1 Cancer

Cancer is one of the leading causes of death worldwide. It was reported that there were 8.2 million of cancer death and 14.1 million new cancer cases in 2012 and it is predicted that the number will rise 19.3 million per year by 2025 [1]. The most prevalence cancer affecting the world population include the lung cancer, breast cancer, prostate cancer and colorectal cancer. Cancer arises from uncontrolled cell growth and proliferation of any different cells in the body. The deregulations of cell growth and proliferation in cancer result from the accumulation of mutations in various genes controlling the cell growth and proliferation overtime. The mutations are acquired in multistep process and this leads to the development of cancerous characteristics known as hallmarks of cancer: *(1)* ability to maintain proliferation either in the presence of growth factor or in their absence, *(2)* ability to evade anti-growth factor suppression, *(3)* ability to evade from cell death, (*4)* ability to sustain limitless replication potential, *(5)* ability to promote angiogenesis, and *(6)* ability to invade the neighboring tissues and metastasize [2]. In addition, improving knowledge of cancer in the recent decade also includes 2 emerging hallmarks of cancer: altering the energy metabolic profile and evasion from the destruction of immune system [3].

1.1.1 Cancer Therapy

The current cancer therapy includes surgery, chemotherapy, radiotherapy, endocrine therapy, immunotherapy and targeted therapy. The choices of the treatment are dependent on many aspects including the age of the patient, types of tumor, localization and stage of the tumor, resistance to previous treatment, responsiveness to the current treatment and so on. Each type of therapeutic intervention has some

limitations, therefore, the combination of the therapies may be required to achieve an optimal result.

Surgery is the most effective way of eliminating primary tumors, which are localized in the organ and have not disseminated through the regional lymphatics [4]. The importance of surgery for the success of solid tumor curative treatment can be especially visible when it is combined with the early detection of the tumor [5]. However, tissue trauma and wound healing associated with the surgery may promote angiogenesis, growth and metastatic potential of micrometastatic disease [6]. At the later stages, as the cancer metastasizes, surgery becomes ineffective and other treatment options that are able to reach cancer cells in different part of the body such as chemotherapy and targeted therapies are required.

Radiotherapy offers another relatively cheap option for the curative therapy of cancer such as head and neck tumors and prostate cancer as a single agent [4]. Radiotherapy involves the delivery of ionizing radiation in a lethal dose to the tumor tissues and this particularly can lead to the damage in the Deoxyribonucleic acid (DNA) and cell death especially when the cell undergoes mitosis [7]. The effect of radiotherapy is more pronounced in tumors compared to the normal tissues because of the differences in their intrinsic radiosensitivity and ability to repair and repopulate [8]. However, in order to achieve high response rate, commonly, the treatment is used in combination with surgery, chemotherapy, and/or targeted therapy. Despite the advantages of radiotherapy, the treatment is still ineffective for metastasized cancer and carries the risk of damaging rapidly proliferating healthy cells. In addition, hypoxic conditions in the tumor site also confer resistance of tumor to radiotherapy [9].

While surgery and radiotherapy are effective for the local treatment of primary tumor, chemotherapy is delivered systematically to reach metastatic tumor tissues [8]. Despite of their effectiveness in killing the cancer cells, chemotherapy produces deleterious side effects to the normal tissues, especially to the cells with high proliferative capacity such as hair follicle cells, gastrointestinal mucosa, hematopoietic stem cells, etc., and in worst cases, sometimes, it can generate life threatening side effects. Generally, chemotherapy drugs target DNA and interferes with DNA

replications leading to apoptosis [10]. In clinical practice, chemotherapy can be used as a single agent or in combination with other chemotherapy drugs and adjuvant or neo-adjuvant to surgery or radiotherapy. The outcomes of the therapies are various; and may range from palliation to completely curing the disease. However, the use of chemotherapy is particularly limited by the development of tumor resistance in addition to their toxic side effects.

The lack of specificity of chemotherapy, along with various side effects and relatively modest improvement in the survival of cancer patients have spurred the development of better cancer therapeutics that are more targeted to the cancer instead of normal tissues. This has largely resulted from better understanding of signaling pathways and genes that are specifically associated with cancer development and are important for their survival and proliferation. Targeted therapies for cancers involves the interference of signaling pathways which are required for cancer progression either by inhibiting the activation of oncogenes or by activating tumor suppression [11].

The molecular targets which have the potential to be candidates of the targeted cancer therapy include growth factor receptor, signaling molecules, proteins controlling the cell cycle and regulators of apoptosis and angiogenesis [8]. Some of the targeted therapeutics in clinical practice has shown significant improvement in progression-free survival while the others are still undergoing clinical trials. For example, as an adjuvant, trastuzumab, an antibody which targets HER-2 receptor on breast cancer cells of some patients is able to improve progression-free survival and overall survival of the patients [8]. Other small molecules and antibodies that are currently used in the clinical setting for targeted therapies include Tyrosine Kinase inhibitors, bevacizumab (Vascular Endothelial Growth Factor (VEGF) targeted monoclonal antibody) , cetuximab and panitumumab (antibodies directed against EGFR), and so on [12] .

1.2 Epidermal Growth Factor Receptor Signaling

Epidermal Growth Factor Receptor (EGFR) / ERBB1 along with ERBB2, ERBB3 and ERBB4 are members of Tyrosine Kinase Receptor family [13]. EGFR is a membrane protein of 170 kDa, consisting of 486 amino acids. It has an extracellular ligand-binding domain, a transmembrane domain, and intracellular domains including protein kinase domain and a regulatory carboxyl terminal [14], [15]. The EGFRs are activated by various different ligands including epidermal growth factor (EGF), transforming growth factor alpha (TGF-α), and amphiregulin [16]. Upon the binding of the ligand, the receptor forms homodimer or heterodimer with other members of the family leading to their phosphorylation and activation [17]. The activation of the receptor leads to the activation of signaling pathways that are important for cellular growth, differentiation and migration [18].

The activations of ERBBs are followed by the activations of downstream pathways that can be overlapping between each type of receptor due to the recruitment of the same molecules by the activated receptor, however, for a given ERBB member some pathways can be unique due to the preferential recruitment of specific effector proteins [13].

The activation of the receptor is connected to major intracellular signaling pathways such as mitogen-activated protein kinase (MAPK), the phosphatidylinositol 3-kinase (PI3K)–AKT, signal transducer and activator of transcription proteins (STATs), Src tyrosine kinase, and mammalian target of rapamycin (mTOR) pathways [19–23] **(Figure 1.1)**. Collectively, these pathways affect cellular proliferation, inhibition of apoptosis, cell division, motility and adhesion, cell survival and invasion, cell cycle progression, and metastasis [13–15, 24].

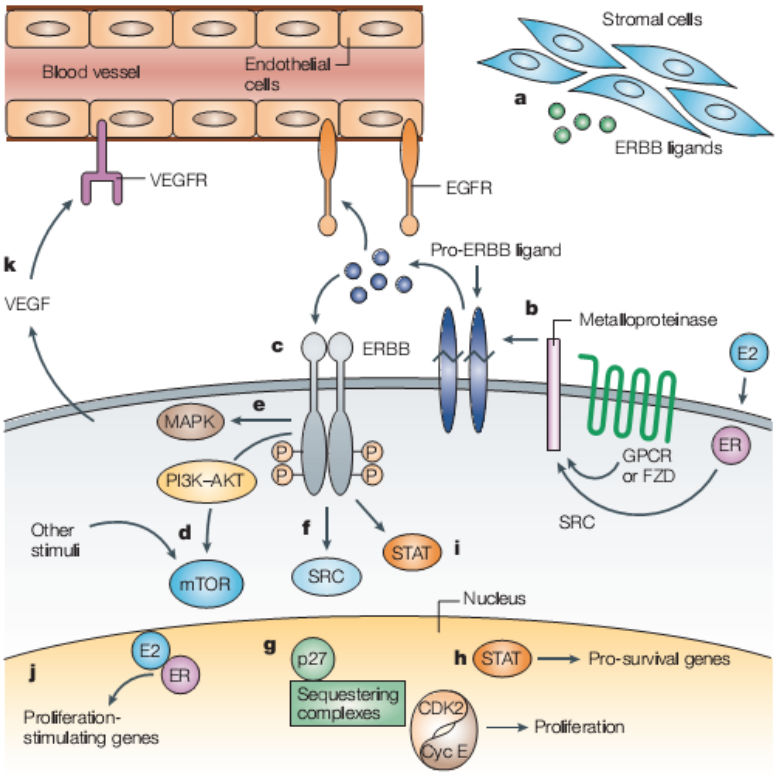

Figure 1.1 The activation of ERBB receptors and downstream signaling pathways in a tumor [13].

1.2.1 EGFR Signaling and Cancer

The deregulation in the activation of ERB family of Tyrosine Kinase Receptor is implicated with many types of epithelial tumors [15] such as head and neck, breast, bladder, ovarian, renal, colon and NSCLC [19]. Receptor activation leads to the phosphorylation of intracellular downstream substrates that activate mitogenic signaling [15]. Many human cancers also harbor gene amplifications that lead to the overexpression of EGFR [25]. Moreover, constitutive activation of EGFR in tumor cells is also triggered by the EGF-related growth factor secretion by the tumor cells itself or tumor's stromal cells [13]. In addition to wild type EGFR, another variant of EGFR, namely EGFR vIII, is also implicated with cancers like glioblastoma, breast, ovarian and NSCLC [26–29] . In gliomas, the loss of exons 1-7 of EGFR gene causes

in-frame deletion in the extracellular domain of the receptor that affects the receptor recycling, leading to its ligand-independent constitutive activation [30–32].

1.2.2 EGFR-Targeted Therapy

The dependency of many types of tumor on the EGFR signaling pathways for their growth and survival and their aberrant activation has encouraged the development of EGFR-targeted therapeutics. The dependency of tumor cells is reflected by the overexpression of EGFR on tumor cell compared to the normal cells. It is estimated that normal cells express $4x10^4$ to $1x10^5$ EGFR per cell while tumor cells can express more than $2x10^6$ receptors per cell [33]. Currently, there are many available EGFR inhibitors in the clinics and they are mainly grouped into either monoclonal antibody (mAbs) directed against extracellular domain of EGFR or Tyrosine Kinase inhibitors [TKIs). Other therapeutics agents that target EGFR include antisense oligonucleotides, nanobodies, affibodies, peptides, antibody-drug conjugates, and EGFR-targeted drug delivery systems.

Cetuximab is a chimeric mouse and human monoclonal antibody that binds to the extracellular domain of EGFR thereby preventing ligand binding and ligand-induced tyrosine kinase activation and induction of receptor internalization [34–36] **(Figure 1.2)**. The inhibitory effect of cetuximab is not only restricted to wild type EGFR as it can also bind to mutant receptor EGFRvIII and abrogate their activation and induce the internalization of the antibody-receptor complex [37].

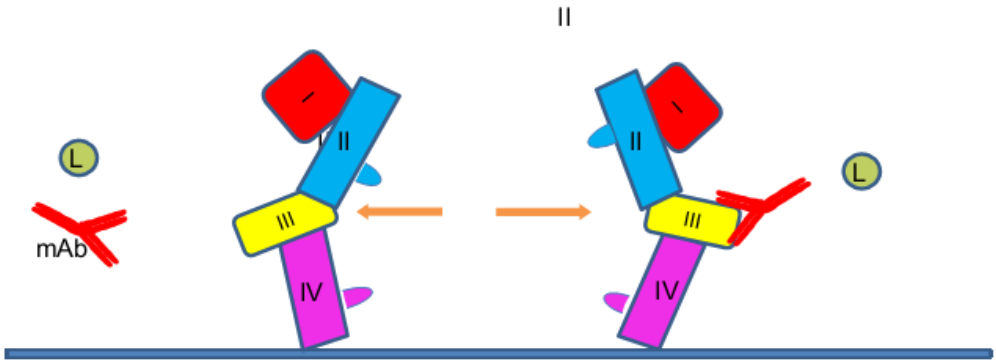

Figure 1.2 Binding of anti-EGFR antibodies to the receptor's extracellular domain. The binding of the antibodies blocking the ligand-binding region and preventing the receptor activation [18].

The anti-tumor activity of cetuximab, as shown in some preclinical studies, includes inhibition of tumor growth, inhibition of angiogenesis, reduction in tumor invasiveness, induction of cell cycle arrest, and apoptosis and increase in sensitivity to radio- and chemotherapy [38–42]. In 2004, cetuximab was approved by the Food and Drug Association (FDA) for the treatment of metastatic colorectal and head and neck cancer [43]. Later, it was also approved for treatment of colon cancer with non-mutated KRAS in 2009 [18].

In addition to cetuximab, the fully humanized version of anti-EGFR antibody, panitumumab, has also been approved by FDA to treat the patients with metastatic colorectal cancer [18]. Panitumumab acts in a similar manner as cetuximab, blocking ligand-binding and inducing EGFR internalization [44] (**Figure 1.2)**. However, it does not cause the receptor degradation [45].

In contrast to mAbs that block the binding of ligand of EGFR, TKIs directly inhibit the tyrosine kinase activity of the receptor which are involved in the activation of downstream signaling pathways [46]. TKIs may act by directly compete with ATP for binding to the kinase, or it can act in an allosteric manner. Currently available TKIs approved by the FDA include gefitinib for the treatment of metastatic non-small cell lung cancer (NSCLC), erlotinib for locally advanced or metastatic NSCLC, and

lapatinib in combination with capecitabine for the treatment of metastatic HER2-overexpressing breast cancer refractory to chemotherapy [18].

Despite of the clinical advantages of mAbs and TKIs, the tumor intrinsic or acquired resistance to these EGFR inhibitors due to mutations and amplifications of the EGFR gene is widespread [47]. Combination therapies such as combining different EGFR inhibitors, the use of inhibitors that target EGFR and other ERRBs receptor family's members, or combining EGFR inhibitor and other agent that target signaling pathways responsible for the development of tumor malignancies are the current approaches to overcome this problem [18]. In addition to the combinatorial therapeutics approach of targeting EGFR, identification of the molecular markers which can predict the patients outcomes to anti-EGFR therapy is also necessary in order to improve the individualize therapy and reduce the treatment cost [18].
For example, the presence of KRAS gene mutation was shown to negatively correlate with the response of patients with colorectal cancer to the therapy [48, 49].

1.3 Cyclooxygenase and Cancer

Cyclooxygenases (COXs) are inflammatory enzymes required for the synthesis of prostaglandin (PG) H2 from arachidonic acid (**Figure 1.3**). PGH2 is then converted by tissue specific PGD synthases (PGDS) into different types of prostaglandins. There are two 2 isoforms of COXs, namely, COX-1 and COX-2. Unlike COX-1, which is expressed constitutively in many types of tissues, COX-2 is expressed transiently and induced by different kinds of ligand including cytokines, lipopolysaccharide (LPS), phorbol myristate acetate (PMA), and growth factors [50–52]. COX-1 is involved in the production of physiologically relevant prostaglandins; on the other hand, an increase in the expression and activity of COX-2 is seen in disease (e.g. cancer) and inflammation [53].

COX-2 is highly expressed in many different cancers including colorectal, breast, lung, head and neck, and prostate cancer [54–57] COX-2 overexpression happens at the early stages of carcinogenesis and acts as a prognostic marker [58], [59]. The expression of COX-2 in human cancer is also associated with the increase of

angiogenic and metastatic potential, inhibition of apoptosis, and cell proliferation [60–62]. The tumor promoting activity of COX-2 mainly is related to the increase in the level of prostaglandins [(PGE_2, PGF_{2a}, PGD_2, TxA_2, PGI_2 and PGJ_2) [63], which can be inhibited by the Non-steroidal anti-inflammatory drugs (NSADs). The inhibition of prostaglandins is associated with analgesic and antipyretic properties of NSADs. Conventional NSADs such as aspirin, ibuprofen, and naproxen inhibit both COX-1 and COX-2 while the new generations NSAIDs such as celecoxib, refocoxib, valdecoxibs, etoricoxib, lumiracoxib specifically inhibit COX-2.

Recently, NSAIDs have been known and studied for their anti-tumorigenic and chemopreventive potentials [64]. For example, the use of aspirin and non-aspirin NSAIDs are reported to decrease the risk of colon cancer [65, 66].

However, the prolonged use of conventional NSAIDs is associated with various side effects such as gastrointestinal tract bleeding and kidney failure, which may result from the inhibition of COX-1 [64].

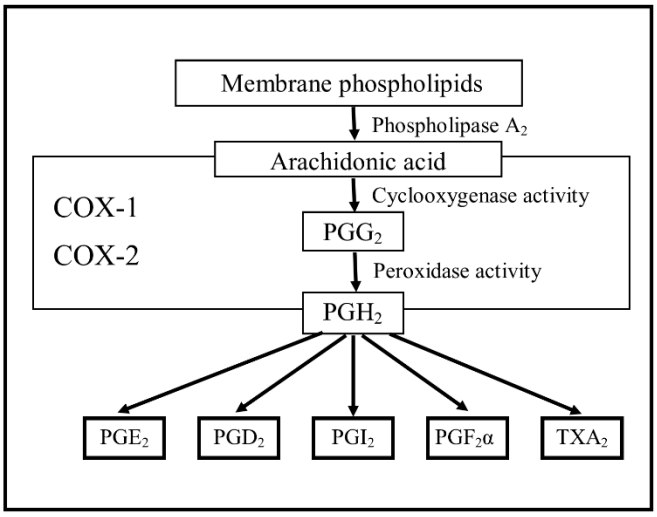

Figure 1.3 The arachidonic acids cascade (modified from [54]).

1.3.1 Celecoxib and Its Anticarcinogenic Effect

To improve the safety of long term consumption of NSAIDs, more selective COX-2 inhibitors were developed. Celecoxib [CLX) (4-[5-(4-Methylphenyl)-3-(trifluoromethyl)-1H-pyrazol-1-yl], a member of COXIBs drug family, was designated to relieve the symptoms of osteoarthritis and rheumatoid arthritis [67]. Celecoxib is a selective COX-2 inhibitor with chemopreventive or anticancer properties in a variety of cancers including colorectal, breast, pancreatic, neuroblastoma, and head and neck cancers [68–72]. Interestingly, the antiproliferative properties of celecoxib are unique among the other members of drug family of COXIBs [73]. According to preclinical studies, celecoxib was shown to increase the tumor response to chemotherapy, radiotherapy, and chemoradiotherapy [74–77]. Currently, their anticarcinogenic effects have been tested for the treatment and prevention of different cancers such as pancreatic, breast, ovarian, non-small cell lung cancer and other human epithelial cancers [78]. In addition, celecoxib has also been approved as an adjuvant for the treatment of patients with familial adenomatous polyposis [79].

The anticarcinogenic properties of CLX are partly attributed to the inhibition of COX-2 (COX-dependent) while in some cases can be COX-2 independent [79]. For example, COX-2 independent effect of CLX includes the induction of cell cycle arrest, induction of apoptosis, inhibition of angiogenesis, and decrease of the membrane fluidity and metastatic potential *in vitro* [79, 80]. The molecular targets of COX-2 independent effects of celecoxib are various, and they range from transcription factors: cyclic adenosine monophosphate (cAMP)-dependent transcription factor (ATF)4, C/EBP-homologous protein (CHOP), Specificity proteins (Sp), Nuclear factor-kB (NF-kappaB); Cell signaling proteins: EGFR, E-cadherin, protein kinase B (Akt), 3-phosphoinositide-dependent protein kinase-1; Cell cycle regulators : p21, cyclin-dependent kinase inhibitors (p21), cyclins [64, 81, 82].

The induction of apoptosis by celecoxib through mitochondrial apoptosis pathways is through the inhibition of anti-apoptotic proteins such as Bcl-2, Mcl-1 and survivin [78]. Therefore, celecoxib has the potential to be used as a single agent to

treat apoptosis resistant tumors with overexpression of Bcl-2, Mcl-1, or survivin or in combinations with other standard therapies [78].

1.3.2 Crosstalk between COX-2 and EGFR Pathways

COX-2 and EGFR are highly upregulated in wide variety of cancers [83]. Interestingly, a crosstalk between COX-2 and EGFR signaling pathways exists (**Figure 1.4**) and the increase of COX-2 expression can lead to an increase in EGFR activation and expression [82]. The crosstalk between (COX-2) and EGFR pathways can synergistically lead to the CRC progression and metastasis [82]. PGE_2 that is generated from the COX-2 pathway can transactivate EGFR through intracellular signaling pathways [84]. PGE_2 is known to promote colorectal carcinoma cell migration and invasion through an EGFR-PI3K-AKT signaling *in vitro* [85].

Furthermore, induction of an EP4/ARRB1/SRC complex by PGE_2 transactivates EGFR which in turn activates AKT signaling leading to stimulation of CRC cell migration *in vitro* and their metastatic spread of to the liver *in vivo* [84]. Therefore, the synergistic effect of COX-2 and EGFR pathways and their positive feedback loop to promote cancer progression and metastasis rationalize the development of the combination therapy targeting both pathways.

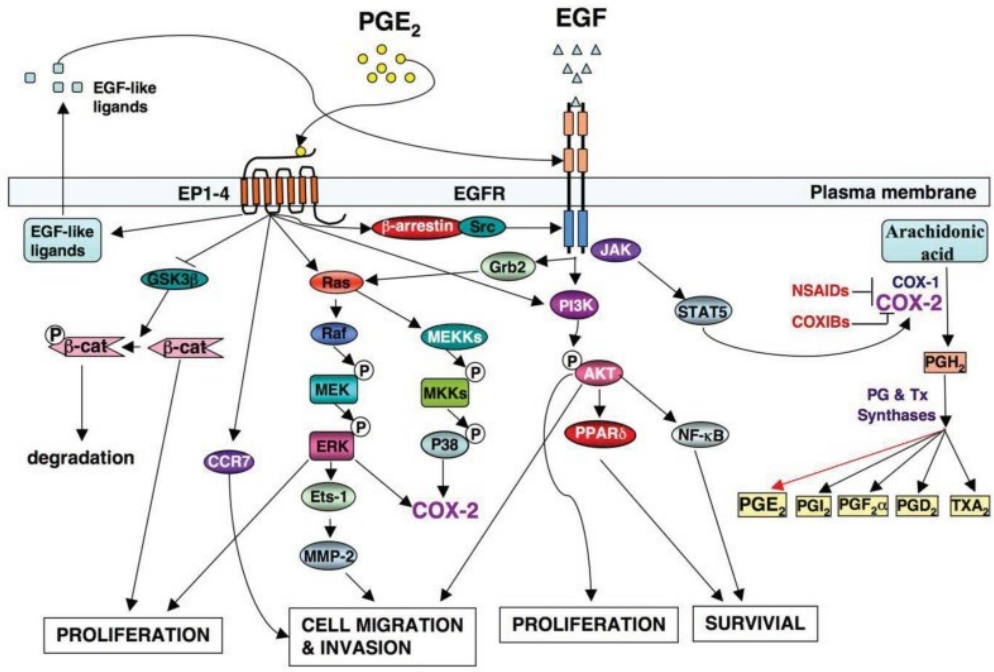

Figure 1.4 The crosstalk between COX-2 and EGFR signaling pathway in colorectal cancer [82].

1.3.3 Combination of Targeted Therapy of the Epidermal Growth Factor Receptor and Cyclooxygenase-2 Pathways

Using a single agent for cancer therapy may suffer from lack of adequate response from the patients because of the development of resistance or poor pharmacokinetic profiles of the drugs. Combining two or more different drugs/ classes of drugs for the treatment of cancer may significantly generate better outcomes. The rationale behind the combination of targeted cancer therapy is to reduce the emergence of resistant cells and fully enhance the cellular response [13]. Drugs that are used in the combination therapy should have non-overlapping toxicities to fully obtain the therapeutic benefit of the drugs and each of them should have an activity against the cancer when use as a single agent [8]. In addition, their mechanism of action should not be overlapping in order to minimize the inherited drug resistance [8].

The use of Cetuximab either as a single agent or in combination with irinotecan or other chemotherapeutic drugs has shown a little success for the treatment of patients

with metastatic colorectal cancer [82]. The reason might be related to the redundancy of EGFR signaling pathways or the transactivation of alternative signaling pathways that reduce the therapeutic benefit of the drugs [82]. In addition, the expression of EGFR is not a good predictor for the patient's response to the therapy, the presence KRAS, BRAF and PI3K mutations and their expression in the patients is valuable to identify the patients that will benefit from the therapies [12]. For example, KRAS mutation in patients with metastatic colorectal cancer diminished the response of the patients to the anti-EGFR therapies [86].

Targeting complementary pathways can provide a better option for the treatment of cancer. It has been shown that the inhibition of both COX-2 and EGFR was able to prevent intestinal adenomas and reduce xenograft tumor volume [87]. Some clinical trials are still on going to test the efficacy of combination therapy targeting of EGFR (tyrosine kinase inhibitor small molecule drugs and anti-EGFR MAbs) and COX-2 pathways in cancer patients. However, a phase II clinical trial of dual blockade of EGFR and COX-2 using cetuximab and celecoxib, respectively, in patients with metastatic colorectal cancer had shown disappointing results since the combination treatments could not improve the clinical outcome of single treatments [88]. The unexpected results of the clinical trial could have been resulted from the low local dose of celecoxib in the tumor site, thereby reducing the potential anticarcinogenic activity of celecoxib (e.g. COX-2 independent effect).

Drug delivery system can be an alternative solution to the problems since it increase the bioavailability of the drug by protecting the drug from premature degradation and enhance their uptake, maintain the drug concentration within their therapeutics window, and reducing their side effect by specifically delivering the drug to the disease site and target cells [89].

1.4 Controlled Drug Delivery Systems and Targeting

Current research in the field of pharmaceutics has been focused in the development of controlled release formulation and drug delivery systems to achieve controlled release of therapeutics drugs [90]. Controlled released systems are designed to control drug exposure over time, enhance the drug penetration across physiological

barriers, protect the drug from premature elimination, and target the drug to site of action. In addition, it also increases the patient compliance by minimizing the frequency of drug administration for the prolonged disease treatment [91]. Several drugs need to be delivered continuously for a period of time to maintain their therapeutic concentration and to reduce any side effect due to rapid delivery [92]. In the paper published by Park [93], the time points of evolution of controlled drug delivery technology was described. Controlled drug delivery technology was initiated in 1952 where the first controlled release formulation was introduced. The first generation of drug delivery systems mainly focused on the mechanisms of drug release such as dissolution, diffusion, osmosis, and ion exchange. The second generation of drug delivery systems moved toward the generation of delivery systems with zero-order release kinetics that maintain constant drug concentration in the blood. However, later, it was found that the constant drug concentration in the blood is not necessary for a drug to have an efficacy as long as the drug concentration is above the minimum effective drug concentration and lower than their minimum toxic concentration in order not to have a drug-associated toxicity (**Figure 1.5**). The early products of the 2nd generation included nanotechnology-based drug delivery systems such as smart polymers and hydrogels, biodegradable microparticles, solid implants, and in situ gel-forming implants [93].

1.4.1 Nanoparticle Drug Delivery System

The field of cancer nanotechnology has allowed the development of nanocarrier/nanoparticle systems containing cancer therapeutic drugs with a minimal toxicity to the healthy tissues and delivered more specifically to the tumor [94–97].

Organic nanomaterial (**Figure 1.6A**) such as liposomes, polymeric nanoparticles, micelles, nanogels, dendrimer, and inorganic nanomaterials (**Figure 1.6B**) such as magnetic nanoparticles, mesoporous silica, gold nanoparticles, and quantum dots are the examples of nanoparticles that are potentially used as a drug delivery systems [98].

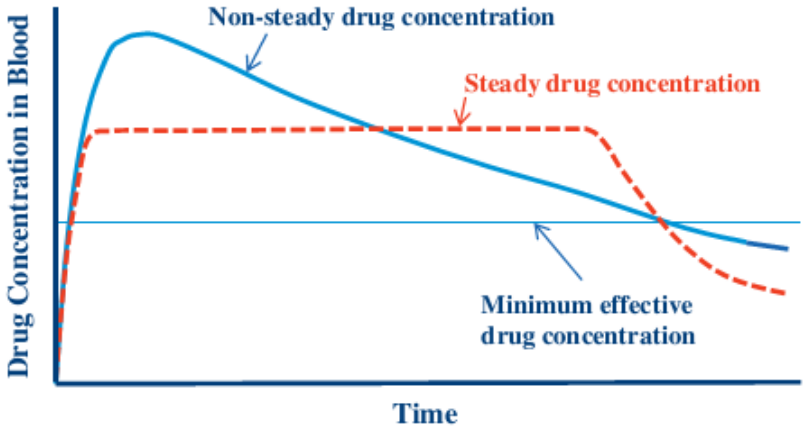

Figure 1.5 The drug is effective as long as its concentration in the blood is above the minimum effective concentration regardless of the pharmacokinetic profiles [93].

The versatility of nanoparticles as drug carrier is mainly because of the ability to control the physical and chemical properties as well as the biocompatibility by which the system will be able to improve the overall profile of therapeutics drug such as bioavailability, plasma solubility, toxicities, and pharmacokinetics. Several modifications on the nanomaterial physical and chemical properties during their formulation may be employed in order to deliver drugs specifically to the dynamics tumor microenvironment so that the drug therapeutic efficacy and toxicity profiles are improved [99]. Such modifications may include the alteration in the surface to volume ratio, size, shape, surface's charge, the addition of stimuli-responsive properties, and functionalization with targeting ligand (e.g. antibodies) in order to target specific sites, protect from the blood clearance, and other functionalities [99].

1.4.2 Cancer Targeting

1.4.2.1 Passive Targeting

Delivery of anticancer drugs can be done either locally or systematically. Local drug delivery is aimed to reach high amount of therapeutic drug directly to the localized site in the body for an extended period of time while reducing the systemic

toxicities by minimizing the exposure to the off target sites [100]. Compartments such as bladder, peritoneum, brain, eye and skin are known to be the sites where drugs may be administered locally [101]. However, the majority of anticancer drugs are administered systematically, which allows for both the treatment of micrometastatic disease and control the local malignancy at the same time [102]. However, this means that normal tissues are also exposed to the drugs. Therefore, the great efforts are being made to improve the systemic delivery of drugs [102].

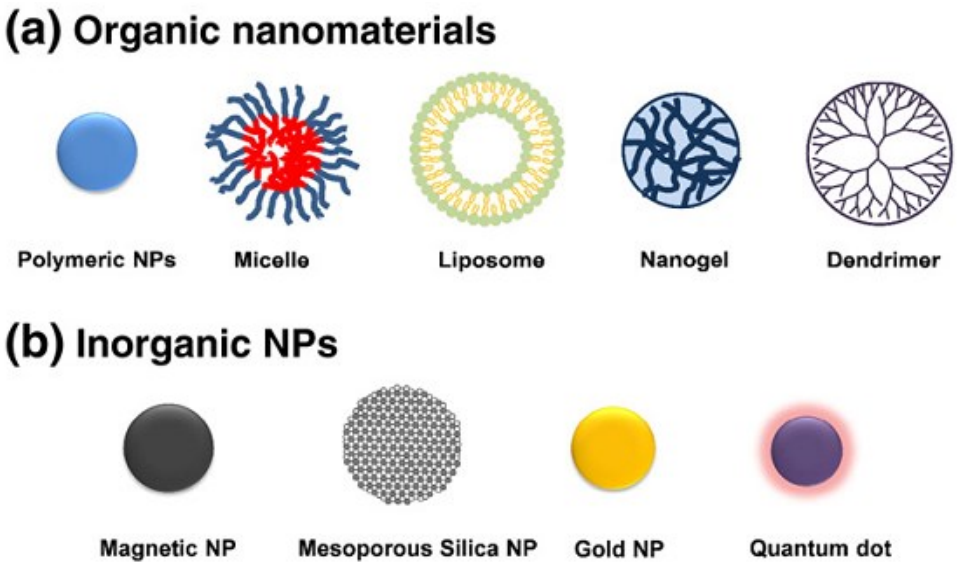

Figure 1.6 Nanoparticles for drug delivery. (A) Organic nanomaterials and (B) Inorganic nanoparticles [98].

In the 1980s, Matsumura and Maeda proposed the concept of Enhanced Permeability and Retention (EPR) effect that became the foundation of cancer targeting by nanoparticle drug delivery systems [103, 104]. Drugs within the nanoparticles with a defined size that are administered systematically can passively accumulate in the tumor site by the EPR effect (**Figure 1.7A**). It is known that a solid tumor for a given size secretes growth factor that promotes rapid angiogenesis leading to the formation of irregular blood vessel [105, 106] with fenestration sizes ranging

from 200 nm to 2000 nm [107]. The enhanced permeation is attributed to the fact that the fenestration will allow the extravasation of any blood components to the tumor sites from the general circulation [108]. On the other hand, the retention and subsequent accumulation of the nanoparticles in the tumor tissue can be attributed to defects in lymphatic drainage and their large size that prevent it from diffusing back into the circulation [108, 109].

EPR effect might be improved by changing the properties of tumor biology [108]. For examples, the modification of tumor microenvironment by remodeling extracellular matrix with injected enzymes was able to enhance the tumor distribution of macromolecules and nanomaterial as it increase the intratumoral mobility of the colloids [110]. In addition, other methods that modify the perivascular environment have also been attempted [111].

Apart from the tumor biology properties, the nanoparticles' physicochemical properties such as blood resident time, size, charge, shape, and the surface properties also affect the EPR effects [108]. The size of the nanoparticle needs to be smaller than the size of the fenestration in order to extravasate. Moreover, the density of collagen may hinder the tumor penetration of particles larger than 60 nm in diameter [112]. However, larger particles can have a similar tumor penetration as the smaller ones at extended times [113, 114]. In addition, negatively charged surface may increase, decrease or not affect the blood clearance of nanoparticles [115–120]. On the other hand, positively charged surface will increase the plasma clearance of the nanomaterial [121, 122]. The shape of nanoparticles can also influence their interaction with mononuclear cells [123, 124]. For instance, single-wall carbon nanotubes with high aspect ratio are cleared by the kidney efficiently although the dimensions are higher than the glomerular filtration threshold [125]. In addition, elongated plant-originated viral nanofilaments are highly accumulated in the tumor compared to the spherical counterpart [126].

Preferential accumulation of macromolecules/nanoparticles in the tumor sites due to the EPR effect has been reported in several publications. PEGylated liposomal formulation of Doxorubicin (Doxil™) was reported to have a 4–16-fold higher tumor deposition compared to free doxorubicin 3 to 7 days after the administration [127,

128]. The higher accumulation of doxorubicin of the liposomes can be attributed to the ability of the PEGylated liposomes to prolong the residence time of the doxorubicin in the blood and therefore, allowing more doxorubicin to accumulate in the tumor [129].

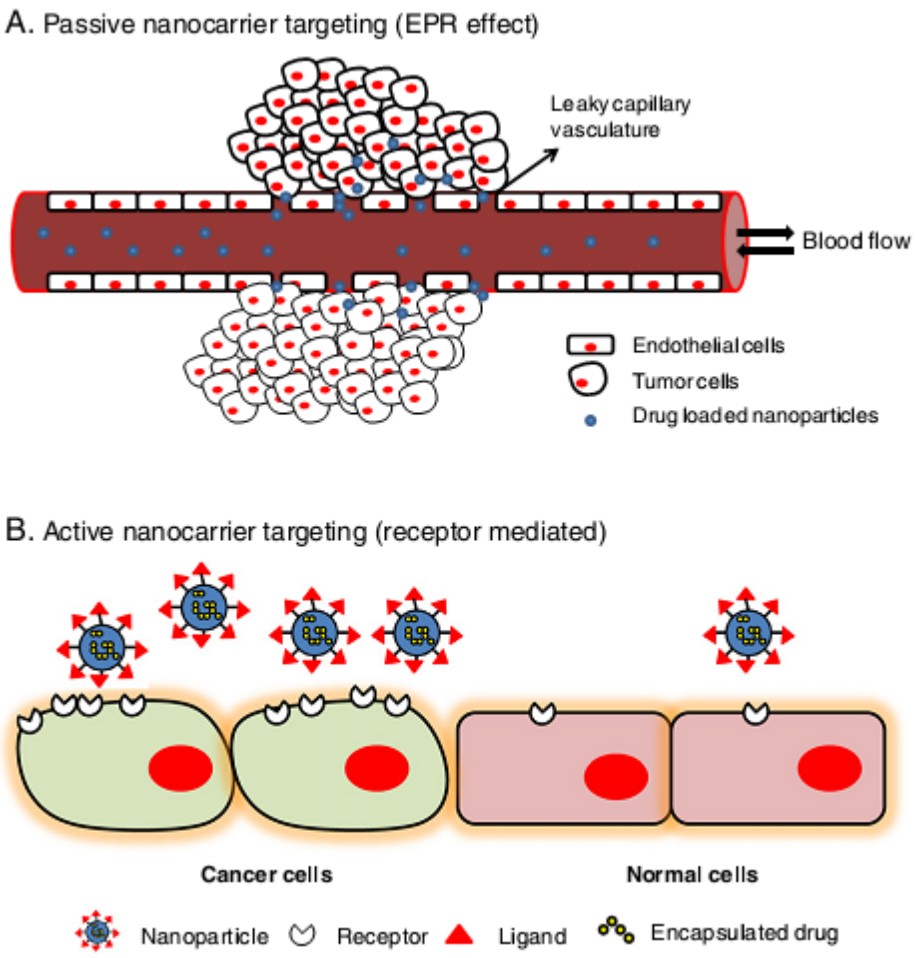

Figure 1.7 Cancer Targeting. Targeting nanopreparations to tumors via (A) Passive (the EPR effect) and (B) active (receptor mediated) targeting [130].

1.4.2.2 Active Targeting

Passive targeting only brings the nanoparticles, typically with size smaller than 200 nm in diameter, around the tumor interstitium; where the question of specificity remains. Grafting or attaching the targeting ligands such as antibodies, proteins, peptides, nucleic acids, sugars, and other small molecules [131] to the surface of nanoparticles will potentially increase the selectivity and cellular interaction of cancer cells with the nanoparticles, which in turn increases their therapeutic efficacy. This ligand-mediated targeting of nanoparticles involving the attachment of affinity ligand on the nanoparticles surface, called as active targeting, enhances the affinity of the particles to the cancer cells, prolong the tumor residence time as well as mediate the efficient uptake of drugs containing nanoparticles through the receptor mediated endocytosis **(Figure 1.7B)** [84]. Molecules which are recognized by the targeting ligands include surface molecules or receptors overexpressed in diseased organs, cells or subcellular domains [132–134]. A single nanoparticle may contain multiple copies of the ligand which increase the avidity of the nanoparticles to their targets [108]. However, in order to interact efficiently, the nanoparticles should be in a close proximity to their target which is usually in the extravascular space of the tumor and therefore it still requires the EPR effect to reach the targets [135, 136]. Moreover, it has also been shown that the active targeting strategies do not change the overall biodistribution profiles of the nanomaterial [137, 138].

Liposomes decorated with anti-HER2 antibodies on the surface have higher internalization to HER-2 expressing cancer cells compared to the non-targeted liposomes [138]. As another example, unlike non-targeted liposomes or non-specific immunoliposomes, EGFR-targeted immunoliposomes derived from Fab' fragments of C225 (Cetuximab) were efficiently bound and internalized in EGFR-overexpressing cancer cells and EGFRvIII stable transfectants [139]. In addition, cellular internalization can also further be improved by combining different targeting ligand on the surface the nanoparticles to target multiple receptors. For example, gold nanoparticles containing dual-ligand targeting (folic acid and glucose) had several fold higher cellular internalization in cancer cells expressing high folate receptor compared to the gold nanoparticles with single targeting ligand [140].

Physicochemical properties of the nanoparticles containing targeting ligand such as density of targeting ligand, size and shape of nanoparticles, surface and ligand charge and surface hydrophobicity are important in mediating interactions with target cells [108]. *In vitro* studies showed that increasing ligand density was followed by an increase in cellular uptake [141]. This might happen because the binding of a ligand to its receptor enhances the binding to nearby ligands [142]. However, the extent in improvement of cell binding was found to be maximum at intermediate ligand density and higher ligand densities may affect the cell binding negatively [143]. In fact, immunoliposomes with high density of intact antibodies as the targeting ligand were cleared faster from the circulation and their localization in the target tissue might decrease [144].

Size or shape of the ligand targeted nanoparticles may influence the extent of cellular internalization [145,146] or the ligand functionalization [136]. The charge of the unfunctionalized nanoparticles and the ligand may affect their conjugation as well as the ligand orientation on the surface [147]. In addition, the overall charge of the particles might also influence the cellular binding and uptake [148]. Besides the overall charge, surface hydrophobicity of the nanoparticles can also affect non-specific interactions with cells [108]. The grafting of hydrophilic polymer like polyethylene glycol (PEG), for example, can increase the surface hydrophilicity of the nanoparticles. The protective layer by PEG surface-functionalization is known to slow down the binding of opsonins and therefore the clearance of liposomes [149, 150]. On the other hand, protein adsorption on sterically unprotected ligand targeted nanoparticles can demise their substrate-binding capacity [151].

1.5 Liposomes as a Drug Delivery System

Liposomes (**Figure 1.8**), lipid bilayered vesicles, are spherical structures with an aqueous compartment in the core and a phospholipid shell surrounding the core. The concept of liposome as a pharmaceutical carrier began 40 years ago when Alec Bangham observed that phospholipids in aqueous solution can form closed bilayers structure [152]. Liposomes have been used as a model of biological membrane as well

as delivery vesicles and controlled release systems of various agents including drugs, diagnostics, nutraceuticals, minerals, food material and some cosmetics [153].

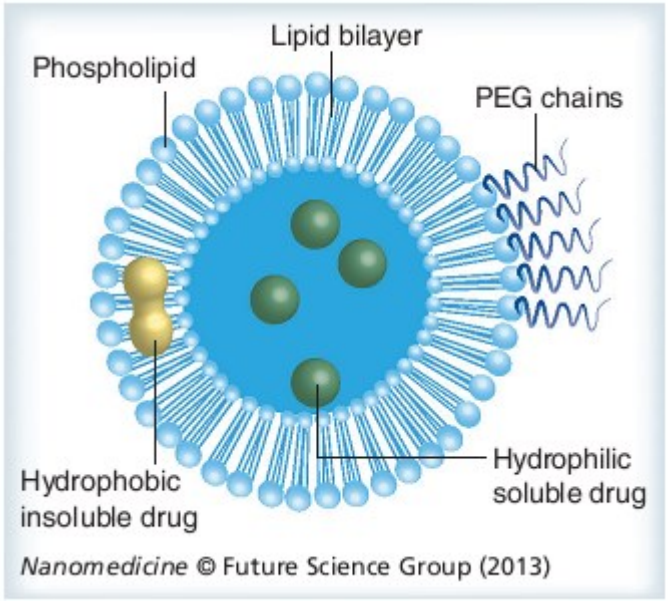

Figure 1.8 Hydrophilic and hydrophobic drugs can be encapsulated within a liposome [154].

As a drug delivery system liposomes offer many advantages over several other delivery systems. Liposomes are biocompatible, biodegradable, little or no toxic, non-immunogenic, and they have the ability to incorporate hydrophobic and hydrophilic drugs [154]. The hydrophobic drugs can be incorporated within the liposomes membrane while the hydrophilic drugs can occupy the aqueous compartment of the liposomes. In addition, as many other drug delivery systems, liposomes also improve the pharmacokinetics and pharmacodynamic profiles of the entrapped-drugs, act as a controlled release system of the drugs, and minimize the systemic toxicity of the associated free drugs [154]. The physical entrapment of the drugs protect them from premature degradation in the blood circulation and therefore prolong their half-life with a subsequent increase in bioavailability and therapeutic efficacy. The significant lowered systemic toxicity and improved therapeutic efficacy of the drugs entrapped

within the liposomes are well documented. For example, liposome-encapsulated doxorubicin (DOXIL) significantly enhanced tumor targeting, lowered the cardiac toxicity of doxorubicin, and improved patient survival and quality of life [155, 156].

1.5.1 Classification and Evolution of Liposomes

Based on the size and number of lamellae, liposomes can be classified into Small Unilamellar Vesicles [SUV), Large Unilamellar Vesicles, and Multilamellar Vesicles (MLV). The size of liposome can vary between 80 nm or less to greater than 1 μm in diameter: SUVs are single layer vesicles and below 100 nm in diameter, LUVs are single layer vesicles with diameters greater than 100 nm and less than 800 nm, and MLVs range from 500 nm up to 5000 nm in diameter and consist of several concentric bilayers [91] (**Figure 1.9**).

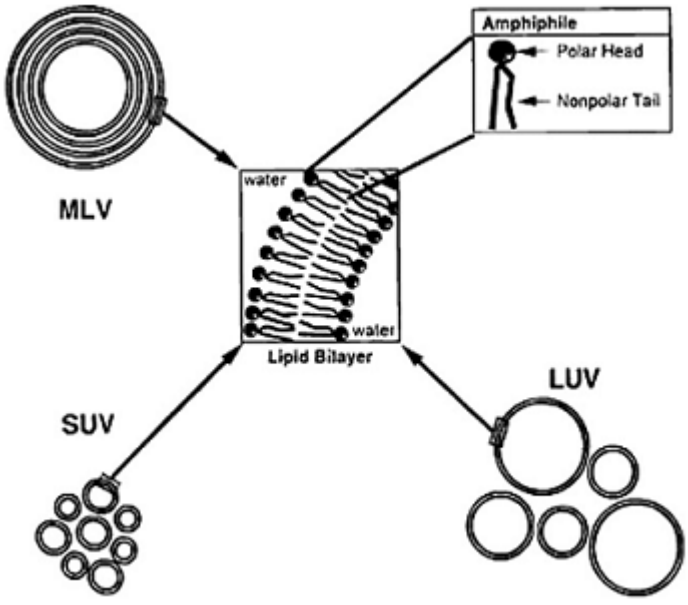

Figure 1.9 The schematic illustration of liposomes based on different size and number of lamellae. SUV : small unilamellar vesicles ; LUV : large unilamellar vesicles ; MLV : multilamellar vesicles [157].

Modification on the surface of the liposomes can generate liposomes with various functionalities for different applications (**Figure 1.10**). The aim of the modification mainly is to increase the life time of liposome in the blood circulation, target the liposomes to specific organelles, cells, or tissues, and provide other functionalities such as stimuli sensitivity and imaging.

The early liposomes produced contained a phospholipid bilayer without any polymers or targeting ligands attached (**Figure 1.10A**). However, these conventional liposome showed rapid clearance from the blood by Reticuloendothelial System (RES) [158].

In an attempt to increase the longevity of liposomes in the circulation, grafting of a biocompatible polymer such as polyethylene glycol (PEG) was done (**Figure 1.10B**) [150]. Steric coating of liposomes with PEG could prolong their half-life by allowing the liposomes to evade from detection of the immune system [97, 155]. For example, PEGylated liposomal vincristine (Marqibo, Talon Therapeutics, Inc.) has a 40-60 fold reduction in their clearance rate compared to the free vincristine [159]. Additionally, compared to the free doxorubicin, PEGylated liposomal formulation of doxorubicin (Doxil) showed a 100-fold increase in the clearance half-life [97]

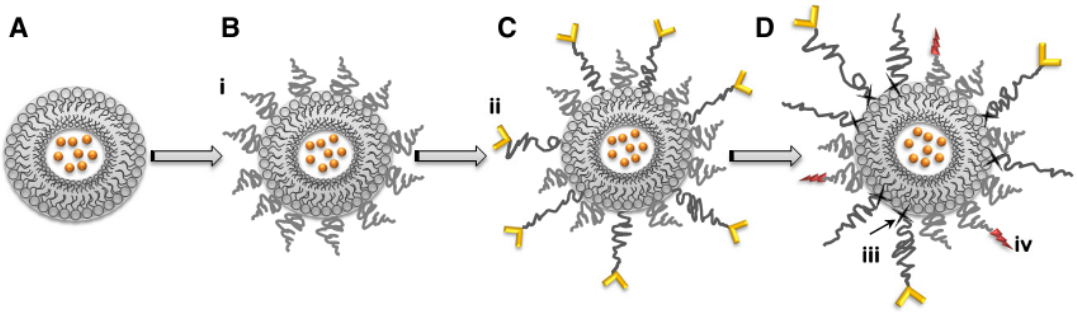

Figure 1.10 Evolution of liposomes. (A) Plain liposome, (B) Long-circulating liposome grafted with a protective polymer (i) such as PEG, (C) Ligand-targeted liposomes. (D) Stimulus-sensitive immuno-targeted liposomes with mAbs attached to long-chain PEG via stimuli-sensitive bonds (iii) [134].

Like other nanoparticles, targetability and selectivity of liposomes can further be improved by attaching targeting ligand on it (**Figure 1.10C**). The targeting ligand can be attached to the distal ends of the protecting polymer such as PEG which can minimize steric hindrance for the binding to the target [152, 160]. Actively targeted liposomes can be generated by conjugating targeting ligand such as small molecules, peptides, and monoclonal antibodies on the surface of liposomes [148]. The targeting ligand also functions to increase the tumor targeting and facilitate intracellular delivery of liposomes present in the tumor interstitium [161].

Liposome internalization through endocytosis pathways is dependent on their size, shape, surface charge, and composition [162, 163]. The targeting ligands especially mediate the uptake of liposomes through receptor-mediated endocytosis (**Figure 1.11**) [162] and the increase of cellular uptake in cancer cells, mediated by the active targeting, is achieved through the presence internalizing and the overexpression of surface receptor [154].

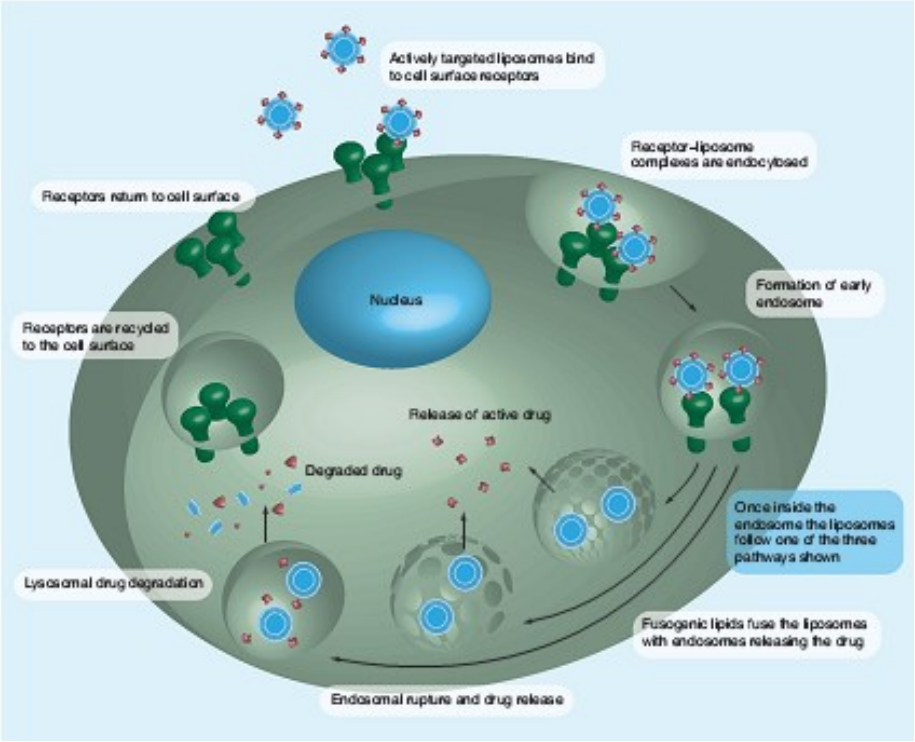

Figure 1.11 Surface receptor-mediated endocytosis [154].

1.5.2 Immunoliposomes for Cancer Therapy

The conjugation of antibodies that recognize receptors or antigens on the cell to the surface of liposomes for generating immunoliposomes (ILs) is a widely used strategy to actively target liposomes to the tumor sites. Among the immunoglobulin classes, IgG is the most widely used for functionalization of liposomes. Whole antibodies, half-IgG, Fab' fragments, and single chain antibodies (ScFv) can be activated and conjugated either directly to the phospholipids or other linkers (such as PEG) on the surface of liposomes [164, 165] . For example, conjugation between antibodies containing thiol group and maleimide functionalized-PEG on the liposomes surface readily generates stable thioether bond between the liposomes and the antibodies [145, 166].

Generally, the targeted drug delivery with immunoliposomes starts with the transport of immunoliposomes from the site of administration to the target cells and followed by the specific binding and the delivery of therapeutics drugs to the target cells [167]. It is presumed that 6 Fab′ fragments per liposome was sufficient to endocytose 55-60% of the cell-associated anti-HER2 immunoliposomes into HER2-overexpressing cells while the optimum ligand density for efficient delivery of anti-HER2 immunoliposomes was seen at density of 40 Fab′ fragments per vesicle [166]. Receptors such as EGFR and HER-2 are overexpressed in many tumors, and are therefore used to target immunoliposomes selectively to tumor cells. For example, HER-2-targeted immunoliposomes successfully increased the tumor delivery and therapeutic efficacy of liposomes containing doxorubicin in mouse xenograft models with HER-2 overexpression [168, 169]. In another study, doxorubicin-loaded immunoliposomes containing EMD72000 (a humanized anti-EGFR monoclonal antibody) were efficiently bound and internalized in different colorectal cancer cells with EGFR overexpression compared to the corresponding non-targeted or non-specific immunoliposomes [170]. In a related study, immunoliposomes with anti-CD19 mAbs or its Fab' fragments as the targeting ligand significantly enhanced the targeting and therapeutic efficacy of doxorubicin in mice model bearing a human CD19+ B-lymphoma [171, 172].

Clinical trials have been conducted with different immunoliposome preparations. For example, MCC-465, immunoliposomes that are targeted to gastric cancer cells, have been shown to have acceptable biodistribution and provide efficient targeted delivery to stomach cancer cells [173]. SGT-53, a transferrin-targeted liposomal formulation containing the p53 gene [174] has resulted in significant growth inhibition of tumors such as head and neck, prostate, and breast in a phase I trial [175]. In another phase 1 dose-escalation study, cetuximab decorated PEGylated DOX (Doxil®/Caelyx®) liposomes were shown to have clinical activity, including 1 with a complete response out of 29 patients, and it was reported that the liposomes may potentially progress to phase 2 clinical study [176].

The development cost of targeted nanomedicine is much higher compared to the non-targeted liposomes [135]. For antibody conjugated nanoparticles, it is difficult to maintain the protein stability in face of environmental challenges. Additionally, the reproducibility for scale up production, the stability and the shelf-life as well as the cost/efficiency of the preparation are also challenging [108].

1.6 Aims of the Study

Deregulation in the of Epidermal Growth Factor Receptor (EGFR) signaling pathway is associated with the development of a wide range of human cancers including head and neck, breast, bladder, ovarian, renal, colon, non-small cell lung cancer. The expression of Cyclooxygenase-2 (COX-2) is associated with bad prognosis in different cancers and can increase the angiogenic and metastatic potential, inhibit apoptosis, and enhance cell proliferation [60–62] . Interestingly, the crosstalk between COX-2 and EGFR signaling pathways exists and the increase of COX-2 expression can lead to the increase of EGFR expression and vice versa. Therefore, targeting these two complementary pathways can be a strategy for cancer therapeutics. However, a phase II clinical trial of dual blockade of EGFR and COX-2 with cetuximab and celecoxib, respectively, in patients with metastatic colorectal cancer had shown disappointing results since the combination treatments could not improve the clinical outcome of single treatments [88]. Drug Delivery System can be an

alternative solution to the lack of clinical outcome since it can increase the bioavailability of the drug by protecting it from premature degradation and enhance uptake, maintain the drug concentration within the therapeutic window, and reduce any side effect by specifically delivering the drug to the disease site and target cells [89] .

Liposomes are a good candidate as a delivery system for celecoxib; owing to its hydrophobicity, celecoxib can be incorporated within the bilayer. Our group has previously shown that high CLX encapsulation can be successfully achieved in different formulations of MLVs and LUVs and the drug was shown to have a sustained release profile from the liposomes, implying the feasibility of a liposomal drug delivery system for CLX [177, 178]. In addition, our group has also shown that non-targeted long circulating liposomes containing CLX can have a functional effect against colorectal cancer cell lines *in vitro* [178]. Liposomes with a defined size, typically less than 200 nm, are passively accumulated in the tumor interstitial through Enhance Permeability and Retention Effect [155, 179]. However, tumor targeting properties of the liposomes can further be improved by attaching targeting ligands such as antibodies or antibody fragments on their surface [161, 165].

The aim of the study can be summarized as:

1. To develop and characterize the EGFR-targeted immunoliposomes for targeted delivery of celecoxib in cancer cells.
2. To study the internalization and cytotoxicity of the immunoliposomes in cancer cell lines with varying expression of EGFR and COX-2.

CHAPTER 2

MATERIALS AND METHODS

2.1 Materials

Celecoxib was purchased from Santa Cruz Biotechnology (Texas, USA) (**Figure 2.1)** [180]. Phosphatidylcholine (1,2-Distearoyl-sn-Glycero-3-Phosphocholine, 18:0, DSPC), Cholesterol (ovine wool, >98%), 18:0 mPEG(2000)-DSPE (1,2-distearoyl-sn-glycero-3-phosphoethanolamine-N-[methoxy(polyethylene glycol)-2000) and DSPE-PEG(2000) Maleimide (**Figure 2.2**), mini-extruder set, filter supports and Nucleopore Track-Etch Polycarbonate (PC) membranes (100 nm) were obtained from Avanti Polar Lipids (Alabaster, Alaska). SP-DiOC18(3) were the products of Invitrogen (Carlsbaad, California). Lissamine™ Rhodamine B 1,2-dihexadecanoyl-sn-glycero-3-phosphoethanolamine, triethylammonium salt (Rhodamine DHPE or Rh-PE) were obtained from Invitrogen (Carlsbaad, California). SlowFade® Gold antifade reagent was purchased from Invitrogen (Oregon, USA). Cysteamine hydrochloride (2-MEA) was purchased from Applichem (Darmstadt, Germany). Mouse IgG (free of azide and BSA, lyophilized) were obtained from Sigma-Aldrich (St Louis,USA). Anti-EGFR monoclonal antibody (chimeric mouse–human IgG1 clone C225; free of azide and BSA) was either purchased from Thermo Scientific, Pierce Protein Research Products (Rockford, IL USA) or LifeSpan BioSciences, Inc (Seattle, WA USA). Chloroform and methanol were obtained from Merck (Munich, Germany). MTT reagent (3-(4,5-Dimethylthiazol-2-yl)-2,5-Diphenyltetrazolium Bromide) was purchased from Invitrogen (Carlsbaad, California). Zeba™ Spin Desalting Columns were obtained from Thermo Scientific, Pierce Protein Research Products (Rockford, IL USA). Ultra filtration device (VivaSpin2) with MWCO 300 kDa membrane was purchased from Sartorius

(Goettingen, Germany). Puradisc^{TM} sterile 0.2 µm Polyethersulfone (PES) filters were purchased from Whatman Inc (New Jersey, USA).

Human colon cancer cell line HCT-116 was purchased from German Collection of Microorganisms and Cell Cultures (DSMZ, Germany) and SW-620 were purchased from American Type Culture Collection (ATCC, USA). MDA-MB-468 (MDA-468) was kindly provided by Assoc. Prof. Dr. Elif Erson from METU, Department of Biological Sciences, Ankara, Turkey. Human colorectal carcinoma cell line HT-29 was purchased from ŞAP Enstitüsü (Ankara, Turkey). Cell culture media and supplements were obtained from Biochrom (Berlin, Germany). Cell culture grade plasticware was obtained from Greiner Bio-One GmbH (Goettingen, Germany).

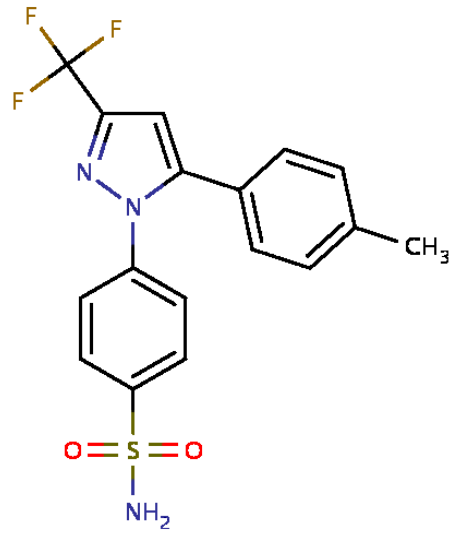

Figure 2.1 Chemical Structure of Celecoxib [180].

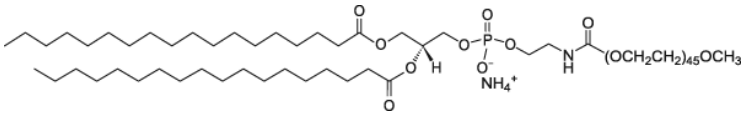

DSPC

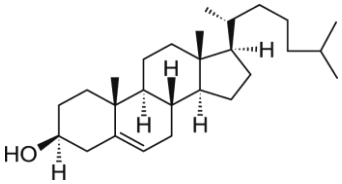

Cholesterol

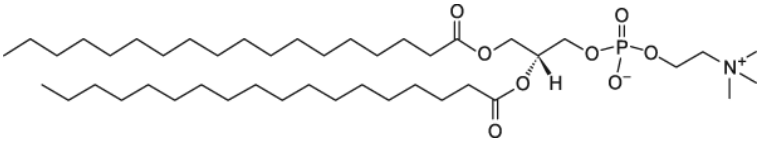

DSPE-mPEG(2000)

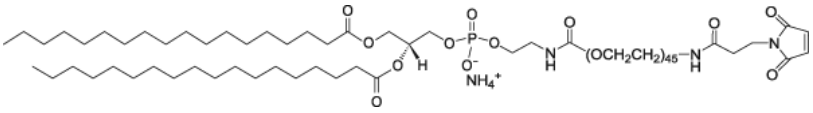

DSPE-PEG(2000) Maleimide

Figure 2.2 Chemical structures of DSPC, Cholesterol, DSPE-mPEG(2000), and DSPE-PEG(2000) Maleimide [181].

2.2 Methods

2.2.1 Preparation of Liposomes

2.2.1.1 Preparation of Unilamellar Liposomes (LUV)

Liposomes were prepared with thin lipid film hydration method [182]. The liposomes were composed of DSPC, CHOL, mPEG(2000)-DSPE (molar ratio 100: 10 : 4) and 7 mol% of Celecoxib (CLX) relative to the total mole number of liposome components. DSPC, cholesterol, mPEG(2000)-DSPE and CLX were dissolved in chloroform to prepare stock solutions and mixed according to the proportion in round bottom Polypropylene (PP) tubes. A stream of argon was used to evaporate chloroform to form a thin lipid film and the residual chloroform was removed by keeping the tubes overnight under vacuum at 100 mbar in HETO-spin vac system

(HETO, Allerod, Denmark). The lipid films were then flushed with argon and stored at 4ºC. Lipid films were hydrated with 1 mL PBS (0.1 M, pH 7.4) for 6 cycles of 4 min heating and vortexing to form MLVs. MLVs were then extruded through 100 nm PC membrane (Avanti Polar Lipids, USA) using a mini-extruder set (Avanti Polar Lipids, USA) at least 15 times to form LUVs (**Figure 2.3**). The extrusion was carried out at 75˚C (above the transition temperature of DSPC at 56°C) after the equilibration of liposome suspension at 75ºC on a heating block provided in the mini extruder set for 10 min. During the extrusion, temperature was maintained at 75°C by putting the heating block on a heater. After the extrusion, the clear liposome suspensions were allowed to re-anneal at 75°C in a water bath for at least 1h. The resulting unilamellar liposomes were purified from un-encapsulated celecoxib using an ultrafiltration device (VivaSpin2) with MWCO 300 kDa membrane (Sartorius, Germany) following the manufacturer's instructions. The purified liposomes were then diluted with PBS (0.1 M, pH 7.4) or complete cell culture medium to obtain 8-10 mM liposomes. For cell culture studies, liposomes diluted with cell culture medium were filter sterilized through sterile 0.2 µm Polyethersulfone (PES) filters (Whatman Puradisc). Aliquots were withdrawn and dried completely under overnight vacuum at 100 mbar in HETO-spin vac system (HETO, Allerod, Denmark) for quantification of CLX and DSPC. The final liposome suspensions were stored at 4°C for further experiments and used up within 1 week.

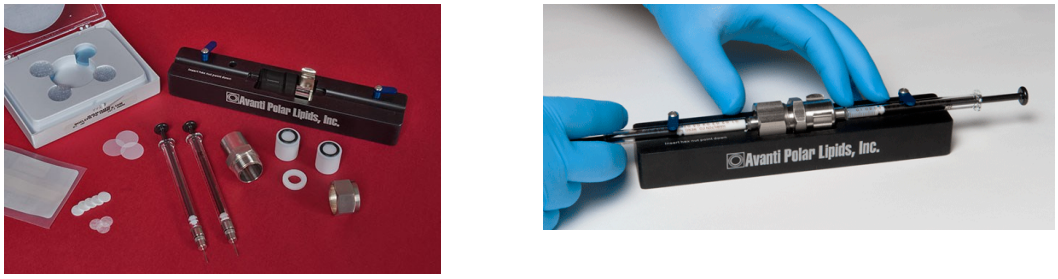

A B

Figure 2.3 Unilamellar vesicles preparation by extrusion method. (A) Mini extruder set for liposome preparation. (B) Liposomes suspension is extruded through PC membrane to produce large unilamellar vesicles [157].

For confocal microscopy and flow cytometry, 0.5 mol % of rhodamine labeled lipid Rh-PE and 0.3 mol % of SP-DiOC18 (3) relative to the total phospholipids were incorporated into the liposome formulations, respectively (please see Section 2.2.1.b for the preparation of immunoliposomes). The liposomes were purified from the excess dye by ultrafiltration using a MWCO of 300 kDa (VivaSpin2). All the procedures involving fluorescence-labeled dyes were carried out in the dark.

2.2.1.2 Preparation of Immunoliposomes

Mouse IgG was used to optimize the preparation of immunoliposomes, their characterization and release of CLX. The monoclonal anti-EGFR mouse IgG (clone C225) was used for confocal microscopy, flow cytometry, and cell cultures study of the immunoliposomes.

For the preparation of immunoliposomes, mPEG(2000)-DSPE and DSPE-PEG(2000)Maleimide were included in the lipid film as 3 mol% and 1 mol% of total phospholipids, respectively, in order to form maleimide functionalized LUVs. The lipid film was hydrated with HBS (HEPES buffered saline: 20 mM HEPES, 140 mM NaCl. pH: 7.4) and the subsequent steps to prepare the maleimide functionalized LUVs were as described in Section **2.2.1.1.** However, the purification of the immunoliposomes from un-encapsulated CLX and un-conjugated antibodies were carried out after the conjugation of antibodies to the surface of LUVs.

Immunoliposomes were prepared by conjugating a half-IgG to the preformed maleimide functionalized unilamellar liposomes. Mouse IgG (200µg) or monoclonal anti-EGFR mouse IgG (clone C225) was reduced with the mild reducing agent 2-MEA at 37°C in order to form half IgG with a free –SH group (**Figure 2.4**) [183]. The reaction was carried out in deoxygenated HBS/EDTA (10 mM EDTA) in order to preserve the reduced ends from metal catalyzed oxidation. For the optimization process, mouse IgG was reduced with a range of concentrations of 2-MEA from 25 mM to 100 mM. The effect of the reaction duration was also evaluated by changing the reaction duration from 30 min to 90 min.

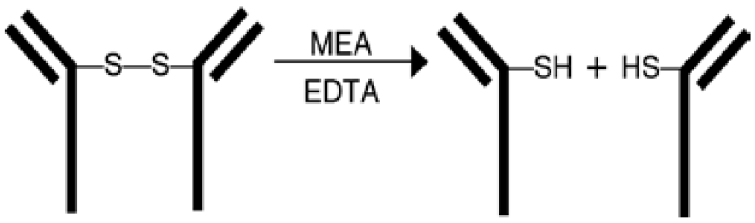

Figure 2.4 2-MEA selectively reduce disulfide bond in the hinge region of IgG [183].

As a positive control, the IgG was fully reduced with β-mercaptoethanol and boiled to separate their heavy and light chains. The reduced IgG fragments were then visualized by Coomassie blue staining after separation by SDS-PAGE.

For preparation EGFR-targeted immunoliposomes, 200 µg anti-EGFR antibody was reduced with 75 mM 2-MEA at 37^{o}C for 90 min in a thermocycler. To remove the reducing agents, a Zeba Desalting column (Thermo Scientific) with MWCO of 7 kDa was pre-equilibrated with HBS/EDTA (EDTA 10 mM) followed by passing the reduced IgG mixtures.

The conjugation of the antibody fragments to the liposomes was carried out by overnight incubation of the purified reduced IgG fragments with 10 mM pre-formed maleimide functionalized unilamellar liposomes at 4^{o}C (**Figure 2.5**) [184]. The un-conjugated antibodies, un-encapsulated celecoxib and other unincorporated components of liposomes were removed from the immunoliposome suspension by ultrafiltration (VivaSpin2). The purified liposomes were diluted with complete cell culture medium to obtain 8-10 mM of liposomes and filter sterilized through sterile 0.2 µm Polyethersulfone (PES) filters (Whatman Puradisc). The liposomes were then stored at 4°C for further experiments.

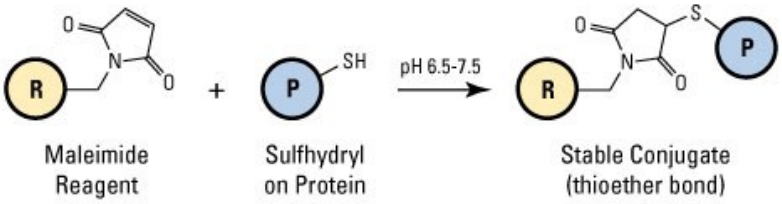

Figure 2.5 Conjugation reaction of maleimide reactive group on a crosslinker and sulfhydryl group on protein generate a stable thioether bond [184].

2.2.2 Quantification of Celecoxib

Celecoxib was quantified by either spectroscopic methods or by HPLC.

2.2.2.1 Spectrophotometric method

Aliquots of liposome samples were initially dried completely under vacuum. The dried samples were dissolved in chloroform and their absorbance was measured at 257 nm. Pure chloroform was used as blank and the concentration of celecoxib was determined from the previously constructed celecoxib calibration curve in chloroform (range: 5-15 µg/mL) (**Figure A.1**)

2.2.2.2 HPLC Method

Celecoxib released from the liposomes into PBS was measured by a modified HPLC method [185]. Samples from PBS media were withdrawn and dried completely under vacuum and then dissolved in pure methanol and filter sterilized through 0.45 µm filters before injection. All samples were analyzed within 8h after reconstitution in methanol. A Shimadzu HPLC equipment and Inertsil ODS-3 C18 column (5µm x 250 mm x 4.6 mm) were used with 85:15 (v/v) methanol:water as mobile phase at a flow rate of 0.8 ml/min. Detection was performed at 254 nm at 25°C (ambient temperature). The amount of celecoxib was then measured from a previously constructed calibration curve in pure methanol (**Figure A.2**).

2.2.3 Quantification of Phospholipids (DSPC)

DSPC was measured by a direct estimation of phospholipids [186]. Aliquots of liposomes were dried completely under vacuum. The dried samples were redissolved and diluted in chloroform. Ammonium ferrothiocyanate solution was added to the samples (1:1 v/v) and mixed by vortex mixing for 20 seconds. After that, the mixture was spun at 300 x *g* for 5 min. The red lower layer (chloroform) phase was withdrawn and the absorbance was measured at 485 nm and DSPC calibration curve (range: 5-50 µg/ml) constructed in chloroform was used for determining the amount of phospholipids (**Figure A.3**).

2.2.4 Characterization of Liposomes

2.2.4.1 Particle Size Analysis

Liposome size distributions of were determined by dynamic light scattering (DLS) using Zeta sizer NanoZS (Dr Irem Erel, METU Chemistry Department). Unilamellar liposomes or immunoliposomes samples (10 mM) were diluted 1:5 with PB (0.1 M, pH 7.4) and the measurement was carried out after the incubation for 1 min at 25°C

The hydrodynamic diameters liposomes were reported as Zavg and the PdI value indicated the homogeneity of the sizes of the particles. PdI <0.2 indicates a homogenous liposome population.

2.2.4.2 Surface Charge Analysis

Zeta potential was determined by Laser Doppler Electrophoresis using zeta sizer NanoZS (Dr Irem Erel, METU Chemistry Department) to assess the surface charge of liposomes. 10 mM unilamellar liposomes or immunoliposomes samples were diluted 1:2 with PB (0.1 M, pH 7.4) and the measurements were carried out under ambient conditions.

2.2.4.3 Drug Encapsulation Efficiency and Drug Loading

50 uL of aliquot of liposomes was allowed to dry under vacuum by using the HETO-spin vac system (HETO, Allerod, Denmark). The dried samples were dissolved in chloroform by vigorous vortex mixing. The CLX and DSPC amounts were calculated using methods that have been described in Sections 2.2.2.1 and 2.2.3, respectively.

Drug encapsulation efficiency was calculated as:

$$Encapsulation\ Efficiency\ (\%) = \frac{CLX\ in\ liposomes\ (mg)}{CLX\ initially\ added\ (mg)} \times 100$$

Drug Loading was calculated as:

$$Drug\ Loading\ (\%) = \frac{mol\ of\ CLX\ in\ liposomes}{mol\ of\ DSPC\ in\ liposomes} \times 100$$

2.2.4.4 *In vitro* release of Celecoxib from Liposomes

Release of celecoxib from unilamellar liposomes and immunoliposomes were analyzed using the dialysis method at 37ºC. The liposomes (1 mL, 8-10 mM) were put inside a celullose acetate dialysis bag (Molecular weight cut off: 12 kDa, Sigma Aldrich, Germany). The bag was immersed in release medium (PBS, pH 7.4) under mild and continuous agitation. The release medium (1 mL) was withdrawn at different time points over a period of 72 h and replaced with the same volume of fresh PBS (pH 7.4). The aliquots were dried completely under vacuum (Labconco FreeZone, Model 77520) and redissolved in 200 µl pure methanol. The amount of celecoxib was determined by HPLC (**section 2.2.2.2**).

2.2.4.5 IgG Conjugation Efficiency

The amount of IgG conjugated to the immunoliposomes was determined indirectly by measuring the amount of unconjugated IgG in the ultrafiltration filtrate. The protein amount was determined by the microplate protocol of Coomassie Plus

(Bradford) assay (Thermo Scientific) following the manufacturer's instructions. The diluted samples (150 µl) were mixed with 150 µl of Coomassie Plus reagent and incubated for 10 min at room temperature. The absorbance at 570 nm was measured by using a Multiskan Go (Thermo scientific) and the protein amount was determined by a constructed calibration curve (range 1-25 µg/ml) (**Figure A.4)**

2.2.5 Cell Culture Conditions

The human colon cancer cell lines HCT-116 and HT-29 cell were cultured in McCOY's 5A modified medium supplemented with 10% FBS, 2 mM L-glutamine and 1% Penicillin-Streptomycin or phenol-red free RPMI 1640 media. The human colon cancer cell line SW-620 and breast cancer cell line MDA-MB-468 were cultured in Leibovitz L-15 medium supplemented with 10% FBS, 2 mM L-glutamine, 1% Penicillin-Streptomycin, and 2 g/L NaHCO3 and maintained in 5% CO_2 at 37ºC. For MTT assays, before the addition of MTT reagent, the medium was replaced with phenol-red free RPMI 1640 media supplemented with 10% FBS, 2 mM L-glutamine and 1% Penicillin-Streptomycin). The characteristics of human colorectal adenocarcinoma cell lines HCT-116, HT-29, SW-620 and breast cancer cell line MDA- -MB-468 are listed in **Table A.1**.

2.2.6 Binding and Internalization of Immunoliposomes

The binding and internalization of immunoliposomes were visualized by using confocal laser scanning microscopy (CLSM) and quantified by flow cytometry.

2.2.6.1 Laser Scanning Confocal Microscopy

SW-620, HCT-116, and MDA-MB-468 cells were seeded on a cover slip in 6 well plates until it reached 80% confluency. The cells were treated with 500µM lipid concentration of Lissamine-Rhodamine labeled-immunoliposomes or unilamellar liposomes at 37ºC for 2 h and 4 h. The untreated cells were used as negative controls. The medium containing labeled liposomes was removed and the cells were washed

three times with cold PBS in order to remove the unbound liposomes. The cells were fixed with 4% paraformaldehyde and mounted on a cover glass with gold antifade reagent as a mounting medium. Images were captured by using Plan-Neofluar 40x/1.3 Oil DIC objective in Zeiss LSM 510 system (METU Central Lab, Molecular Biology and Biotechnology Research Center) at excitation wavelength of 543 nm and emission wavelength of 583 nm. For the emission and imaging, LP560 filter was used.

2.2.6.2 Flow Cytometry

For flow cytometry analysis, SW-620, HCT-116 and MDA-MB-468 cells were seeded in 6 well plates and cultured until they reached 60-70 % confluency. The medium was withdrawn and the cells were treated with SpDiOC(18)-labeled immunoliposomes or unilamellar liposomes at 500 uM lipid concentration. The cells were incubated with the liposomes at 37ºC and 4ºC in order to distinguish between non-specific binding and internalization of liposomes. At 4°C, the cells are not expected to actively internalize the liposomes; therefore any cell association can be assumed to be non-specific [187]. Untreated cells were used as negative controls in every experiment. After 2 h or 4 h of treatments, the medium was removed and the cells were washed 3 times with cold PBS. The cells were detached by trypsinization, collected, and centrifuged at 1000 rpm. The pellet was then washed twice with cold PBS. The cells were then fixed by 100 µL drop-wise addition of 4% paraformaldehyde (freshly prepared) and vortex mixing. After 15 min of fixation, 2 mL of 1% (g/mL) of BSA in PBS was added to terminate the fixation. The cells were then collected by centrifugation; the pellet was washed with PBS and re-suspended in 300 µL of PBS. Fixed cells were analyzed in AccuriC6 Flow cytometer and CFlow software (METU, Department of Biological Sciences) by collecting 10,000 events for each sample in FL-1 channel. Live-gating was performed by using forward vs side scatter to exclude debris and dead cells. The gating was performed separately on MDA-MB-468, HCT-116 and SW-620 cell populations.

2.2.7 Western Blot Analysis

COX-2 and EGFR expressions in HT-29, HCT-116, SW-620, and MDA-MB-468 cell lines were visualized by Western blot analysis. Proteins were isolated using M-PER mammalian protein extraction reagent (Pierce, Rockford, IL, USA) supplemented with protease inhibitors (Roche, USA). The protein content was determined by standard microplate protocol of Coommasie Plus (Bradford) assay (Thermo Scientific). Proteins (50–80 μg) were subjected to SDS-PAGE on a 10% polyacrylamide gel and transferred onto a PVDF membrane (Bio-Rad, Hercules, CA, USA) for 1-2 hours. The membranes were blocked in 5% skim milk in PBST (0.1 M PBS, 0.1 % Tween 20, pH 7.4) for 1 h at room temperature and then incubated overnight at 4^{o}C with primary antibodies: COX-2 (1:200 dilution; Cayman Chemical, Ann Arbor, MI, USA) or EGFR (1:200 dilution; Santa Cruz Biotechnology, Santa Cruz, CA, USA). The membrane was rinsed with PBST for 30 min with at least 3 changes and incubated for 1 h at room temperature with a HRP-conjugated goat anti-rabbit (1:2000) or goat anti-mouse (1:2000) secondary antibody. After that, the membrane was washed extensively 3 times with PBST (10 min for each wash). The proteins were detected by using an enhanced chemiluminescence kit (ECL Plus; Pierce) following the manufacturer's instructions.

2.2.8 Cellular Viability Assay

10^4 cells/well were seeded in 96-well plates and allowed to recover for 48 h. The CLX was solubilized in DMSO and then diluted in cell culture medium as required. The cells were treated with different concentrations of CLX (25 – 150 μM) to determine the concentration of CLX resulting in 50% growth inhibition. After 24 h, the medium was then replaced with 100 μL of phenol red free complete medium and 10 μL of the MTT labeling reagent (5 mg/ mL) was added to the medium and incubated for 4 h. The cells were lysed with HCl-SDS (0.01 M HCl, 1 % SDS w/v) solution. After 18 hours, the absorbance was measured by using a Multitaskan Go (Thermo Scientific) microplate reader at 570 nm. IC_{50} was determined graphically from the concentration-effect curve, in which the viability of the control cells was considered

as 100%. Additionally, in different set-up of the experiments, the cells were treated separately with 100 μM of free CLX, empty liposomes, CLX loaded unilamellar liposomes and the EGFR-targeted immunoliposomes with 100 μM of CLX concentration, in complete media supplemented with 10% FBS. In order to determine lipid associated toxicity, the dose of the empty liposomes used was equal to the lipid concentration of the ILs. After 4h of treatment, the medium was replaced with 100 μL of phenol red free complete medium and MTT assay was carried out as described above.

2.2.9 Statistical Analysis

All experiments were carried out with 2-3 independent replicates. Data analysis and graphing were performed using the GraphPad Prism 6 (San Diego, California). One-way ANOVA and Tukey's multiple comparison post-hoc test were used to determine the level of significance between the groups with different treatments. The difference between the means were considered to be statistically significant at level of $P<0.05$.

CHAPTER 3

RESULTS AND DISCUSSIONS

3.1 Characterization of CLX Loaded ILs

3.1.1 Encapsulation Efficiency and Drug Loading of ILs

Despite the anti-inflammatory and anticarcinogenic activities of CLX, its long-term use is associated with the increased incidence of cardiovascular risks [68, 188]. The development of a drug delivery system (DDS) for CLX may possibly overcome the unfavourable side effects of CLX. Controlled drug delivery may improve bioavailability by preventing premature degradation and enhancing uptake, maintain drug concentration within the therapeutic window by controlling the drug release rate, and reduce side effects by targeting to disease site and target cells [89]. Liposomes, polymers, and micelles are DDS's, which are frequently used. The use of liposomes as DDS is more beneficial compared to several others since it is biocompatible, biodegradable, non-toxic, non-immunogenic, and non-pyrogenic. Moreover, CLX is a highly hydrophobic drug with poor plasma solubility; therefore, it is a good candidate to be formulated in liposomes. The incorporation of CLX in the liposomes can improve its plasma solubility, pharmacokinetics profile as well as its accumulation in the target tissue.

Some studies have reported liposomal formulations of CLX for different purposes, including for the cancer treatment [177, 178, 189–193]. For example, Erdog et al has reported the successful encapsulation of the CLX within the PEGylated LUVs [178]. The LUVs containing CLX was shown to have a desirable characteristics DDS for such as sustained release profile and high encapsulation efficiency of CLX. The generated liposomes were also shown to be functionally active against different colorectal cancer cell lines with varying expression of COX-2. Another study also reported that liposomal celecoxib was able to inhibit colon cancer *in vitro* and DMBA-

induced tumor in a rat model [189]. However, the use of non-targeted PEGylated liposomes is not completely devoid of off-target associated toxicities. For example, for DOXIL® (PEGylated liposomal doxorubicin), an increase in the incidence of palmar-plantar erythrodysesthesia ('hand-foot' syndrome) in patients receiving liposomal doxorubicin versus those receiving free doxorubicin was observed [194]. Therefore, the targeting of liposomes containing CLX with a targeting ligand such as an antibody may enhance the specificity and efficacy of the therapeutic drug. EGFR-specific antibody C225 (cetuximab) can be considered as a promising candidate for targeting the CLX to cancer since EGFR overexpression is seen in human tumors and the antibody is among the ones the most ahead in clinical development.

In this study, we prepared the EGFR-targeted immunoliposomes, with composition: DSPC, Cholesterol, CLX, mPEG, and mal-PEG. As a control, non-targeted LUVs containing the same composition as those of EGFR-targeted immunoliposomes except mal-PEG was prepared. Non-specific IgG containing immunoliposomes were also constructed for the optimization studies including antibody conjugation to the liposomes, *in vitro* release, as well as size analysis and zeta potential measurements. DSPC was used in the formulation because it is phospholipid with saturated fatty acids and melting point about 55^{o}C. This is higher than normal body's temperature of 37°C. We could expect the formulation containing DSPC to be at the gel phase at 37°C and maintain their rigidity and in turn their retention of the encapsulated materials. In addition, the saturated lipids can also prevent the dissociation of the liposomal membrane by plasma proteins [195, 196]. Addition of cholesterol to the liposome formulations was shown to decrease the loading of hydrophobic drugs such as paclitaxel [197] and CLX [177]. However, all the formulations were supplemented with a low amount of cholesterol at 10 mol% of the total phospholipid, which can have an optimum advantage in the encapsulation and retention of CLX [177]. In fact, the cholesterol was provided in order to increase the compactness of the bilayer and minimize drug leakage [198].

In the first part of the study, we characterized both ILs and LUVs in terms of encapsulation and loading of celecoxib **(Table 3.1)**. The encapsulation efficiency was determined as ratio between the amount of CLX present in the liposome formulation

after filter sterilization and the CLX added in the lipid film. On the other hand, the drug loading is the ratio between the mole number of CLX and mole number of DSPC in the final product. The drug loading was used to determine the efficiency of liposomes preparation independent of the formulations. In other words, it is the real measurement of drug entrapment efficiency of a given liposome formulation since its values is independent of the lipid recovery of liposome preparation.

Initial studies were carried out to optimize the CLX content in order to generate ILs with high stability, less prone to vesicle aggregation, and high encapsulation efficiency. For the optimization, the CLX was added to the lipid film in a range of 3-22 mol % of the total liposome constituents. It was seen that 7 mol% of CLX was the most optimized formulation for the ILs containing CLX (data not shown). Inclusion of more than 7 mol% of CLX in the liposomal formulation resulted in significant aggregation of the vesicles, while at 7 mol% of CLX no significant aggregates were observed. Decreasing the CLX content further in the formulation resulted in lower drug loading compared to the formulation with 7 mol% of CLX. Therefore, 7 mol% of CLX in the IL and LUV formulations were used for further studies.

The LUVs had an encapsulation efficiency of 55%, on the other hand, isotype specific IgG immunoliposomes and EGFR-targeted immunoliposomes had encapsulation efficiencies of 46.5% and 43.9%, respectively (**Table 3.1**). The drug loading was similar in both the ILs prepared with non-specific IgGs and anti-EGFR mAbs. On the other hand, the LUVs had higher drug loading compared to the ILs. The lower encapsulation efficiency of ILs compared to the LUVs could be related to the longer preparations step of ILs (eg. conjugation of antibody) compared to those of LUVs, therefore, it was more likely to lose the drug during the ILs preparation steps. At the end of conjugation reaction minimum aggregation of the liposomes was observed, to some extent, it might also be correlated with the lower encapsulation efficiency of the ILs compared to the non-ILs. However, the encapsulations efficiency of the liposomes is sufficient to reach the in-vitro IC_{50} of CLX in different cancer cell lines. The lower percentage of encapsulation of CLX in ILs is also reflected by the lower drug loading in the ILs compared to the drug loading of LUVs. Therefore, we suggest that the lower encapsulation efficiency of the ILs was related to the release of

the drug from the liposomes during the antibody conjugation and it was not related with the difference in the lipid recovery at the end of the liposome preparations.

Table 3.1 Encapsulation efficiency and drug loading of ILs and LUVs.

Liposome formulations (n≥3)	EE (%)	Drug Loading (mol/mol)
LUVs	55.0 ± 2.6	7.70 ± 2.19
IgG-ILs	46.5± 0.56 *	5.48± 0.21
EGFR-ILs	43.9 ± 3.3 *	5.00 ± 1.35

Values denote Mean ± S.D.

Results analyzed by One-way ANOVA, Tukey's Multiple Comparison Test.

* $P< 0.05$ compared to LUVs.

Several studies have reported the encapsulation efficiency of liposomes containing CLX. For example, Perumal et al. reported 46% encapsulation efficiency of CLX in unilamellar liposomes composed of DSPC only prepared by sonication [189]. The reported value was smaller than our observed value of CLX encapsulation efficiency in LUVs. This could have resulted from the absence of cholesterol in the formulation that might decrease the stability of liposomes to maintain the encapsulated materials as well as the sonication method that the authors used. In another study, anti-VCAM-1-Fab'-immunoliposomes containing 1,2-dimyristoyl-sn-glycero-3-phosphocholine (DMPC), cholesterol, and 1,2-dipalmitoyl-sn-glycero-3-phosphoethanolamine-N-(glutaryl) (glutaryl-N-PE) for the targeted delivery of CLX prepared by sonication was reported to have 308 ± 34 μg/mL of CLX in the non-targeted liposomes and 281.1 ± 29 μg/mL of CLX in the ILs [192]. These values correspond to 3.00% and 2.73% of drug loading, respectively [192]. The lower reported drug loading could be related to the difference in the method of liposome preparation and the inclusion of DMPC that has a phase transition temperature at room

temperature. In a related study by Ju et al., non-targeted CLX liposomes and PTDHIV-1 peptide-targeted-CLX liposomes composed of egg phosphatidylcholine (EPC), cholesterol, DSPE-PEG2000, and 2.6 mol% of CLX was prepared by sonication and subsequent extrusion methods [190]. The reported encapsulation efficiency of CLX for non-targeted liposomes and targeted liposomes were 91.18 ± 1.18 and 83.47 ± 0.72, respectively. The higher encapsulation efficiency could be related to the lower amount of initial CLX that they used in the liposome formulations. Our liposomes formulation was started with 7 mol% of CLX in the lipids film and resulted with a final encapsulation efficiency of 40% to 55%. Therefore, the CLX concentration in the final liposome product described in this study is comparable to the values reported by Ju et al.

3.1.2 Antibody Conjugation to LUVs

Antibody is widely used as a targeting ligand for active delivery of nanoparticles, including liposomes, to the tumor cells / tissues. In the field of cancer targeted drug delivery, EGFR is an interesting antigen target for ligand-targeted liposomes, particularly, because of their overexpression in a wide range of cancers including head and neck, breast, renal, non-small cell lung, colon, ovarian, glioma, pancreatic, and bladder cancers [18]. In an attempt to develop anti-EGFR-immunoliposomes containing CLX, antibody conjugation to the functionalized LUVs was carried out. LUVs were functionalized with the DSPE-PEG (2000) Maleimide by anchoring it within the LUVs membrane during its formation and before the conjugation reactions were performed. Like other components of the liposomes such as phospholipids, cholesterol, celecoxib, and DSPE-PEG (2000), simply, maleimide was incorporated in the lipid films as 1 mol% of the total phospholipids. At pH 6.8-7.5, Maleimide reacts with sulfidryl group in proteins or peptide to form a covalent and stable thioether bond [184]. The reactions at these pH range is specific for thiols rather than amine group [199], therefore, allowing the site specific conjugation between the reduced IgG and maleimide functionalized PEG-DSPE molecules.

For the optimization of immunoliposomes preparation, to make the experiments more cost effective, non-specific mouse IgG was used in place of anti-EGFR monoclonal antibody (cetuximab). As the conjugation reaction involved the presence of thiol group in the protein, a free thiol group was introduced to IgG by reducing selectively the hinge region of IgG with mild reducing agent, 2-MEA, to form 2 equal half IgGs each with an antigen binding site [200]. Conjugation at the hinge region is favorable particularly because it orients the ligand binding site of antibody in a proper way, thus, preserving their binding to the antigens [199]. For the optimization, 200 μg of mouse IgG was reduced with different concentrations of MEA ranging from 25 to 100 mM for 90 minutes. The reactions were also carried in the presence of EDTA, as it was important to prevent metal catalyzed oxidation of the sulfhydryl groups [199]. Moreover, a 63-90 % loss in sulfhydryl group was also reported after 40 hours life-span of reduced IgG in the absence of EDTA [201].

The resulting IgG fragments from the reactions were then separated with SDS-PAGE and the protein bands were visualized with Coomassie Blue staining (**Figure 3.1A**). As a positive control, intact IgG was fully reduced with 2-mercaptoethanol and boiled in order to generate heavy and light chains of the antibody. The band of about 150 kDa in size indicated the intact IgG and the 25 kDa and 55 kDa bands in bottom of the gel indicated the presence of light and heavy chains of IgG, respectively. It seems that the reduction of IgG with 25 mM of 2-MEA was enough to generate half-IgG, however, there was still large portion of the un-reduced IgG. The large portion of half-IgG as the reduction product was clearly observed at 75 mM of MEA and further increase in the concentration of the reducing agent did not significantly improve the half-IgG yield. Apart from that, in all conditions the reduction also proceeded outside the hinge region of IgG as it can be inferred from the generation of other antibody fragments instead of half-IgG and this could have been resulted from a partial reduction of disulfide bonds in the heavy and light chains due to a prolonged exposure of the antibodies to 2-MEA [145]. However, these non-specific fragments are minimal, therefore it was assumed that this product would not affect the subsequent conjugation reaction involving the reduced IgG products.

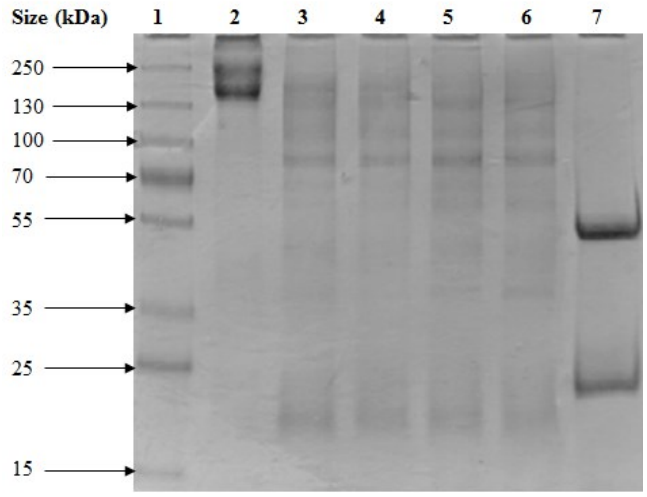

A

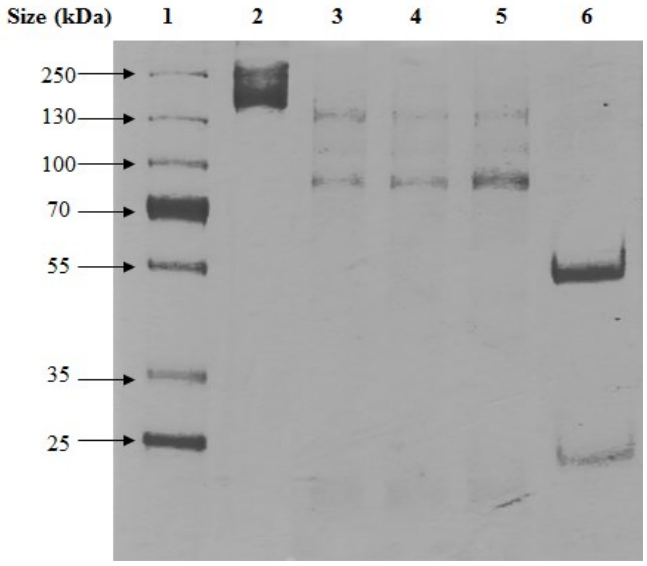

B

Figure 3.1 SDS-PAGE analysis of reduced IgG molecules at different concentrations of 2-MEA (A) and at different reduction durations (B).

For A, Lanes : 1. Marker; 2. Unreduced IgG; 3-6. 25 – 100 mM of 2-MEA; 7. IgG reduced with β-ME and boiled (+C).

For B, Lanes: 1. Marker ; 2. Unreduced IgG; 3. 30 min reduced IgG; 4. 60 min reduced IgG; 5. 90 min reduced IgG; 6. IgG reduced with β-ME and boiled (+C).

The duration of reduction reaction was also optimized by varying the reduction time between 30-90 minutes at 75 mM concentration of 2-MEA (**Figure 3.1B**). Half-IgG was generated in the first 30 minutes of the reaction, however, half-IgG as the major product was detected at 90 minutes of the reaction. Therefore, for further experiments involving anti-EGFR immunoliposomes, the reaction conditions for reducing IgG was 75 mM of 2-MEA for 90 minutes.

After the IgG was reduced, the generated product was purified from the remaining reducing agent by passing the reaction product through Zeba desalting column. This ensured that the reducing agent would not interfere with the subsequent conjugation reaction of reduced IgG and maleimide functionalized liposomes. For the conjugation reaction, 200 μg of the reduced IgG was mixed with 10 mM of preformed-liposomes containing maleimide and the reaction was allowed to proceed overnight at 4^{o}C. The reaction between sulfhydryl group and maleimide can proceed at room temperature as well as at 4^{o}C with prolonged duration [199]. The lower temperature was chosen because it could minimize the CLX release from the liposomes to the medium during the conjugation reaction. In order to achieve maximum systemic targeting effect, immunoliposomes must have efficient loading and retention of the anticancer drug [167]. At the end of conjugation reaction, the excess maleimide was quenched with 2-mercaptoethanol in order to prevent cross-reaction between liposomes that may lead to immunoliposome aggregation, fusion, and leakage of celecoxib. To separate the immunoliposomes from the unconjugated antibody fragments, lipids and any leaked celecoxib, the mixture was passed through an ultrafiltration column with a MWCO of 300 kDa. The immunoliposomes, being larger, were not filtered and retained above the ultrafiltration membrane, whereas all other materials smaller than 300 kDa were filtered out.

The conjugation efficiency of antibody to the surface of liposomes was measured indirectly by determining the concentration of unconjugated antibody obtained from the ultrafiltration filtrate. The protein amount in the filtrate was measured by Bradford assay and the initial protein amount was assumed to be the same as that at the beginning of the reduction reaction (200 μg). The conjugation efficiencies of non-specific IgG ILs and anti-EGFR ILs are represented in the **Table 3.2.** In order

to understand the effect of CLX on the conjugation efficiency of immunoliposomes, the conjugation of non-specific IgG on LUVs without CLX (Empty-ILs) is also provided.

Table 3.2 Conjugation efficiency of immunoliposomes containing CLX.

Formulations (n ≥ 3)	**Conjugation Efficiency (%)**
IgG-IL	40.1 ± 4.40 *
EGFR-IL	34.0 ± 7.00 **
Empty-IL	54.0 ± 0.02

Values denote Mean ± S.D.

Results analyzed by One-way ANOVA, Tukey's Multiple Comparison Test.

* $P< 0.05$ compared to Empty-IL, ** $P<0.01$ with respect to Empty-IL.

Accordingly, the conjugation efficiency of antibodies to the surface of maleimide functionalized LUVs was about 40%. The coupling yield is relatively higher than that reported by Huwyler & Pardridge, where the liposomes functionalized with maleimide group was conjugated with OX26 MAb [202]. The difference might be related to the targeting ligand that they used for conjugation to the liposomes. The whole antibody might generate more steric repulsion to the liposomes surface grafted with PEG, therefore, at molecular level, less antibody was available for the reaction with maleimide group, which in turn led to the decrease in the conjugation efficiency. Immunoliposomes with 40% coupling efficiency will have about 6 half-IgG per vesicle. Although the number of antibody per liposome is fewer than those are reported for optimum internalization of anti-HER2 immunoliposomes [166], the same, publication also reported that 6 Fab′/liposome was sufficient to endocytose 55-60% of the cell-associated anti-HER2 immunoliposomes into HER2-overexpressing cells. The difference in the ligand density /vesicles to some extent was related to the initial amount of antibody used for the reaction. In our case, we used 100 µg/mL of whole

antibodies as a starting amount, on the other hand, the anti HER-2 immunoliposomes were prepared with 300 µg/mL of Fab' fragments.

As expected, since anti-EGFR mAb are also IgG molecules, the conjugation efficiency values were similar in both IgG-IL and anti-EGFR-ILs. The conjugation efficiency of empty immunoliposomes is significantly higher than the celecoxib-containing ones ($P< 0.05$). Therefore, the presence of CLX in the liposomal membrane might affect the efficiency of the coupling reaction. It was reported that CLX reduced the fluidity of model membranes containing DSPC and cholesterol [193]. Regarding this observation, the mobility of maleimide functionalized DSPE-PEG in the liposome bilayer might be restricted in the presence of CLX in the membrane, thus, it became less likely for it to collide and react with half-IgG containing thiol groups.

3.1.3 Particles size distribution and zeta potential analysis

3.1.3.1 Particles Size Distribution

Zetasizer measures the particles size based on the Dynamic Light Scattering (DLS) methods. DLS method measures the Brownian motion of the particles and then will correlate the velocities with their size based on the Stokes-Einstein equation. To do that, laser is applied to the particles, the change in intensity of the scattering pattern is then analyzed within very small time scales, and the intensity fluctuation is correlated with the size of particles. Therefore, as a general rule, small particles move faster and the intensity fluctuations occur rapidly. On the contrary, large particles move slower and the intensity fluctuations occur slowly.

Here, the particle size of liposomes was measured as the Z-average size. The Z-average size is the most important and reproducible number generated by Dynamic Light Scattering (DLS) technique. Particularly, the value can be used for comparing the size of particles from batch to batch as long as the dispersion medium of the particles is the same. In addition, the Z-average is calculated from the mean of signal intensity instead of a mass or number mean. The distribution of the particle population size is represented by the poly-dispersity index (PdI) [203]. It reflects the homogeneity of the particles' sizes in suspension. Liposomes populations with PdI values <0.2 are

said to be homogenous, on the other hand, the ones with PdI >0.3 are said to be heterogeneous [204]. Previously, it was described that preparation of liposomes by extrusion through polycarbonate membrane with a particular size could generate liposome suspensions with defined size distributions [205]. Our research group's finding also showed that LUVs containing CLX could be generated by extruding the MLVs suspension through polycarbonate membrane with 100 nm of pores in size [178]. The mean particle sizes of the LUVs and ILs are shown in **Figure 3.2 and 3.4** and **Table 3.3**

Accordingly, the mean particles size of LUVs containing CLX was about 120 nm **(Figure 3.2** and **Table 3.3).** ILs have a slight increase in the size, which is about 5 nm, irrespective of the CLX content compared to LUVs (**Figure 3.3 and Figure 3.4** and **Table 3.3**) and this can be attributed to the surface decoration of maleimide functionalized with thiol-containing half-IgGs. Although, the conjugation efficiency of empty ILs is higher than the CLX-loaded ILs, their size was similar. This could be explained by the difference in the conjugation efficiency that corresponded to only 1-2 half-IgG/ vesicles difference between empty ILs and CLX-loaded ILs. In all formulations, the PdI values were smaller than 0.2, indicating a homogenous vesicles population (**Table 3.3**)

The passive accumulation of the immunoliposomes in the tumor site is a prerequisite for the antibody fragments on the ILs to bind to receptors on the target cells and get internalized. Large fenestrations and poor lymphatic drainage in the pathological site, including the tumor site, allows liposomes and other nanoparticles up to 200 nm in size to penetrate and accumulate in the tumor interstitium, on the other hand, healthy vasculature only allow particles less than <1–2 nm in size to penetrate [206, 207]. Therefore, nanoparticle-based drug delivery systems with diameters in between 10–200 nm was shown to improve the efficacy and systemic toxicity profile of the therapeutic drugs [148, 208, 209].

Table 3. 3 Particle size distribution and zeta potential of liposome formulations.

Formulations (n ≥ 3)	Z_{ave} (d.nm)	Polydispersity index (PdI)	Zeta Potentials (mV)
ILs	124.3 ± 1.26	0.064 ± 0.019	-2.97 ± 1.41
Empty ILs	124.7 ± 0.14	0.058 ± 0.028	-3.06 ± 1.30
LUVs	120.0 ± 1.80	0.055 ± 0.014	-1.87 ± 0.71

Values denote Mean ± S.D.

Z_{avg}: Average hydrodynamic diameter of particles. PdI: Polydispersity Index.

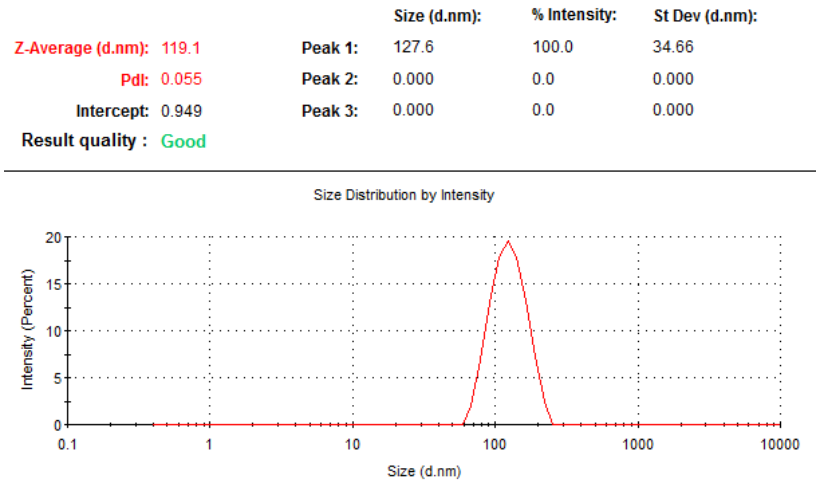

Figure 3.2 Representative image for particle size distribution of CLX-loaded LUVs.

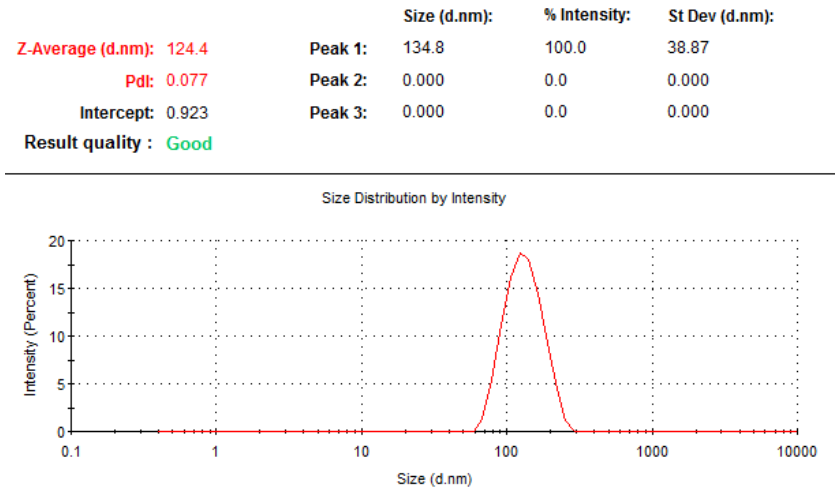

Figure 3.3 Representative image for particle size distribution of empty-ILs

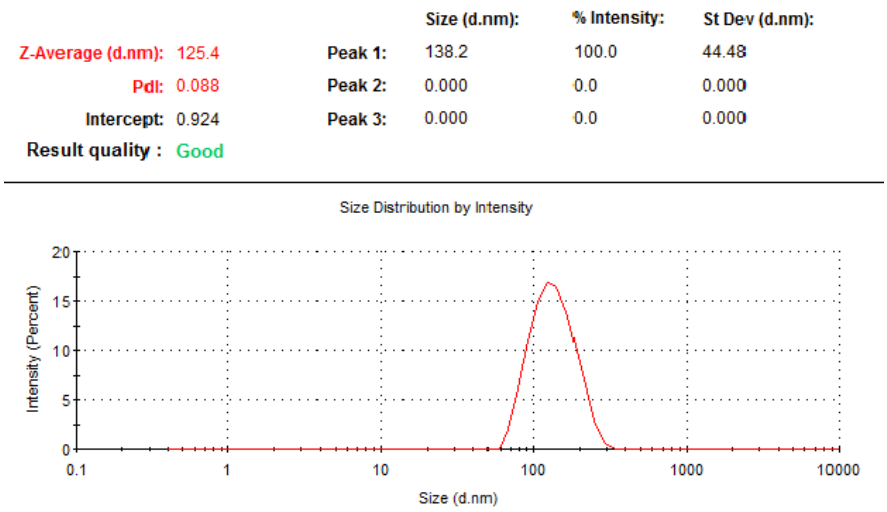

Figure 3.4 Representative image for particle size distribution of CLX-loaded ILs.

The size of liposomes is not only important for their preferential accumulation in the tumor site but also contributes to their shelf-life and clearance from the blood circulation. Particles with size less than 5.5 nm clears from the circulation by renal filtration [210]. Minimal liver uptake was observed in liposomes with 100 nm in size compared to particles smaller than 50 nm and larger than 300 nm, in fact, clearance by

the spleen was seen in particles larger than 400 nm [211]. Therefore, in general, optimum particles size in order to exploit the EPR effect optimally and minimize clearance was determined to be close to 100 nm [212].

The CLX-containing ILs with a diameter 125 nm, in term of the size, matched with the desirable nano-drug formulation properties. Thus, a selective passive accumulation of the CLX-loaded ILs in the tumor site and minimal clearance from the circulation could be expected.

3.1.3.2 Zeta Potentials

The potential at the slipping plane between the particle surface and the dispersing liquid is called the zeta potential. Simply, it is the net charge on the surface of particles. Zeta potential determines the ionic stability of colloidal particles in the dispersing medium. Particles with very positive or very negative zeta potentials tend to be more stable in suspension. On the other hand, particles with zeta potential close to zero tend to come together and flocculate. Since pH affects the degree of ionization of particles, the value of zeta potential is specific for a particular pH. Zeta potential is measured by using Laser Doppler Electrophoresis technique. The method is able to measure the velocity of particles in a liquid when an electrical field is applied. Velocity of particles, the applied electric field, viscosity and dielectric constant of the samples are correlated with **Henry equation** to determine the zeta potential.

It was seen that the zeta potentials of the immunoliposomes, and non-immunoliposomes were not significantly different **(Table 3.3)**. As can be inferred from the zeta potential of empty ILs and CLX-loaded ILs, CLX appeared not to affect the zeta potential of the immunoliposomes. The different components of LUVs and ILs including DSPC, Chol, PEG, are also neutral at physiological pH, therefore, zeta potentials that are close to zero (neutral) were expected in all liposomes formulations. Although the low zeta potential in the liposome formulations indicate the colloidal instability, surface modification of liposomes with hydrophilic polymer such as PEG may improve its steric stability. The immunoliposomes containing CLX was formulated to include 3.5 mol% of PEG. Therefore, it could provide steric stabilization

of the liposomes in suspension. In fact, surface PEGylation of nanoparticles is known to prevent the nanoparticles aggregation and minimize non-specific interactions [213]. Moreover, steric protection by PEG prevents the adsorption of opsonins and other serum protein that are involved in the clearance of nanoparticles thereby helping the nanoparticles to remain in blood circulation for extended periods [161].

Maintaining relatively neutral surface charge of the liposomes is also beneficial for improving their pharmacokinetics and biodistribution. Negatively charged particles with zeta potential ≤ -10 mV can be significantly taken up by reticuloendothelial system (RES), positively charged particles with zeta potential greater than 10 mV may induce serum protein aggregation; on the other hand, neutral nanoparticles with zeta potential between + 10 and – 10 mV generally show minimum RES uptake and prolonged shelf-life in the circulation [212]. In addition, liposomes with a nearly neutral charge (−2 to −5mV) were shown to penetrate the tumor tissue 14 times faster than the positively charged liposomes (+48 mV) [214].

3.1.4 *In vitro* Release Studies of CLX from ILs

Optimum drug delivery formulations should have high entrapment efficiency and controlled release profiles of the therapeutic drugs. The capability of nanoparticles to maintain high retention of the encapsulated materials and prevent the rapid leakage of the drug in the blood circulation is necessary in order to have an optimum dose of the drug in the tumor sites. Therefore, the physicochemical properties of the drug carrier need to be tailored carefully to achieve maximum benefit from the nano drug delivery systems.

A lipophilic drug like CLX is favourably incorporated within the liposomal membrane. Therefore, the composition of the constituents of the liposomal membrane will greatly influence the encapsulation and retention of CLX within the membrane. It was proposed that in the presence of cholesterol, CLX was confined to the inner core of the hydrocarbon tails of the phospholipids and this may contribute to the slower release of the CLX from the liposomes containing cholesterol [177]. It has also been stated in **Section 3.1.1** that saturated phospholipid was incorporated in the liposomal formulation of CLX as they can minimize the drug leakage and increase the stability of the liposomes. In addition, PEGylation of both LUVs and the ILs may also involve

in slowing down the release of the drugs from the liposomes. Several studies have shown experimentally that PEGylated liposomes had a slower drug release profile compared to the conventional liposomes [215–217].

The *in vitro* release profile of CLX from the ILs using IgG-IL and non-targeted LUV was studied at 37^{o}C in PBS (pH 7.4) for 72h, under mild agitation in order to mimic the body's physiological condition **(Figure 3.5)**. Lipophilic drugs within the liposomes bilayer as well as natural membrane components may transfer to another lipid domain (e.g from the donor liposomes to the acceptor liposomes) through 2 mechanisms: direct transfer to the acceptor membrane with minimal exposure to aqueous phase upon the collision of the liposomes or diffusion through the aqueous phase [218, 219]. Therefore, under the *in vitro* conditions within the context of this study, if the CLX released from the liposomes were not transferred to another liposome it might simply diffuse to the surrounding aqueous medium or bind to the dialysis membrane. Overall, both the ILs and the LUVs showed a sustained release profile for up to 72 h. There was no significant difference in the release of CLX from the LUVs and the ILs for each time point used in this study (P> 0.05). This indicated that the decoration of antibody on the surface of ILs did not change the membrane integrity of the liposomes. Within the first 10 hours, only 13.6% of the CLX was released from the LUVs whereas 19.2% of the drug was released from the ILs. The release rate of CLX from both formulations was decreased after 10 hours and it reached a plateau at 24 hours of incubation. At 72 hours of incubation, most of the drug was retained within the liposomes and only 27% and 23% of the drug was released from the ILs and LUVs, respectively. The ability of the ILs to maintain relatively high retention of CLX (>70%) suggests that the ILs were a suitable platform for the delivery of the drugs. The high retention of the CLX for 72 hours within the ILs will also allow the liposomes to deliver effective dose of CLX with enough time to the tumor site by exploring the EPR effect. In addition, the targeted ILs with slow release characteristics should have higher therapeutic efficacy since their uptake mechanism is facilitated by receptor mediated endocytosis, therefore, with a high retention of the encapsulated drugs more drug payloads are delivered to a given target cell.

Since the IgG-ILs showed a high stability, high encapsulation efficiency of CLX, and slow release profile of the drug, after these optimization studies, the EGFR-targeted immunoliposomes of CLX, by including anti-EGFR mAbs instead of non-specific mouse IgG, were prepared using the same protocols.

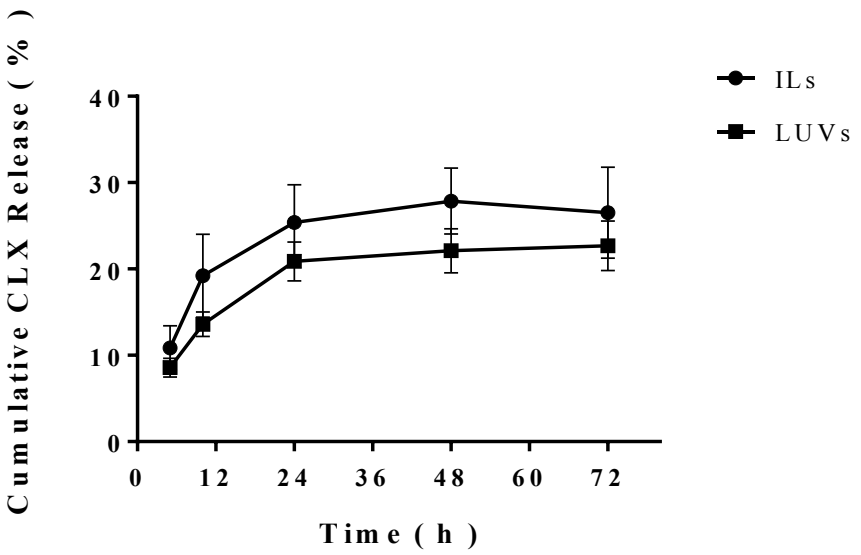

Figure 3.5 *In vitro* CLX release from IgG-ILs and LUVs in PBS at 37°C. Values denote Mean ± S.D., n≥3.

3.2 Cell Association of Immunoliposomes

Immunoliposomes are designed to improve the cellular uptake liposomes as well as their selectivity toward the target. Employing anti-EGFR mAb as a targeting ligand of the liposomes is promising strategy to combat tumors with high level expression of EGFR. Fortunately, EGFR is expressed in wide variety of tumors. Therefore, the application of EGFR-targeted immunoliposomes as delivery vesicles is more diverse as it can be encapsulated with different types of anticancer drugs to target many types of cancers. In our study, the functionality of EGFR-targeted ILs containing CLX to target multiple cancer cell lines with varying expression of EGFR was quantitatively evaluated with Flow Cytometry.

Three different cell lines, including MDA-MB-468, HCT-116, and SW-620 were used to measure the cellular internalization of the ILs. The EGFR expression of these cell lines as well as HT-29 cells were evaluated by using western blotting analysis **(Figure 3.6)**. From the western blotting analysis, MDA-MB-468 cell line was highly expressing EGFR. On the other hand, HCT 116 and SW-620 cell lines expressed moderate to low and low level of EGFR, respectively. These findings were also supported by work of other research group [218, 219] .

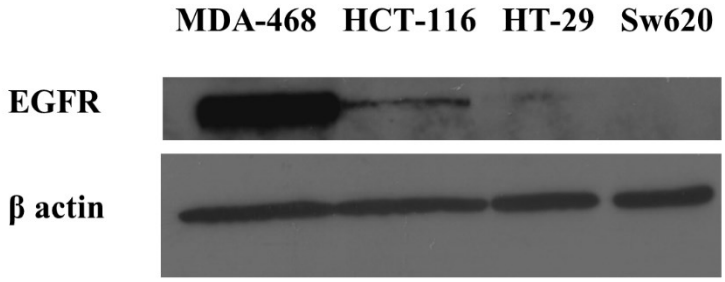

Figure 3.6 Western blot analysis of the expression of EGFR in MDA-MB-468, HCT-116, HT-29, and SW-620 cell lines.

3.2.1 Fluorescence Activated Cell Sorting Analysis (FACS)

For the flow cytometry analysis, LUVs and immunoliposomes were labeled with SP-DiOC18(3), a sulfonated carbocyanine tracer. The labeling of liposomes with the dye appeared to be compatible with aldehyde fixation and show persistent retention of the dye. In the lipid environment, lipophilic carbocyanines have high extinction coefficients and moderate fluorescence quantum yields. SP-DiIC18(3) and SP-DiOC18(3) generate more fluorescent quantum yields than DiI and DiO [222]. The dyes are also highly fluorescent and photostable in the membranes, but weakly fluorescent in water [223].

The extent of cellular internalization of the EGFR-targeted ILs and non-targeted LUVs were evaluated in MDA-MB-468, HCT-116 and SW-620 cells for 2 hours and 4 hours of treatment both at 4^{o}C and 37^{o}C. The signal detected after incubation at 4°C was assumed to be originated from liposomes bound to surface of

the cells, since active endocytosis was inhibited at low temperature. On the other hand, after the incubation at 37°C, the signal was assumed to be originated from both bound and internalized liposomes [187]. Before the treatment, the liposomes were purified from the un-incorporated dyes, filter sterilized, and their lipid content was measured. This ensured that fluorescence –associated signal was coming from the liposomes, not from the unincorporated dyes. For the treatment, the dose of liposomes used was adjusted according to phospholipid concentration.

Dot plots and single parameter histograms associated with FL1-H signal from labeled-liposomes in each cell line are shown in the **Figure 3.7 and Figure 3.9**. In the MDA-MB-468 cell population (**Figure 3.7**), a greater fraction of cells internalized the anti-EGFR ILs compared to the non-targeted LUVs after 2 hours (53.4% vs 15.2%) and 4 hours (70.6% vs 17.9 %) incubation with the liposomes. On the other hand, there was no significant difference in the fraction of cells that internalized ILs compared to non-targeted liposomes, even after 4 hours incubation with the liposomes, in HCT 116 cells (40.5% vs 47.7%) (**Figure 3.8**) and SW-620 cells (28.9% vs 21.7%) (**Figure 3.9**). The single parameter histogram also confirmed the dot plot result where the histogram of cell populations treated with ILs was shifted more to the right compared to the ones treated with the non-targeted LUVs in MDA-MB-468 cells but not in HCT-116 and SW-620 (**Figure 3.10**). In all cell lines, the liposomes' uptake by the cell in populations, for both ILs and LUVs, happened in a time dependent manner with the cell populations internalizing liposomes more at longer incubation times. The internalization of ILs in all the cell lines was also abrogated at 4^{o}C, the histogram of cells incubated with ILs at 4^{o}C overlapped with those of control cells indicating that the fluorescence signal originating from the surface-bound liposomes was much lower compared to the signal obtained from the cells incubated at 37^{o}C. In the other words, at 37^{o}C most of FL1-H associated signal originated from the active internalization of liposomes into the cells.

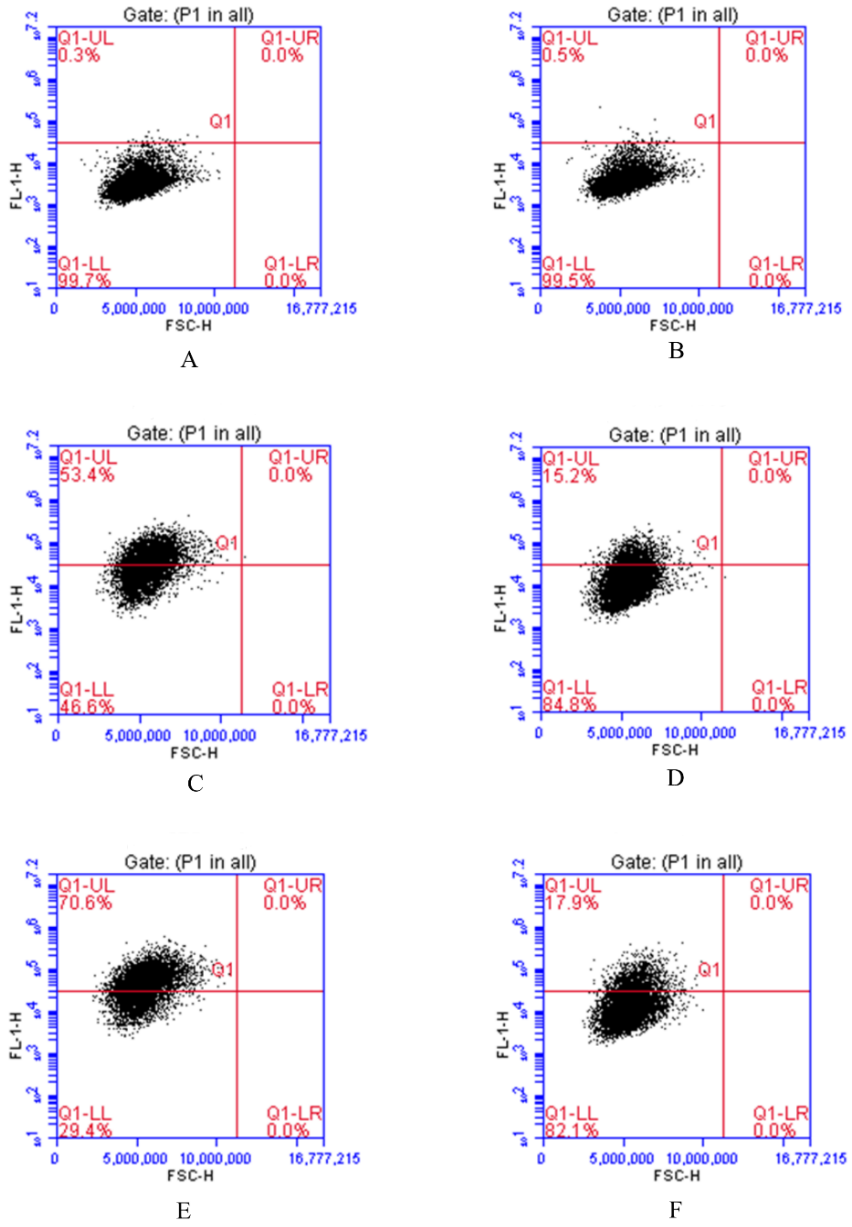

Figure 3.7 Dot plots for MDA-MB-468 cell populations associated with fluorescently labeled liposomes.

Representative images. x-axis: Forward Scatter Height, y-axis: FL1 signal Height. Cells were treated with SP-DiOC18(3)-labeled-EGFR targeted ILs (B, C & E) or Non-targeted LUVs (D & F) either at 4°C (B) or at 37°C (C, D, E, F). The controls cells were not treated with liposomes and incubated at 37°C (A).

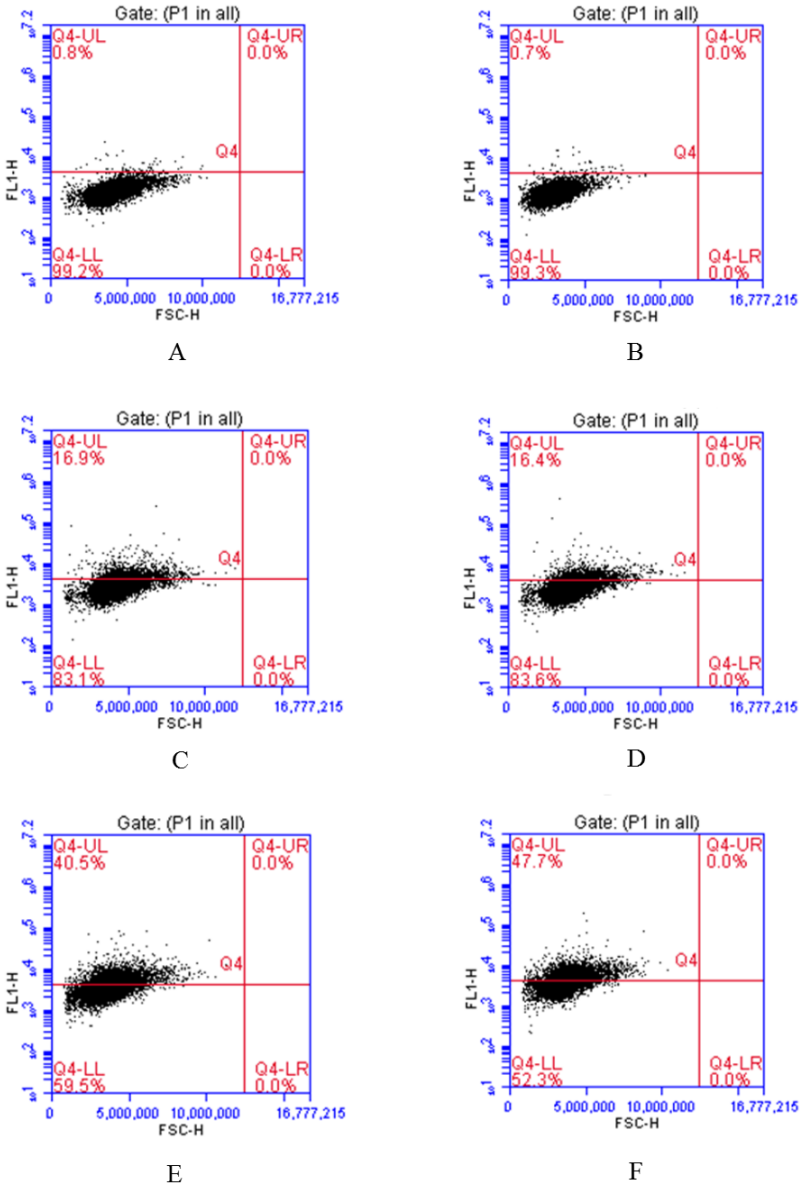

Figure 3.8 Dot plots for HCT-116 cell populations associated with fluorescently labeled liposomes.

Representative images. x-axis: Forward Scatter Height, y-axis: FL1 signal Height. Cells were treated with SP-DiOC18(3)-labeled-EGFR targeted ILs (B, C & E) or Non-targeted LUVs (D & F) either at 4°C (B) or at 37°C (C, D, E, F). The controls cells were not treated with liposomes and incubated at 37°C (A).

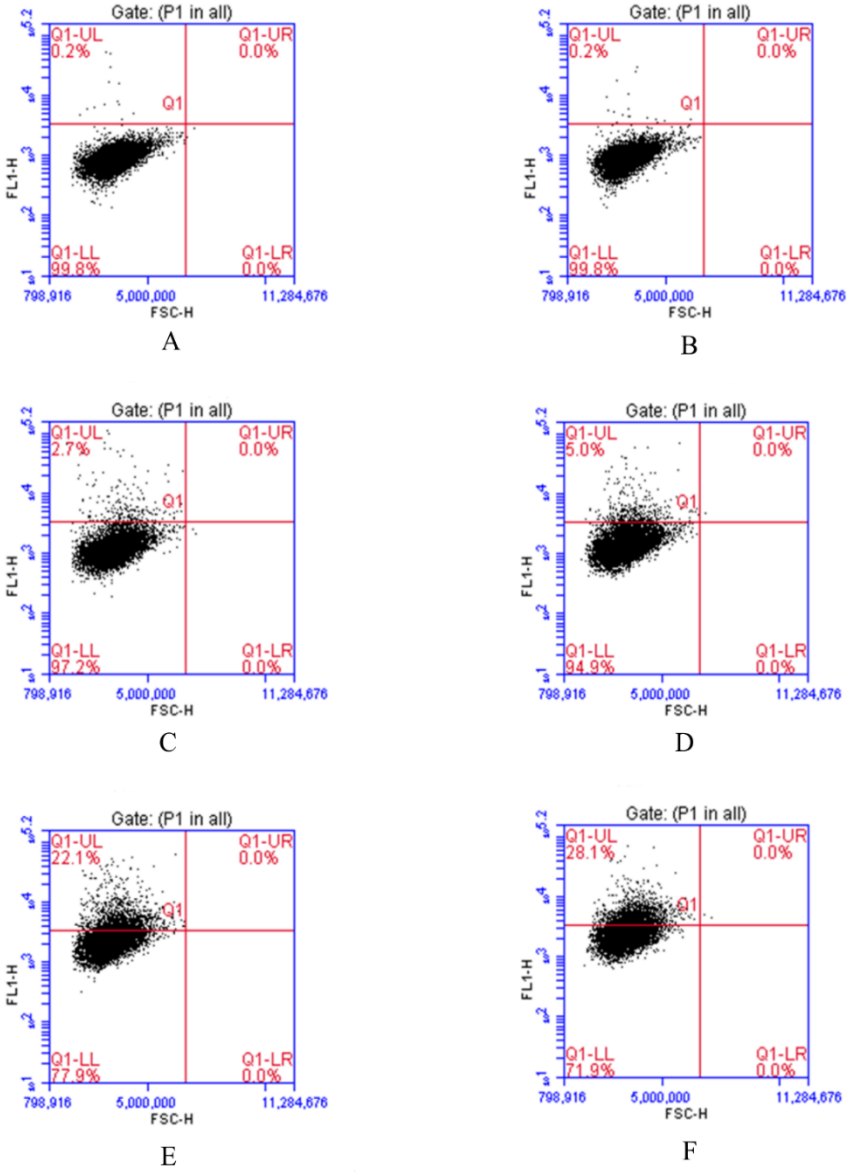

Figure 3.9 Dot plots for SW-620 cell populations associated with fluorescently labeled liposomes.

Representative images. x-axis: Forward Scatter Height, y-axis: FL1 signal Height. Cells were treated with SP-DiOC18(3)-labeled-EGFR targeted ILs (B, C & E) or Non-targeted LUVs (D & F) either at 4ºC (B) or at 37ºC (C, D, E, F). The controls cells were not treated with liposomes and incubated at 37ºC (A).

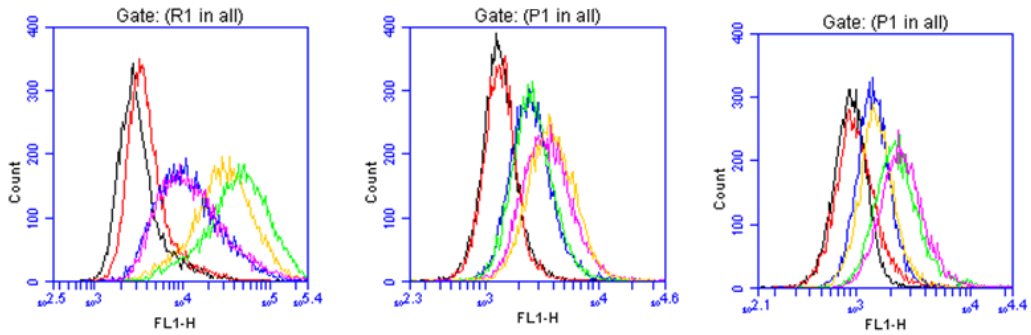

Figure 3.10 Single parameter histograms for cell populations associated with fluorescently labeled liposomes.

For MDA-MB-468 cells (left); black line represents negative control, red line represents treatments with EGFR-targeted ILs at 4°C, blue and purple line represents 2 and 4 hours treatment with non-targeted LUVs at 37°C, respectively, yellow and green line represents 2 and 4 hours treatments with EGFR-targeted ILs at 37°C, respectively.

For HCT-116 cells (middle); black line represents negative control, red line represents treatments with EGFR-targeted ILs at 4°C, green and yellow line represents 2 and 4 hours treatment with non-targeted LUVs at 37°C, respectively, blue and purple line represents 2 and 4 hours treatments with EGFR-targeted ILs at 37°C, respectively.

For SW-620 cells (right); black line represents negative control, red line represents treatments with EGFR-targeted ILs at 4°C , blue and green line represents 2 and 4 hours treatment with non-targeted LUVs at 37°C, respectively, yellow and purple line represents 2 and 4 hours treatments with EGFR-targeted ILs at 37°C, respectively .

3.2.2 Laser Scanning Confocal Microscopy Analysis

The cellular internalization of EGFR-targeted immunoliposomes containing CLX was also visualized with LSCM in MDA-MB-468 and SW-620 cell lines. The extent of cellular internalization was compared for both non-targeted LUVs and EGFR-targeted immunoliposomes for 2 hours and 4 hours incubations with the liposomes at 37^{o}C. Negative control was prepared by incubating the cells with liposome-free medium both for 2 hours and 4 hours treatments. At the end of the treatment, medium-containing liposomes was withdrawn and the cells were washed with PBS in order to remove free liposomes and ensure that the fluorescence signal was mostly originated from the cell associated liposomes. In this study, Rhodamine labeled DHPE was chosen to tag the liposomes because it was stably incorporated in the liposomal membrane and exhibited no lateral diffusion to the plasma membrane [224].

The confocal microscopy study showed that the EGFR-targeted liposomes were more efficiently internalized in the MDA-MB-468 cell populations compared to the non-targeted liposomes (**Figure 3.11**). In MDA-MB-468 cell population, within 2 hours of incubation with the targeted immunoliposomes, a significant portion of the liposomes was present in the cytoplasm and nuclear periphery. On the other hand, non-targeted LUVs showed minimum uptake in the cell lines. At 2 hours of incubation with the liposomes, only a small portion of the liposomes was internalized, even some of the liposomes were still located on the plasma membrane, indicating non-specific binding of liposomes. At 4 hours of incubation, the extent of the cellular internalization for both the immunoliposomes and non-targeted liposomes increased in this cell line, however, more immunoliposomes were internalized compared to the non-targeted liposomes. On the contrary, in SW-620 cell populations, internalization of both immunoliposomes and non-immunoliposomes were minimal at 2 hours and 4 hours of treatment. Therefore, EGFR-targeted immunoliposomes were selectivity internalized in cell lines with a high expression of EGFR (MDA-MB-468) and not in the cell lines with low expression of EGFR (SW-620). As can be seen from the **Figure 3.11**, MDA-MB-468 cells also internalized more non-targeted liposomes at 2 hours and 4 hours

treatment compared to the SW-620 cells. Therefore, to some extent, the internalization of liposomes might also be related with the intrinsic difference between the cell lines.

Selective delivery of CLX with EGRR-targeted ILs to cancer cell lines with varying expression of EGFR was quantitatively evaluated with flow cytometry and qualitatively visualized with LSCM. The extent of internalization of ligand-targeted nanoparticles, including immunoliposomes, is dependent on the density of targeting ligand on the surface of liposomes as well as the density of the target receptor/ antigens on the surface of target cells. MDA-MB-468 cells with high overexpression of EGFR will be suitable target of the immunoliposomes. The flow cytometry and the confocal microscopy results have shown that the EGFR-targeted ILs were internalized more efficiently compared to the non-targeted liposomes in the MDA-MB-468 cells where a high expression of EGFR was observed, but not in the HCT-116 or SW-620 cells in which the EGFR expression is relatively lower. This could be explained by the fact that the MDA-MB-468 cells express 5 x 10^5 EGFR per cell [225], whereas the other cells lines, as can be depicted from the western blot analysis, have much more lower expression of EGFR. Moreover, according to a previous finding, no significant accumulation of EGFR-targeted ILs was observed in MCF-7 cells where the expression of EGFR is low (10^4 receptor/cell) and non-transformed (normal) epithelial cells with EGFR expression up to 10^3-10^4 receptors/cell may be spared from toxicity implicated by the targeted drug delivery [139]. Thus, anti-EGFR-immunoliposomes can provide s an efficient targeted delivery vehicle for CLX in cancer cells with a high level expression of EGFR.

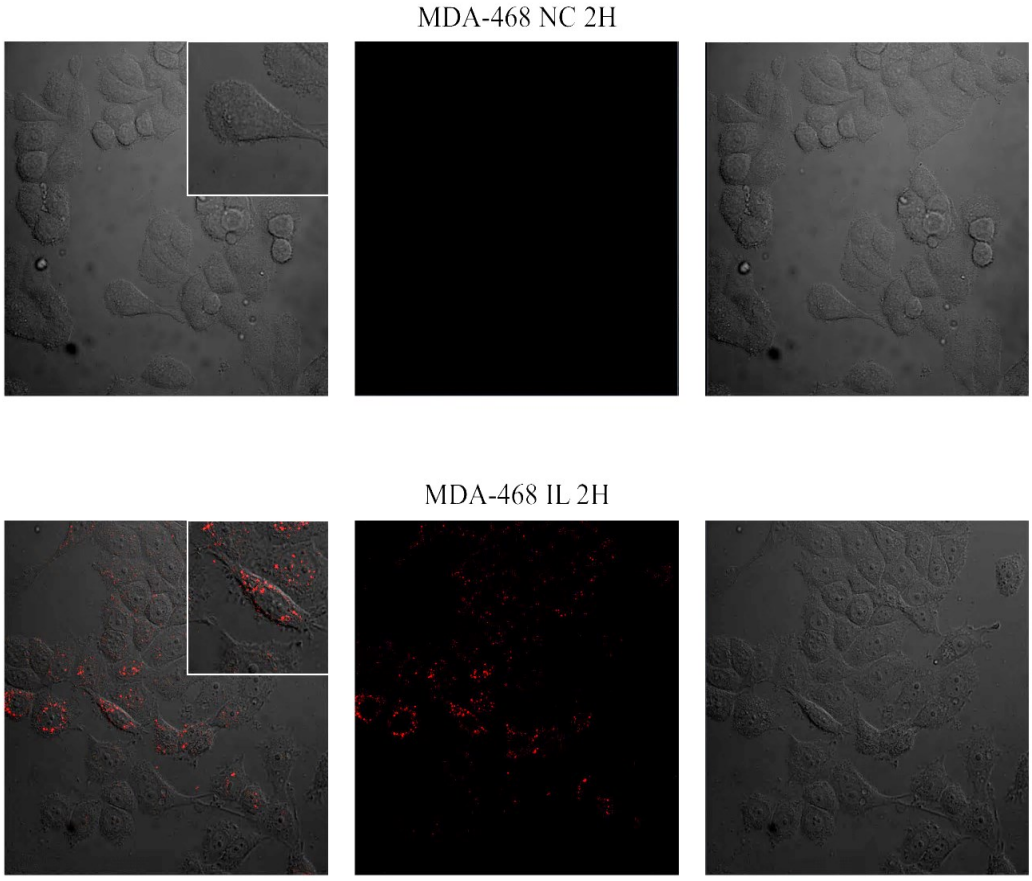

Figure 3.11 LSCM analysis of cell associated Rhodamine labeled anti-EGFR immunoliposomes (IL) or non-targeted LUVs (NT) containing CLX in MDA-MB-468 or SW-620 cells.

The cells were treated with 500 µM liposomes for 2 hours (2 H) and 4 hours (4 H). The images are represented as phase contrast images (right), red channel image (middle) and merged image (right). Untreated cells were used as negative control (NC) and representative images are shown for each cell line. Rhodamine signal was pseudo colored as red, brightness and contrast of the images were adjusted for optimum visualization.

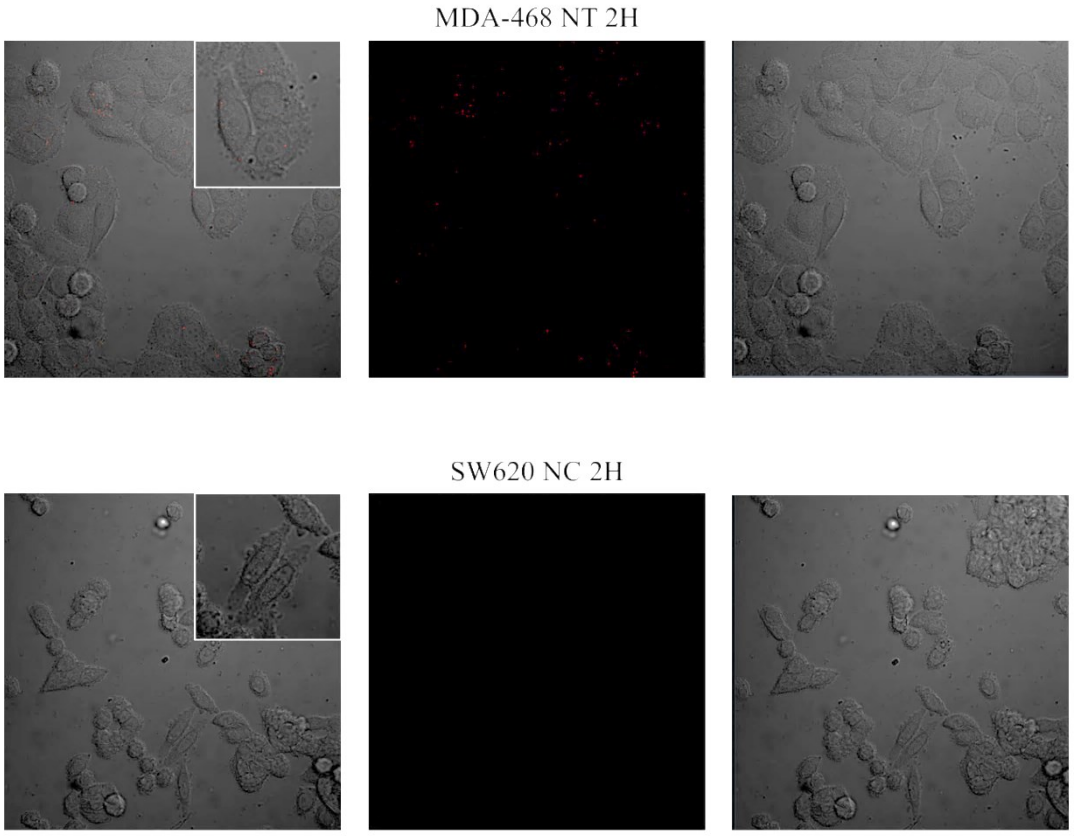

Figure 3.11 continued.

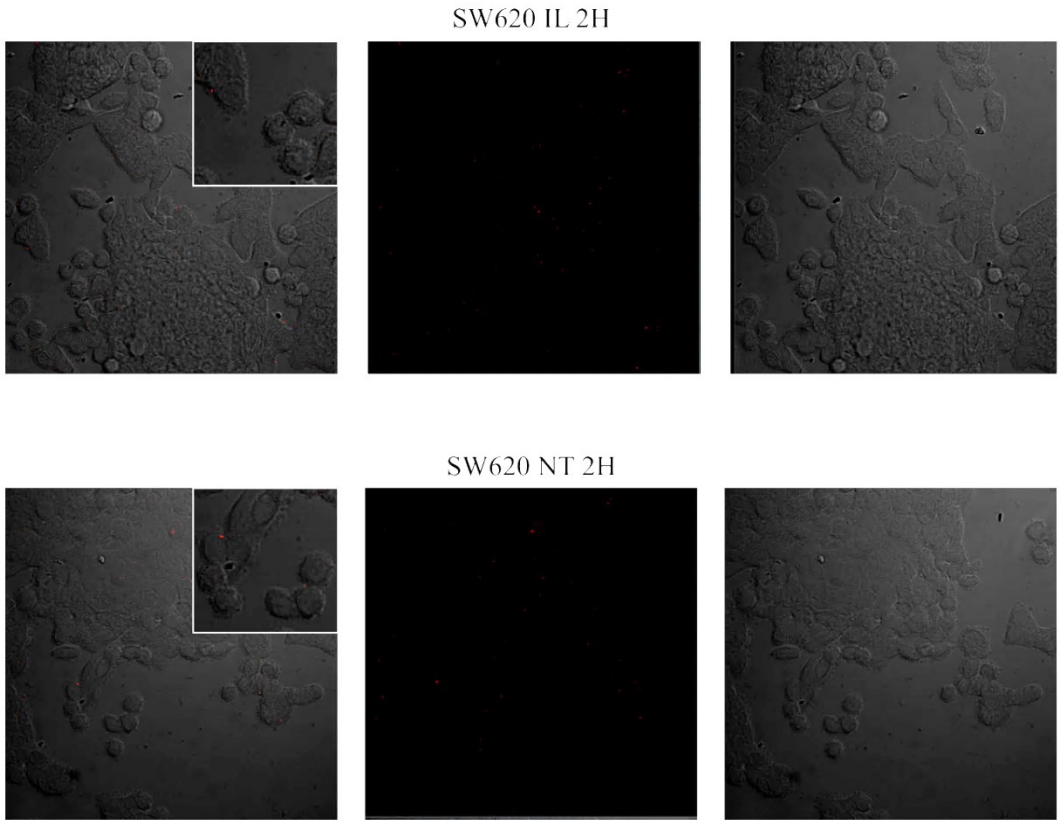

Figure 3.11 continued.

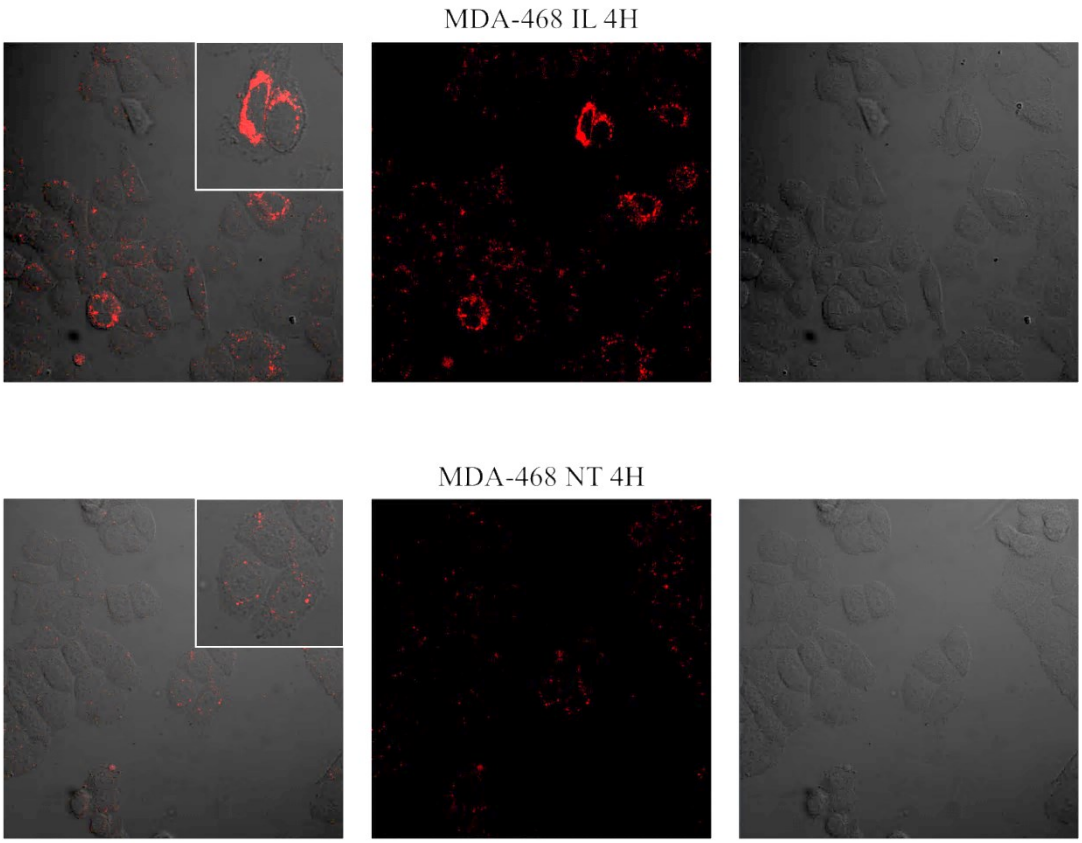

Figure 3.11 continued.

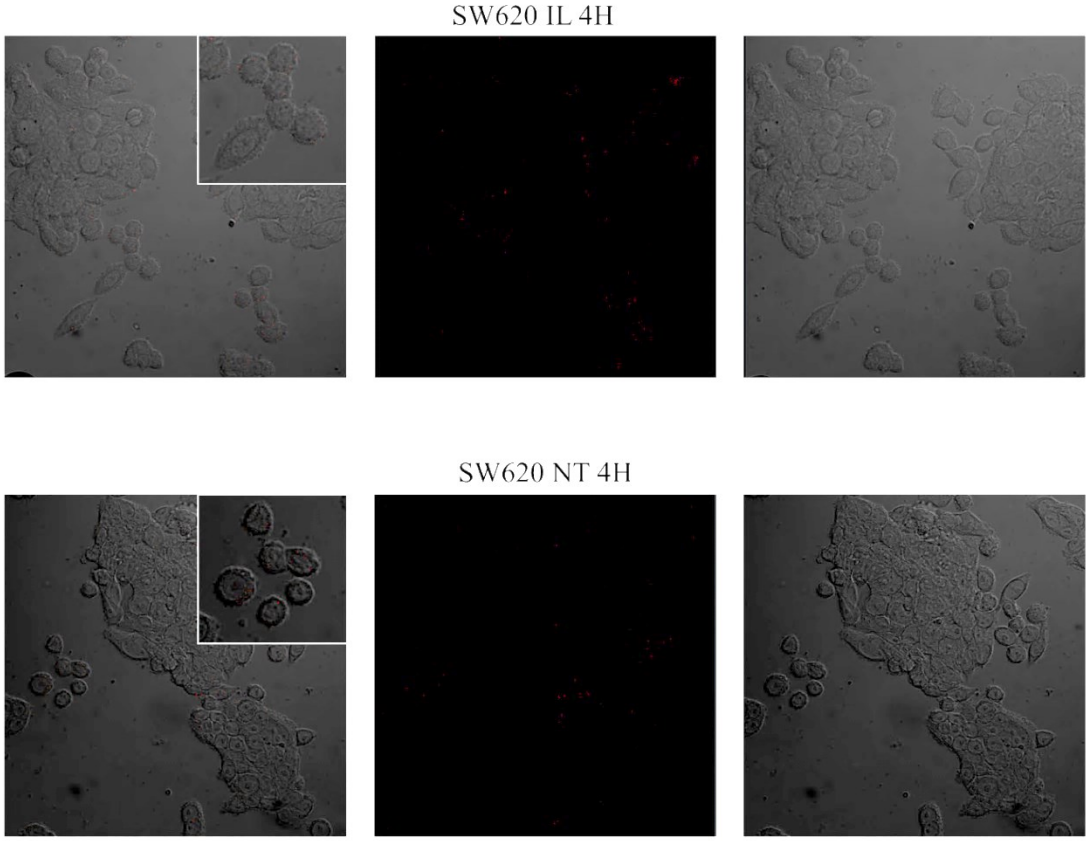

Figure 3.11 continued.

3.3 Cellular Toxicity of Pure CLX and EGFR-Targeted Immunoliposomes Containing CLX

In vitro cytotoxicity of pure CLX was tested in 4 different cell lines with varying expressions of COX-2. The COX-2 expression in these cell lines was evaluated by western blotting analysis (**Figure 3.12**). From the analysis, it was shown that HT-29 had a high expression of COX-2 whereas HCT-116 and MDA-MB-468 cells expressed low levels of COX-2 and SW-620 had almost undetectable levels of COX-2 expression. All cell lines were treated with 25-150 μM of CLX for 24 hours (**Figure 3.13**). The concentration of the DMSO (vehicle) was kept at less than 0.1% in order to prevent any toxicity. Control cells were incubated with medium only containing 0.1% of DMSO. In HCT-116, SW-620, and MDA-MB-468 cells, 25 μM

of CLX did not inhibit the proliferation of the cells. On the other hand, 25 μM of CLX significantly inhibited the proliferation of HT-29 (COX-2 overexpressing) cells to 86% ($P< 0.05$). Increasing the CLX concentration to 50 μM resulted in 20% and 15% decrease in cellular proliferation of HCT-116 and MDA-MB-468 cells, respectively. However, at the same concentration no significant decrease in the proliferation of SW-620 cells compared to the non-treated controls was observed. In all cell lines about 50% cellular proliferation inhibition was observed at 100 μM of CLX concentration. Further increase in the concentration of CLX to 125 μM or higher resulted in more than 90% decrease in the proliferation of HT-29, SW-620, and MDA-MB-468 cells. In addition, only at 150 μM of CLX, HCT 116 cells showed 90% inhibition in cellular proliferation.

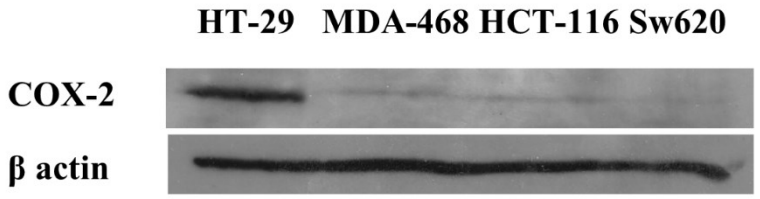

Figure 3.12 Western blot analysis of the expression of COX-2 in MDA-MB-468, HTT-116, HT-29, and SW-620 cell lines.

COX-2 expression is seen in wide range of cancers and several studies have shown that it could be a molecular target for cancer treatment or prevention [56, 223–226]. COX-2 inhibitors, including CLX, were documented to have an antitumorigenic effect *in vitro*, *in vivo*, and in clinical studies [227–231] . The anticarcinogenic effect of CLX occurs through both COX-2 dependent and COX-2 independent manner [79]. COX-2 independent effect of CLX includes the induction of cell cycle arrest, induction of apoptosis, inhibition of angiogenesis, and decrease in membrane fluidity and metastatic potential *in vitro* [79, 80].

In this study, CLX was shown to have a dose dependent inhibition in cellular proliferation in HT-29, HCT-116, SW-620, and MDA-MB-468 cell lines. The

inhibitory effect of CLX that was observed at low concentration of CLX (25 μM) in HT-29 cells might indicate that the COX-2 dependent effect of CLX was present on the COX-2 overexpressing cells (HT-29) but not in the low COX-2 expressing cells (HCT-116, MDA-MB-468, and SW-620). At concentrations greater than 50 μM of CLX, all the cells lines showed significant decrease in the cellular proliferation compared to the control cells ($P< 0.05$) and this effect to some extent could be related to COX-2 independent effect of CLX since these effects occurred in cells with low expression of COX-2 and at concentrations higher than the physiological concentration of CLX to inhibit COX-2. Furthermore, the COX-2 expression status was demonstrated not always to correlate with the response to CLX [232, 233]. The 50% inhibition (IC_{50}) in the cellular proliferation in all the cell lines within the scope of this study was observed at the concentration of CLX of about 100 μM (**Table 3.4**). The similarity in the IC_{50} values of CLX in the cell lines with low and high COX-2 expressions may indicate mechanisms in inhibiting the growth of cancer cells other than COX-2 inhibition. For example, it was suggested that CLX was able to induce cell cycle arrest at the G0/G1 checkpoint in MDA-MB-468 cells [237]. In agreement with this, numerous studies also demonstrated that the anticarcinogenic effect of CLX did not rely on the involvement of its target protein COX-2 [79, 235]. The requirement of a large concentration of COX-2 in order to achieve COX-2 independent effect of CLX (>50 μM of CLX) *in vitro* exceeds the plasma concentrations of CLX that can be achieved upon a daily intake of 200–400 mg CLX. However, the concentration is still clinically relevant as most of the *in vitro* studies, including this study, have been performed in short duration of treatment. With a prolonged treatment period the effective dose of CLX could still be reduced [239]. Therefore, the plasma concentrations of CLX needed to generate a significant anticarcinogenic effect might be achieved *in vivo* with a longer treatment period [78]. In fact, inhibition of prostate cancer growth through COX-2 independent mechanism of CLX *in vivo* could be attained under a clinically relevant concentration [239].

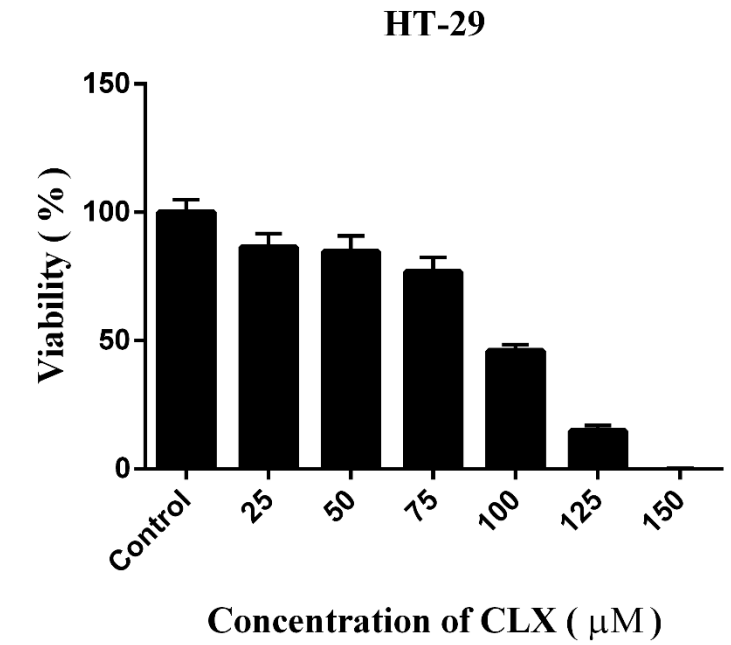

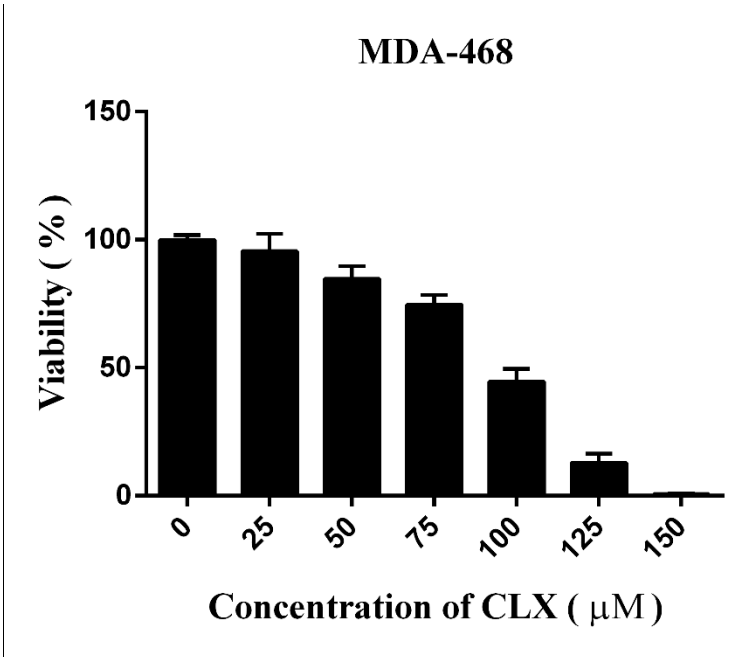

Figure 3.13 Representative image of cellular toxicity of pure CLX on HT-29, MDA-MB-468, and SW-620 cells by MTT assay.

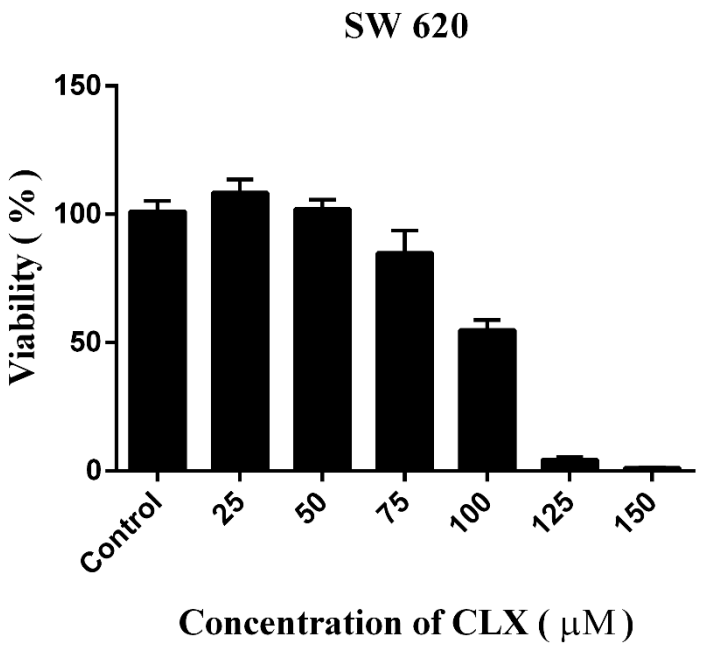

Figure 3.13 continued**.**

The cells were treated with various concentrations of celecoxib (25-150 μM) for 24 h. The graph is a representative of three independent experiments. Columns represent means; bars represent S.D.

Table 3.4 IC_{50} values for the inhibition of cellular proliferation in HT29, HCT-116, MDA-MB-468, and SW-620 cells after 24 h treatment with CLX (0–150 μM).

Cell Lines	**IC_{50} Value (μM)**
HT-29	87
MDA-MB-468	94
SW-620	93

Cellular toxicity of EGFR-targeted ILs with encapsulated CLX content of 100 µM was tested on MDA-MB-468, SW-620, and HT-29 cell lines for 4 h of treatment (**Figure 3.14**). MDA-MB-468 cells highly expressed EGFR, while HT-29 and SW-620 cells expressed low and no detectable level of EGFR, respectively. HT-29 cells expressed high level of COX-2 and SW-620 and MDA-MB-468 cells expressed low level of COX-2. For comparison with the targeted ILs, the toxicity of non-targeted LUVs was also examined. In addition, the toxicity of components of the ILs including 100 µM of pure CLX and empty liposomes were also carried out. 100 µM of CLX was chosen because it was close to the IC_{50} of CLX in these cell lines. On the other hand, the empty liposomes dose use in the treatment was equal to the lipid concentration of the ILs with highest amount of CLX in order to determine the lipid associated toxicity.

A

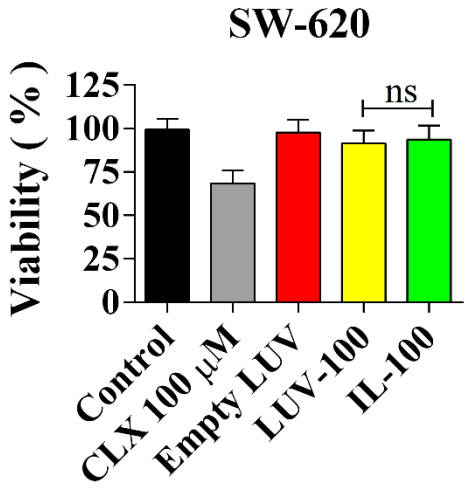

Figure 3.14 Cellular toxicity of CLX loaded EGFR targeted liposomes.
Values denote Mean ± S.D. (A) SW-620, (B) MDA-MB-468 and (C) HT-29 were treated with 100 µM of free CLX, empty liposomes, or LUVs (LUV-100) and EGFR-targeted ILs (IL) loaded with 100 µM of CLX for 4 h. The cells were then allowed to recover for 24 h and the MTT assay was used to evaluate their viability.

B

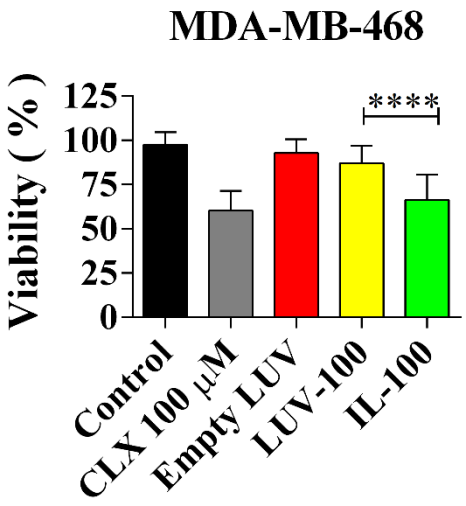

C

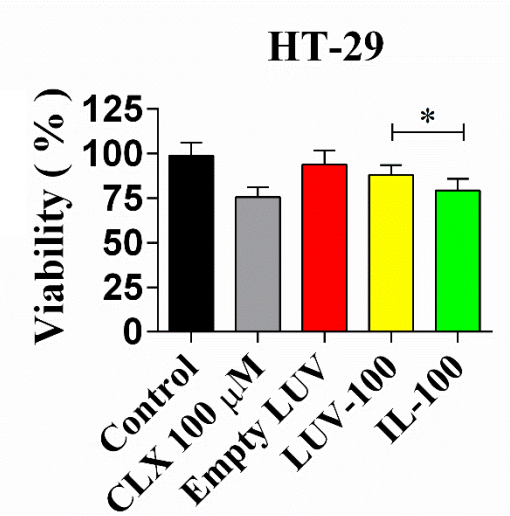

Figure 3.14 continued.

Values denote Mean ± S.D of percentage of viable cells with respect to untreated control cells from 2 independent experiments. Significance with respect to the control group was analyzed by one-way ANOVA using Tukeys's multiple comparison test. 'ns' stands for not significant, * P<0.05, **** P<0.0001.

In all cell lines, the empty liposomes did not show any significant toxicity compared to the control cells indicating that the lipids were not toxic at the concentrations used (**Figure 3.14**). The cytotoxicity of the EGFR-targeted ILs was compared with the non-targeted LUVs in order to evaluate the effectiveness of the EGFR targeting. In SW-620 cells, where EGFR expression is low, there was no significant difference between the toxicities of ILs and non-targeted liposomes ($P>0.05$) (**Figure 3.14A**). The free CLX was significantly more toxic in this cell line compared to LUVs or ILs ($*P<0.05$). On the other hand, in MDA-MB-468 cells, EGFR-targeted ILs were significantly more toxic compared to the non-targeted LUVs ($*P<0.05$) (**Figure 3.14B**). In fact, the toxicity of the EGFR-targeted ILs was comparable to free CLX treatment. This might indicate that the EGFR-targeted ILs could deliver CLX as rapidly as the easy diffusion of free CLX into the cells. On the other hand, in all cell lines, the treatment with the LUVs was less toxic than that of with free CLX. According to the *in vitro* release study of CLX from LUVs, only less than 30% of the drugs was released to the medium during the first 72 h of incubation at 37^{o}C. Therefore, in case of LUVs, the amount of CLX that could functionally inhibit the proliferation of the cancer cells was only a small portion of the encapsulated drugs, which mainly originate from the drug's diffusion from the liposomes. In other words, the rate of diffusion of CLX encapsulated within the LUVs to the cells was the limiting factor for the therapeutic efficacy of CLX-loaded LUVs. Interestingly, although the EGFR expression is low in HT-29 cells (please see **Figure 3.6**), the EGFR-targeted ILs were slightly more toxic compared to the non-targeted LUVs and the toxicity is comparable to the treatment with free CLX (**Figure 3.14C**). This could have resulted from the blockage of EGFR signaling subsequent to the internalization of the receptor upon the binding of EGFR-targeted ILs in these cells. HT-29 cells were shown to have an intermediate response to Cetuximab (anti EGFR mAB) therapy [86]. We have also observed that after 24h of treatment with 10μg/ml EGFR mAb (similar to the amount of mAB present on the ILs), the viability of HT-29 cells decreased to 73% (data not shown).

In this study, the generated ILs contain only about 6 half-IgG molecules/ liposomes and with this number of targeting ligand, probably the CLX-loaded ILs was

not able to deliver the drug exceeding the diffusion of the free drug to the target cells including MDA-MB-468 cells. In fact, it is presumed that in order to have an optimum intracellular delivery of the drugs within the liposomes, 40 targeting ligands/liposome was required. However, it was reported that 6 Fab′ fragments per liposome was sufficient for endocytosis of 55-60% of the cell-associated anti-HER2 immunoliposomes into HER2-overexpressing cells [166].

Apart from that, the EGFR-targeted ILs were significantly more toxic compared to the non-targeted liposomes in MDA-MB-468 cells despite its low COX-2 expression. To some extent, it can be attributed to the improvement in the intracellular delivery of CLX due to the presence of the EGFR antibody as the targeting ligand on the surface of the liposomes. An additional reason for the selective toxicity of the ILs in MDA-MB-468 cells could be related to the very high expression of EGFR in these cells compared to the other cell lines. The selective toxicity of the EGFR-targeted immunoliposomes makes it more advantageous over the non-targeted liposomes since it is estimated that normal cells express several fold lower EGFR per cell compared to the tumor cells [33]. Therefore, it could spare the normal cells from toxicity of the EGFR-targeted ILs.

Although MDA-MB-468 cells overexpress EGFR, in this cell, the cytotoxicity of the EGFR-targeted ILs may not be related to the inhibition of EGFR signaling pathway by the antibodies on the surface of the ILs. We have shown that the treatment of MDA-MB-468 cells with 10 μg/ml EGFR mAb alone for 24 h resulted in decrease its viability only by 6% (Data not shown). Additionally, the effect of combination treatment between 10 μg/ml EGFR mAb and 100 μM of CLX resulted in significant additive effect of inhibition in the proliferation only in HT-29 cells but not in MDA-MB-468 cells (Data not shown). This could have resulted from the responsiveness of the HT-29 cells to the individual therapy, whereas MDA-MB-468 cells were highly responsive only to CLX but not to the anti-EGFR mAbs treatment. Therefore, the effect of the combination treatment in these cell lines mainly could be attributed to anticarcinogenic effect of the CLX. Our results along with the discrepancy between response to Cetuximab and the EGFR cell surface expression status reported in phase 2 and phase 3 studies of patients with lung, gastric, esophageal, and pancreatic cancer

[238–240] further validated that the response to anti-EGFR mAb therapy was not correlated with EGFR expression status.

Regardless of the less efficient intracellular delivery of the encapsulated drug exhibited by non-ligand targeted liposomes compared to the free drugs, the high retention of the drugs within the liposomes is still necessary for effective *in vivo* delivery since the free drugs, especially CLX here, will have a large volume distribution and will be more prone to clearance by RES compared to the corresponding drug inside the liposomes. Therefore, ideally, in a similar manner like the non-ligand targeted liposomes, the ILs should have the ability to maintain the retention of the encapsulated materials during its circulation in the blood and after extravasation to the tumor interstitium as well as sufficient number of targeting ligands to optimally deliver the encapsulated drug to the target cells.

As a continuation of our studies, in order to further increase the internalization of the EGFR-targeted liposomes for enhancing the delivery of CLX into the cancer cell with EGFR overexpression, it might be necessary to increase the density of the targeting ligand on the surface of liposomes. One of the attractiveness in using ILs for the cancer therapy is their ability to deliver high payload of the drugs to their target with relatively few number of antibodies per liposome [243]. The ILs were designated to improve the intracellular delivery of CLX through receptor mediated endocytosis of the liposomes [162]. In addition, the mechanistic action of immunoliposomes that can improve the therapeutic efficacy of anticancer drug is facilitated through the increased internalization and intracellular delivery of the drugs independent of the inhibition of intracellular signaling pathways [139, 222]. Therefore, as long as the extracellular domain of the target receptor is recognized by the antibody on the liposomes surface, the targeted ILs can be used to treat cancers with mutations that diminish the inhibitory effect of ligand binding blocking by mAbs.

CHAPTER 4

CONCLUSIONS

Since EGFR is highly expressed in a wide range of solid tumors, among the currently available targeting ligands, cetuximab (anti-EGFR monoclonal antibody) is a viable candidate for targeting liposomes to cancer cells. In the presented thesis, we aimed to develop EGFR-targeted immunoliposomes for enhancing the delivery of CLX to cancer cells. Our previous studies have shown the successful encapsulation of CLX within non-targeted Large Unilamellar Vesicles [178]. This formulation was shown to have desirable characteristics of a Drug Delivery System for CLX as well as functional efficacy (inhibition of proliferation and motility) against colorectal cancer cells [178] .

In the current study, the characteristics of targeted CLX-loaded immunoliposomes including encapsulation efficiency, drug loading, *in vitro* release profile of CLX, and the conjugation of antibody on the surface of the liposomes were evaluated and the major observations are as follows:

1. The ILs formulation of CLX was able to incorporate 40% of the CLX, maintain a sustained (not burst) release profile of CLX from the liposomes *in vitro*, and showed around 40% conjugation of the antibody.
2. The extent of the cellular internalization of the EGFR-targeted ILs was compared with the non-targeted LUVs. The internalization was qualitatively visualized with Laser Scanning Confocal Microscopy (LSCM) and quantitatively measured with flow cytometry. In accordance with the flow cytometry data, confocal microscopy showed a significant accumulation of the ILs within the EGFR-overexpressing cells compared to the non-targeted liposomes and the z-stacks indicated that the internalized liposomes were localized within the cytoplasm.
3. The cellular toxicity data revealed that 4 hours of treatment with the EGFR-targeted ILs loaded with CLX was more toxic to the EGFR overexpressing cell lines compared

to the non-targeted liposomes. In addition, the cellular toxicity of the CLX containing EGFR targeted ILs were comparable to that of free CLX only in EGFR overexpressing cell lines. The cytotoxicity studies also showed that pure CLX (non-liposomal) or the CLX-loaded liposomes were toxic to both COX-2 positive and COX-2 negative cells.

All in all, functional studies carried out in this thesis have shown that surface decoration of CLX-loaded liposomes with the EGFR antibodies resulted in increase the selective toxicity and intracellular delivery of the liposomes to EGFR-overexpressing cancer cells but not to cancer cells with a low expression of EGFR. The internalized CLX-loaded ILs can then exert their anticarcinogenic properties through both COX-2 dependent and independent functions. However, according to our cellular association studies, targeting the CLX loaded liposomes with anti-EGFR mAbs significantly improved the cellular uptake of the liposomes in the EGFR-overexpressing cell lines implying an improvement in the ligand targeted liposomes over the non-targeted ones. We believe that the major role played by the EGFR mAb on the liposome surface was to enhance the internalization of the liposomes; rather than bind to EGFR and interfere with the EGFR signaling pathway. Consequently, the main mechanism of cell death resulting from these immunoliposomes could have resulted from the COX-2 independent effects of CLX.

FUTURE DIRECTIONS

The results presented in this study are important in that they provide an insight that ligand targeted liposomes could improve tumor targeting as well as the intracellular delivery of CLX. Further studies employing higher ligand density on the surface of the liposomes may be necessary in order to make the *in vitro* delivery liposomal CLX comparable to the cellular uptake of free CLX. In addition, *in vivo* studies to test the efficacy of targeted or non-targeted liposomal CLX will also be essential. This could potentially lead to the advancement in the nanoparticles based drug delivery system over the conventional systemic administration of drug by increasing the dose of the therapeutic drug at the target site and thereby preclude the development of systemic side effects.

REFERENCES

[1] F. Ferlay, J : Soerjomataram, I:Ervik, M:Dikshit, R:Eser, S:Mathers, C:Rebelo, M: Parkin, DM:Forman, D:Bray, "Cancer Incidence and Mortality Worldwide: IARC CancerBase No. 11," *GLOBOCAN*, 2012. [Online]. Available: http://globocan.iarc.fr. [Accessed: 20-Aug-2014].

[2] D. HANAHAN, "The Hallmarks of Cancer," *Cell*, vol. 100, pp. 57–70, 2000.

[3] D. Hanahan and R. A. Weinberg, "Hallmarks of cancer: The next generation," *Cell*, vol. 144. pp. 646–674, 2011.

[4] A. Urruticoechea, R. Alemany, J. Balart, A. Villanueva, F. Viñals, and G. Capellá, "Recent advances in cancer therapy: an overview.," *Curr. Pharm. Des.*, vol. 16, pp. 3–10, 2010.

[5] T. Hussain and Q. T. Nguyen, "Molecular imaging for cancer diagnosis and surgery," *Advanced Drug Delivery Reviews*, vol. 66. pp. 90–100, 2014.

[6] W. Ceelen, P. Pattyn, and M. Mareel, "Surgery, wound healing, and metastasis: Recent insights and clinical implications," *Critical Reviews in Oncology/Hematology*, vol. 89. pp. 16–26, 2014.

[7] L. J. Murray and M. H. Robinson, "Radiotherapy: technical aspects," *Medicine (Baltimore).*, vol. 39, no. 12, pp. 698–704, Dec. 2011.

[8] V. Brown, T. Sridhar, and R. P. Symonds, "Principles of chemotherapy and radiotherapy," *Obstet. Gynaecol. Reprod. Med.*, vol. 21, pp. 339–345, 2011.

[9] K. Symonds, P., Jones, D., Good, J., & Harrington, "Advances in Clinical Radiobiology," *Clin. Oncol.*, vol. 25, no. 10, pp. 567–568, 2013.

[10] A. Caley and R. Jones, "The principles of cancer treatment by chemotherapy," *Surgery*, vol. 30. pp. 186–190, 2012.

[11] I. Goldstein, S. Madar, and V. Rotter, "Cancer research, a field on the verge of a paradigm shift?," *Trends in Molecular Medicine*, vol. 18. pp. 299–303, 2012.

[12] S. Banerjee and H. Flores-Rozas, "Monoclonal antibodies for targeted therapy in colorectal cancer.," *Cancer Biol. Ther.*, vol. 9, pp. 563–571, 2010.

[13] N. E. Hynes and H. A. Lane, “ERBB receptors and cancer: the complexity of targeted inhibitors.,” *Nat. Rev. Cancer*, vol. 5, pp. 341–354, 2005.

[14] M. D. Siegelin and A. C. Borczuk, “Epidermal growth factor receptor mutations in lung adenocarcinoma.,” *Lab. Invest.*, vol. 94, no. 2, pp. 129–37, Feb. 2014.

[15] J. Mendelsohn and J. Baselga, “Epidermal Growth Factor Receptor Targeting in Cancer,” *Semin. Oncol.*, vol. 33, pp. 369–385, 2006.

[16] K. Khazaie, V. Schirrmacher, and R. B. Lichtner, “EGF receptor in neoplasia and metastasis.,” *Cancer Metastasis Rev.*, vol. 12, pp. 255–274, 1993.

[17] M. A. Lemmon and J. Schlessinger, “Cell signaling by receptor tyrosine kinases,” *Cell*, vol. 141. pp. 1117–1134, 2010.

[18] C. Yewale, D. Baradia, I. Vhora, S. Patil, and A. Misra, “Epidermal growth factor receptor targeting in cancer: A review of trends and strategies,” *Biomaterials*, vol. 34. pp. 8690–8707, 2013.

[19] Y. Yarden and M. X. Sliwkowski, “Untangling the ErbB signalling network.,” *Nat. Rev. Mol. Cell Biol.*, vol. 2, pp. 127–137, 2001.

[20] J. Schlessinger, “Common and distinct elements in cellular signaling via EGF and FGF receptors.,” *Science*, vol. 306, pp. 1506–1507, 2004.

[21] H. Yu and R. Jove, “The STATs of cancer--new molecular targets come of age.,” *Nat. Rev. Cancer*, vol. 4, pp. 97–105, 2004.

[22] R. Ishizawar and S. J. Parsons, “C-Src and cooperating partners in human cancer,” *Cancer Cell*, vol. 6. pp. 209–214, 2004.

[23] M.-A. Bjornsti and P. J. Houghton, “The TOR pathway: a target for cancer therapy.,” *Nat. Rev. Cancer*, vol. 4, pp. 335–348, 2004.

[24] Y. Guo, J. Du, and D. J. Kwiatkowski, “Molecular dissection of AKT activation in lung cancer cell lines.,” *Mol. Cancer Res.*, vol. 11, pp. 282–93, 2013.

[25] A. Gschwind, O. M. Fischer, and A. Ullrich, “The discovery of receptor tyrosine kinases: targets for cancer therapy.,” *Nat. Rev. Cancer*, vol. 4, pp. 361–370, 2004.

[26] L. Frederick, X. Y. Wang, G. Eley, and C. D. James, “Diversity and frequency of epidermal growth factor receptor mutations in human glioblastomas.,” *Cancer Res.*, vol. 60, pp. 1383–1387, 2000.

[27] I. E. G. De Palazzo, G. P. Adams, P. Sundareshan, L. Carcinomas, A. J. Wong, J. R. Testa, D. D. Bigner, L. M. Weiner, and I. E. Garcia de Palazzo, "Expression of Mutated Epidermal Growth Factor Receptor by Non-Small Cell Lung Carcinomas," *Cancer Res.*, vol. 53, pp. 3217–20, 1993.

[28] D. K. Moscatello, M. Holgado-Madruga, A. K. Godwin, G. Ramirez, G. Gunn, P. W. Zoltick, J. A. Biegel, R. L. Hayes, and A. J. Wong, "Frequent expression of a mutant epidermal growth factor receptor in multiple human tumors.," *Cancer Res.*, vol. 55, pp. 5536–5539, 1995.

[29] C. J. Wikstrand, L. P. Hale, S. K. Batra, M. L. Hill, P. A. Humphrey, S. N. Kurpad, R. E. McLendon, D. Moscatello, C. N. Pegram, and C. J. Reist, "Monoclonal antibodies against EGFRvIII are tumor specific and react with breast and lung carcinomas and malignant gliomas.," *Cancer Res.*, vol. 55, pp. 3140–3148, 1995.

[30] A. J. Ekstrand, N. Sugawa, C. D. James, and V. P. Collins, "Amplified and rearranged epidermal growth factor receptor genes in human glioblastomas reveal deletions of sequences encoding portions of the N- and/or C-terminal tails.," *Proc. Natl. Acad. Sci. U. S. A.*, vol. 89, pp. 4309–4313, 1992.

[31] S. K. Batra, S. Castelino-Prabhu, C. J. Wikstrand, X. Zhu, P. A. Humphrey, H. S. Friedman, and D. D. Bigner, "Epidermal growth factor ligand-independent, unregulated, cell-transforming potential of a naturally occurring human mutant EGFRvIII gene.," *Cell Growth Differ.*, vol. 6, pp. 1251–1259, 1995.

[32] H. S. Huang, M. Nagane, C. K. Klingbeil, H. Lin, R. Nishikawa, X. D. Ji, C. M. Huang, G. N. Gill, H. S. Wiley, and W. K. Cavenee, "The enhanced tumorigenic activity of a mutant epidermal growth factor receptor common in human cancers is mediated by threshold levels of constitutive tyrosine phosphorylation and unattenuated signaling.," *J. Biol. Chem.*, vol. 272, pp. 2927–2935, 1997.

[33] R. S. Herbst and D. M. Shin, "Monoclonal antibodies to target epidermal growth factor receptor-positive tumors a new paradigm for cancer therapy," *Cancer*, vol. 94, pp. 1593–1611, 2002.

[34] A. Zaczek, B. Brandt, and K. P. Bielawski, "The diverse signaling network of EGFR, HER2, HER3 and HER4 tyrosine kinase receptors and the consequences

for therapeutic approaches.," *Histol. Histopathol.*, vol. 20, pp. 1005–1015, 2005.

[35] H. Bier, T. Hoffmann, I. Haas, and A. Van Lierop, "Anti-(epidermal growth factor) receptor monoclonal antibodies for the induction of antibody-dependent cell-mediated cytotoxicity against squamous cell carcinoma lines of the head and neck," *Cancer Immunol. Immunother.*, vol. 46, pp. 167–173, 1998.

[36] et al. Hadari, Y,. Doody, J,. Wang, Y,. Patel, S,. Apblett, R,. Loizos, N, "The IgG1 monoclonal antibody cetuximab induces degradation of the epidermal growth factor receptor," *ASCO Gastrointest Cancers Symp*, pp. 22–24, 2004.

[37] S. M. Huang, J. M. Bock, and P. M. Harari, "Epidermal growth factor receptor blockade with C225 modulates proliferation, apoptosis, and radiosensitivity in squamous cell carcinomas of the head and neck," *Cancer Res.*, vol. 59, pp. 1935–1940, 1999.

[38] M. Perez-Torres, M. Guix, A. Gonzalez, and C. L. Arteaga, "Epidermal growth factor receptor (EGFR) antibody down-regulates mutant receptors and inhibits tumors expressing EGFR mutations.," *J. Biol. Chem.*, vol. 281, pp. 40183–40192, 2006.

[39] F. Ciardiello, R. Bianco, V. Damiano, S. De Lorenzo, S. Pepe, S. De Placido, Z. Fan, J. Mendelsohn, A. R. Bianco, and G. Tortora, "Antitumor Activity of Sequential Treatment with Topotecan and Anti-Epidermal Growth Factor Receptor Monoclonal Antibody C225," *Clin Cancer Res*, vol. 5, pp. 909–916, 1999.

[40] H. Mellstedt, "Monoclonal antibodies in human cancer.," *Drugs Today (Barc).*, vol. 39 Suppl C, pp. 1–16, 2003.

[41] D. Peng, Z. Fan, Y. Lu, T. DeBlasio, H. Scher, and J. Mendelsohn, "Anti-epidermal growth factor receptor monoclonal antibody 225 up-regulates p27KIP1 and induces G1 arrest in prostatic cancer cell line DU145.," *Cancer Res.*, vol. 56, pp. 3666–3669, 1996.

[42] P. Perrotte, T. Matsumoto, K. Inoue, H. Kuniyasu, B. Y. Eve, D. J. Hicklin, R. Radinsky, and C. P. Dinney, "Anti-epidermal growth factor receptor antibody

C225 inhibits angiogenesis in human transitional cell carcinoma growing orthotopically in nude mice.," *Clin. Cancer Res.*, vol. 5, pp. 257–265, 1999.

[43] S.-F. Wong, "Cetuximab: an epidermal growth factor receptor monoclonal antibody for the treatment of colorectal cancer.," *Clin. Ther.*, vol. 27, pp. 684–694, 2005.

[44] X. D. Yang, X. C. Jia, J. R. F. Corvalan, P. Wang, and C. G. Davis, "Development of ABX-EGF, a fully human anti-EGF receptor monoclonal antibody, for cancer therapy," *Critical Reviews in Oncology/Hematology*, vol. 38. pp. 17–23, 2001.

[45] D. H. Lynch and X.-D. Yang, "Therapeutic potential of ABX-EGF: a fully human anti-epidermal growth factor receptor monoclonal antibody for cancer treatment.," *Semin. Oncol.*, vol. 29, pp. 47–50, 2002.

[46] L. Nicola, N,. Maria, P,. Alessia, L,. & Antonella De, "Mechanisms of action of EGFR inhibitors, EGFR Inhibitors in Cancer Treatment, Future Medicine," *Futur. Med.*, pp. 6–17, 2012.

[47] S. Aifa, J. Aydin, G. Nordvall, I. Lundström, S. P. S. Svensson, and O. Hermanson, "A basic peptide within the juxtamembrane region is required for EGF receptor dimerization," *Exp. Cell Res.*, vol. 302, pp. 108–114, 2005.

[48] A. Lièvre, J.-B. Bachet, D. Le Corre, V. Boige, B. Landi, J.-F. Emile, J.-F. Côté, G. Tomasic, C. Penna, M. Ducreux, P. Rougier, F. Penault-Llorca, and P. Laurent-Puig, "KRAS mutation status is predictive of response to cetuximab therapy in colorectal cancer.," *Cancer Res.*, vol. 66, pp. 3992–3995, 2006.

[49] S. Benvenuti, A. Sartore-Bianchi, F. Di Nicolantonio, C. Zanon, M. Moroni, S. Veronese, S. Siena, and A. Bardelli, "Oncogenic activation of the RAS/RAF signaling pathway impairs the response of metastatic colorectal cancers to anti-epidermal growth factor receptor antibody therapies.," *Cancer Res.*, vol. 67, pp. 2643–2648, 2007.

[50] W. L. Smith, D. L. DeWitt, and R. M. Garavito, "Cyclooxygenases: structural, cellular, and molecular biology.," *Annu. Rev. Biochem.*, vol. 69, pp. 145–182, 2000.

[51] H. R. Herschman, “Prostaglandin synthase 2.,” *Biochim. Biophys. Acta*, vol. 1299, no. 1, pp. 125–40, Jan. 1996.

[52] T. Tanabe and N. Tohnai, “Cyclooxygenase isozymes and their gene structures and expression,” *Prostaglandins Other Lipid Mediat.*, vol. 68–69, pp. 95–114, 2002.

[53] T. D. Warner and J. A. Mitchell, “Cyclooxygenases: new forms, new inhibitors, and lessons from the clinic.,” *FASEB J.*, vol. 18, pp. 790–804, 2004.

[54] J. R. Brown and R. N. DuBois, “COX-2: a molecular target for colorectal cancer prevention.,” *J. Clin. Oncol.*, vol. 23, pp. 2840–2855, 2005.

[55] R. A. Soslow, A. J. Dannenberg, D. Rush, B. M. Woerner, K. Nasir Khan, J. Masferrer, and A. T. Koki, “COX-2 is expressed in human pulmonary, colonic, and mammary tumors,” *Cancer*, vol. 89, pp. 2637–2645, 2000.

[56] G. Chan, J. O. Boyle, E. K. Yang, F. Zhang, P. G. Sacks, J. P. Shah, D. Edelstein, R. A. Soslow, A. T. Koki, B. M. Woerner, J. L. Masferrer, and A. J. Dannenberg, “Cyclooxygenase-2 expression is up-regulated in squamous cell carcinoma of the head and neck.,” *Cancer Res.*, vol. 59, pp. 991–994, 1999.

[57] S. Gupta, M. Srivastava, N. Ahmad, D. G. Bostwick, and H. Mukhtar, “Over-expression of cyclooxygenase-2 in human prostate adenocarcinoma,” *Prostate*, vol. 42, pp. 73–78, 2000.

[58] M. Ladetto, S. Vallet, A. Trojan, M. Dell’Aquila, L. Monitillo, R. Rosato, L. Santo, D. Drandi, A. Bertola, P. Falco, F. Cavallo, I. Ricca, F. De Marco, B. Mantoan, B. Bode-Lesniewska, G. Pagliano, R. Francese, A. Rocci, M. Astolfi, M. Compagno, S. Mariani, L. Godio, L. Marino, M. Ruggeri, P. Omedè, A. Palumbo, and M. Boccadoro, “Cyclooxygenase-2 (COX-2) is frequently expressed in multiple myeloma and is an independent predictor of poor outcome,” *Blood*, vol. 105, pp. 4784–4791, 2005.

[59] G. Ferrandina, L. Lauriola, M. G. Distefano, G. F. Zannoni, M. Gessi, F. Legge, N. Maggiano, S. Mancuso, A. Capelli, G. Scambia, and F. O. Ranelletti, “Increased cyclooxygenase-2 expression is associated with chemotherapy resistance and poor survival in cervical cancer patients.,” *J. Clin. Oncol.*, vol. 20, pp. 973–981, 2002.

[60] G. Li, T. Yang, and J. Yan, “Cyclooxygenase-2 increased the angiogenic and metastatic potential of tumor cells,” *Biochem. Biophys. Res. Commun.*, vol. 299, pp. 886–890, 2002.

[61] X. Tang, Y. J. Sun, E. Half, M. T. Kuo, and F. Sinicrope, “Cyclooxygenase-2 overexpression inhibits death receptor 5 expression and confers resistance to tumor necrosis factor-related apoptosis-inducing ligand-induced apoptosis in human colon cancer cells.,” *Cancer Res.*, vol. 62, pp. 4903–4908, 2002.

[62] R. Chinery, R. J. Coffey, R. Graves-Deal, S. C. Kirkland, S. C. Sanchez, W. E. Zackert, J. A. Oates, and J. D. Morrow, “Prostaglandin J2 and 15-deoxy-delta12,14-prostaglandin J2 induce proliferation of cyclooxygenase-depleted colorectal cancer cells.,” *Cancer Res.*, vol. 59, pp. 2739–2746, 1999.

[63] F. Li, Y. Liu, H. Chen, D. Liao, Y. Shen, F. Xu, and J. Wang, “EGFR and COX-2 protein expression in non-small cell lung cancer and the correlation with clinical features.,” *J. Exp. Clin. Cancer Res.*, vol. 30, p. 27, 2011.

[64] J. L. Liggett, X. Zhang, T. E. Eling, and S. J. Baek, “Anti-tumor activity of non-steroidal anti-inflammatory drugs: Cyclooxygenase-independent targets,” *Cancer Letters*, vol. 346. pp. 217–224, 2014.

[65] W. Smalley, W. A. Ray, J. Daugherty, and M. R. Griffin, “Use of nonsteroidal anti-inflammatory drugs and incidence of colorectal cancer: a population-based study.,” *Arch. Intern. Med.*, vol. 159, pp. 161–166, 1999.

[66] R. S. Sandler, S. Halabi, J. A. Baron, S. Budinger, E. Paskett, R. Keresztes, N. Petrelli, J. M. Pipas, D. D. Karp, C. L. Loprinzi, G. Steinbach, and R. Schilsky, “A randomized trial of aspirin to prevent colorectal adenomas in patients with previous colorectal cancer.,” 2003.

[67] M. M. Goldenberg, “Celecoxib, a selective cyclooxygenase-2 inhibitor for the treatment of rheumatoid arthritis and osteoarthritis.,” *Clin. Ther.*, vol. 21, pp. 1497–1513; discussion 1427–1428, 1999.

[68] M. M. Bertagnolli, “Chemoprevention of colorectal cancer with cyclooxygenase-2 inhibitors: two steps forward, one step back,” *Lancet Oncol.*, vol. 8, pp. 439–443, 2007.

[69] R. E. Harris, J. Beebe-Donk, and G. A. Alshafie, “Reduction in the risk of human breast cancer by selective cyclooxygenase-2 (COX-2) inhibitors.,” *BMC Cancer*, vol. 6, p. 27, 2006.

[70] S. Ali, B. F. El-Rayes, F. H. Sarkar, and P. A. Philip, “Simultaneous targeting of the epidermal growth factor receptor and cyclooxygenase-2 pathways for pancreatic cancer therapy.,” *Mol. Cancer Ther.*, vol. 4, pp. 1943–1951, 2005.

[71] J. I. Johnsen, M. Lindskog, F. Ponthan, I. Pettersen, L. Elfman, A. Orrego, B. Sveinbjörnsson, and P. Kogner, “Cyclooxygenase-2 is expressed in neuroblastoma, and nonsteroidal anti-inflammatory drugs induce apoptosis and inhibit tumor growth in vivo.,” *Cancer Res.*, vol. 64, pp. 7210–7215, 2004.

[72] Y.-Y. Kim, E.-J. Lee, Y.-K. Kim, S.-M. Kim, J.-Y. Park, H. Myoung, and M.-J. Kim, “Anti-cancer effects of celecoxib in head and neck carcinoma.,” *Mol. Cells*, vol. 29, pp. 185–194, 2010.

[73] S. Schiffmann, T. J. Maier, I. Wobst, A. Janssen, H. Corban-Wilhelm, C. Angioni, G. Geisslinger, and S. Grösch, “The anti-proliferative potency of celecoxib is not a class effect of coxibs,” *Biochem. Pharmacol.*, vol. 76, pp. 179–187, 2008.

[74] T. Hida, K. Kozaki, H. Muramatsu, A. Masuda, S. Shimizu, T. Mitsudomi, T. Sugiura, M. Ogawa, and T. Takahashi, “Cyclooxygenase-2 inhibitor induces apoptosis and enhances cytotoxicity of various anticancer agents in non-small cell lung cancer cell lines.,” *Clin. Cancer Res.*, vol. 6, pp. 2006–11, 2000.

[75] H. Choy and L. Milas, “Enhancing radiotherapy with cyclooxygenase-2 enzyme inhibitors: a rational advance?,” *J. Natl. Cancer Inst.*, vol. 95, pp. 1440–1452, 2003.

[76] T. W. Davis, J. M. O’Neal, M. D. Pagel, B. S. Zweifel, P. P. Mehta, D. M. Heuvelman, and J. L. Masferrer, “Synergy between celecoxib and radiotherapy results from inhibition of cyclooxygenase-2-derived prostaglandin E2, a survival factor for tumor and associated vasculature.,” *Cancer Res.*, vol. 64, pp. 279–285, 2004.

[77] P. Wardman, “Chemical Radiosensitizers for Use in Radiotherapy,” *Clin. Oncol.*, vol. 19, pp. 397–417, 2007.

[78] V. Jendrossek, “Targeting apoptosis pathways by Celecoxib in cancer,” *Cancer Letters*, vol. 332. pp. 313–324, 2013.

[79] S. Grösch, T. J. Maier, S. Schiffmann, and G. Geisslinger, “Cyclooxygenase-2 (COX-2)-independent anticarcinogenic effects of selective COX-2 inhibitors.,” *J. Natl. Cancer Inst.*, vol. 98, pp. 736–747, 2006.

[80] A. Sade, S. Tunçay, İ. Çimen, F. Severcan, and S. Banerjee, “Celecoxib reduces fluidity and decreases metastatic potential of colon cancer cell lines irrespective of COX-2 expression,” *Bioscience Reports*, vol. 32. pp. 35–44, 2011.

[81] H.-P. Lin, S. K. Kulp, P.-H. Tseng, Y.-T. Yang, C.-C. Yang, C.-S. Chen, and C.-S. Chen, “Growth inhibitory effects of celecoxib in human umbilical vein endothelial cells are mediated through G1 arrest via multiple signaling mechanisms.,” *Mol. Cancer Ther.*, vol. 3, pp. 1671–1680, 2004.

[82] D. Wang, D. Xia, and R. N. DuBois, “The Crosstalk of PTGS2 and EGF Signaling Pathways in Colorectal Cancer,” *Cancers*, vol. 3. pp. 3894–3908, 2011.

[83] G. J. Kelloff, J. R. Fay, V. E. Steele, R. A. Lubet, C. W. Boone, J. A. Crowell, and C. C. Sigman, “Epidermal growth factor receptor tyrosine kinase inhibitors as potential cancer chemopreventives,” *Cancer Epidemiol. Biomarkers Prev.*, vol. 5, pp. 657–666, 1996.

[84] F. G. Buchanan, D. L. Gorden, P. Matta, Q. Shi, L. M. Matrisian, and R. N. DuBois, “Role of beta-arrestin 1 in the metastatic progression of colorectal cancer.,” *Proc. Natl. Acad. Sci. U. S. A.*, vol. 103, pp. 1492–1497, 2006.

[85] F. G. Buchanan, D. Wang, F. Bargiacchi, and R. N. DuBois, “Prostaglandin E2 regulates cell migration via the intracellular activation of the epidermal growth factor receptor.,” *J. Biol. Chem.*, vol. 278, pp. 35451–35457, 2003.

[86] M. Jhawer, S. Goel, A. J. Wilson, C. Montagna, Y.-H. Ling, D.-S. Byun, S. Nasser, D. Arango, J. Shin, L. Klampfer, L. H. Augenlicht, R. Perez-Soler, and J. M. Mariadason, “PIK3CA mutation/PTEN expression status predicts response of colon cancer cells to the epidermal growth factor receptor inhibitor cetuximab.,” *Cancer Res.*, vol. 68, pp. 1953–1961, 2008.

[87] F. G. Buchanan, V. Holla, S. Katkuri, P. Matta, and R. N. DuBois, “Targeting cyclooxygenase-2 and the epidermal growth factor receptor for the prevention and treatment of intestinal cancer.,” *Cancer Res.*, vol. 67, pp. 9380–9388, 2007.

[88] E. Chan, B. Lafleur, M. L. Rothenberg, N. Merchant, A. C. Lockhart, B. Trivedi, C. H. Chung, R. J. Coffey, and J. D. Berlin, “Dual blockade of the EGFR and COX-2 pathways: a phase II trial of cetuximab and celecoxib in patients with chemotherapy refractory metastatic colorectal cancer.,” *Am. J. Clin. Oncol.*, vol. 34, pp. 581–6, 2011.

[89] Y. Zhang, H. F. Chan, and K. W. Leong, “Advanced materials and processing for drug delivery: the past and the future,” *Adv Drug Deliv Rev*, vol. 65, pp. 104–120, 2013.

[90] M. P. A. Lim, W. L. Lee, E. Widjaja, and S. C. J. Loo, “One-step fabrication of core–shell structured alginate–PLGA/PLLA microparticles as a novel drug delivery system for water soluble drugs,” *Biomater. Sci.*, vol. 1, p. 486, 2013.

[91] R. A. Siegel and M. J. Rathbone, “Overview of Controlled Release Mechanisms,” in *Fundamentals and Applications of Controlled Release*, 2012, pp. 19–44.

[92] M. Kim, B. Jung, and J. H. Park, “Hydrogel swelling as a trigger to release biodegradable polymer microneedles in skin,” *Biomaterials*, vol. 33, pp. 668–678, 2012.

[93] K. Park, “Controlled drug delivery systems: Past forward and future back.,” *J. Control. Release*, 2014.

[94] J. Nicolas, S. Mura, D. Brambilla, N. Mackiewicz, and P. Couvreur, “Design, functionalization strategies and biomedical applications of targeted biodegradable/biocompatible polymer-based nanocarriers for drug delivery,” *Chem. Soc. Rev.*, vol. 42, pp. 1147–1235, 2013.

[95] N. R. Patel, B. S. Pattni, A. H. Abouzeid, and V. P. Torchilin, “Nanopreparations to overcome multidrug resistance in cancer,” *Advanced Drug Delivery Reviews*, vol. 65. pp. 1748–1762, 2013.

[96] R. van der Meel, L. J. C. Vehmeijer, R. J. Kok, G. Storm, and E. V. B. van Gaal, “Ligand-targeted particulate nanomedicines undergoing clinical evaluation:

Current status," *Advanced Drug Delivery Reviews*, vol. 65. pp. 1284–1298, 2013.

[97] Y. Barenholz, "Doxil?? - The first FDA-approved nano-drug: Lessons learned," *Journal of Controlled Release*, vol. 160. pp. 117–134, 2012.

[98] F. Jia, X. Liu, L. Li, S. Mallapragada, B. Narasimhan, and Q. Wang, "Multifunctional nanoparticles for targeted delivery of immune activating and cancer therapeutic agents," *Journal of Controlled Release*, vol. 172. pp. 1020–1034, 2013.

[99] M. Kanapathipillai, A. Brock, and D. E. Ingber, "Nanoparticle targeting of anti-cancer drugs that alter intracellular signaling or influence the tumor microenvironment.," *Adv. Drug Deliv. Rev.*, May 2014.

[100] J. R. Weiser and W. M. Saltzman, "Controlled release for local delivery of drugs: barriers and models," *Journal of Controlled Release*, 2014.

[101] M. J. Cima, H. Lee, K. Daniel, L. M. Tanenbaum, A. Mantzavinou, K. C. Spencer, Q. Ong, J. C. Sy, J. Santini, C. M. Schoellhammer, D. Blankschtein, and R. S. Langer, "Single compartment drug delivery," *Journal of Controlled Release*, 2014.

[102] M. J. Ewesuedo, Reginald B. : Ratain, "Systemically Administered Drugs," in *Drug Delivery Systems in Cancer Therapy*, D. M. Brown, Ed. New Jersey: Humana Press Inc, 2004, pp. 3–4.

[103] Y. Matsumura and H. Maeda, "A new concept for macromolecular therapeutics in cancer chemotherapy: mechanism of tumoritropic accumulation of proteins and the antitumor agent smancs.," *Cancer Res.*, vol. 46, pp. 6387–6392, 1986.

[104] D. Brambilla, P. Luciani, and J.-C. Leroux, "Breakthrough discoveries in drug delivery technologies: The next 30years.," *J. Control. Release*, Apr. 2014.

[105] R. K. Jain, "The next frontier of molecular medicine: delivery of therapeutics.," *Nat. Med.*, vol. 4, pp. 655–657, 1998.

[106] R. K. Jain and T. Stylianopoulos, "Delivering nanomedicine to solid tumors.," *Nat. Rev. Clin. Oncol.*, vol. 7, pp. 653–664, 2010.

[107] S. K. Hobbs, W. L. Monsky, F. Yuan, W. G. Roberts, L. Griffith, V. P. Torchilin, and R. K. Jain, "Regulation of transport pathways in tumor vessels:

role of tumor type and microenvironment.," *Proc. Natl. Acad. Sci. U. S. A.*, vol. 95, pp. 4607–4612, 1998.

[108] N. Bertrand, J. Wu, X. Xu, N. Kamaly, and O. C. Farokhzad, "Cancer nanotechnology: the impact of passive and active targeting in the era of modern cancer biology.," *Adv. Drug Deliv. Rev.*, vol. 66, pp. 2–25, Feb. 2014.

[109] T. P. Padera, B. R. Stoll, J. B. Tooredman, D. Capen, E. di Tomaso, and R. K. Jain, "Pathology: cancer cells compress intratumour vessels.," *Nature*, vol. 427, p. 695, 2004.

[110] T. D. McKee, P. Grandi, W. Mok, G. Alexandrakis, N. Insin, J. P. Zimmer, M. G. Bawendi, Y. Boucher, X. O. Breakefield, and R. K. Jain, "Degradation of fibrillar collagen in a human melanoma xenograft improves the efficacy of an oncolytic herpes simplex virus vector.," *Cancer Res.*, vol. 66, pp. 2509–2513, 2006.

[111] W. P. Caron, G. Song, P. Kumar, S. Rawal, and W. C. Zamboni, "Interpatient pharmacokinetic and pharmacodynamic variability of carrier-mediated anticancer agents.," *Clin. Pharmacol. Ther.*, vol. 91, pp. 802–12, 2012.

[112] S. Ramanujan, A. Pluen, T. D. McKee, E. B. Brown, Y. Boucher, and R. K. Jain, "Diffusion and convection in collagen gels: implications for transport in the tumor interstitium.," *Biophys. J.*, vol. 83, pp. 1650–1660, 2002.

[113] H. Lee, H. Fonge, B. Hoang, R. M. Reilly, and C. Allen, "The effects of particle size and molecular targeting on the intratumoral and subcellular distribution of polymeric nanoparticles.," *Mol. Pharm.*, vol. 7, no. 4, pp. 1195–208, Aug. 2010.

[114] N. M. La-Beck, B. A. Zamboni, A. Gabizon, H. Schmeeda, M. Amantea, P. A. Gehrig, and W. C. Zamboni, "Factors affecting the pharmacokinetics of pegylated liposomal doxorubicin in patients," *Cancer Chemother. Pharmacol.*, vol. 69, pp. 43–50, 2012.

[115] T. S. Levchenko, R. Rammohan, A. N. Lukyanov, K. R. Whiteman, and V. P. Torchilin, "Liposome clearance in mice: The effect of a separate and combined presence of surface charge and polymer coating," *Int. J. Pharm.*, vol. 240, pp. 95–102, 2002.

[116] R. R. Arvizo, O. R. Miranda, D. F. Moyano, C. A. Walden, K. Giri, R. Bhattacharya, J. D. Robertson, V. M. Rotello, J. M. Reid, and P. Mukherjee, "Modulating pharmacokinetics, tumor uptake and biodistribution by engineered nanoparticles," *PLoS One*, vol. 6, 2011.

[117] A. Gabizon and D. Papahadjopoulos, "Liposome formulations with prolonged circulation time in blood and enhanced uptake by tumors.," *Proc. Natl. Acad. Sci. U. S. A.*, vol. 85, pp. 6949–6953, 1988.

[118] E. Roux, M. Lafleur, É.́ Lataste, P. Moreau, and J. C. Leroux, "On the characterization of pH-sensitive liposome/polymer complexes," *Biomacromolecules*, vol. 4, pp. 240–248, 2003.

[119] D. Peer and R. Margalit, "Tumor-Targeted Hyaluronan Nanoliposomes Increase the Antitumor Activity of Liposomal Doxorubicin in Syngeneic and Human Xenograft Mouse Tumor Models," *Neoplasia*, vol. 6, pp. 343–353, 2004.

[120] Y. Yamamoto, Y. Nagasaki, Y. Kato, Y. Sugiyama, and K. Kataoka, "Long-circulating poly(ethylene glycol)-poly(D,L-lactide) block copolymer micelles with modulated surface charge.," *J. Control. Release*, vol. 77, no. 1–2, pp. 27–38, Nov. 2001.

[121] K. Y. Win and S.-S. Feng, "Effects of particle size and surface coating on cellular uptake of polymeric nanoparticles for oral delivery of anticancer drugs.," *Biomaterials*, vol. 26, pp. 2713–2722, 2005.

[122] R. B. Campbell, D. Fukumura, E. B. Brown, L. M. Mazzola, Y. Izumi, R. K. Jain, V. P. Torchilin, and L. L. Munn, "Cationic charge determines the distribution of liposomes between the vascular and extravascular compartments of tumors.," *Cancer Res.*, vol. 62, pp. 6831–6836, 2002.

[123] J. A. Champion and S. Mitragotri, "Shape induced inhibition of phagocytosis of polymer particles," *Pharm. Res.*, vol. 26, pp. 244–249, 2009.

[124] Y. Geng, P. Dalhaimer, S. Cai, R. Tsai, M. Tewari, T. Minko, and D. E. Discher, "Shape effects of filaments versus spherical particles in flow and drug delivery.," *Nat. Nanotechnol.*, vol. 2, pp. 249–255, 2007.

[125] A. Ruggiero, C. H. Villa, E. Bander, D. A. Rey, M. Bergkvist, C. A. Batt, K. Manova-Todorova, W. M. Deen, D. A. Scheinberg, and M. R. McDevitt, "Paradoxical glomerular filtration of carbon nanotubes.," *Proc. Natl. Acad. Sci. U. S. A.*, vol. 107, pp. 12369–12374, 2010.

[126] S. Shukla, A. L. Ablack, A. M. Wen, K. L. Lee, J. D. Lewis, and N. F. Steinmetz, "Increased tumor homing and tissue penetration of the filamentous plant viral nanoparticle potato virus X," *Mol. Pharm.*, vol. 10, pp. 33–42, 2013.

[127] A. Gabizon, R. Catane, B. Uziely, B. Kaufman, T. Safra, R. Cohen, F. Martin, A. Huang, and Y. Barenholz, "Prolonged circulation time and enhanced accumulation in malignant exudates of doxorubicin encapsulated in polyethylene-glycol coated liposomes.," *Cancer Res.*, vol. 54, pp. 987–992, 1994.

[128] D. W. Northfelt, F. J. Martin, P. Working, P. A. Volberding, J. Russell, M. Newman, M. A. Amantea, and L. D. Kaplan, "Doxorubicin encapsulated in liposomes containing surface-bound polyethylene glycol: pharmacokinetics, tumor localization, and safety in patients with AIDS-related Kaposi's sarcoma.," 1996.

[129] H. Maeda, "SMANCS and polymer-conjugated macromolecular drugs: Advantages in cancer chemotherapy," *Advanced Drug Delivery Reviews*, vol. 46. pp. 169–185, 2001.

[130] S. Biswas and V. P. Torchilin, "Nanopreparations for organelle-specific delivery in cancer," *Advanced Drug Delivery Reviews*, vol. 66. pp. 26–41, 2014.

[131] R. N. Saha, S. Vasanthakumar, G. Bende, and M. Snehalatha, "Nanoparticulate drug delivery systems for cancer chemotherapy.," *Mol. Membr. Biol.*, vol. 27, pp. 215–231, 2010.

[132] N. Kamaly, Z. Xiao, P. M. Valencia, A. F. Radovic-Moreno, and O. C. Farokhzad, "Targeted polymeric therapeutic nanoparticles: design, development and clinical translation," *Chemical Society Reviews*, vol. 41. p. 2971, 2012.

[133] J. Shi, Z. Xiao, N. Kamaly, and O. C. Farokhzad, "Self-assembled targeted nanoparticles: Evolution of technologies and bench to bedside translation," *Accounts of Chemical Research*, vol. 44. pp. 1123–1134, 2011.

[134] A. Koshkaryev, R. Sawant, M. Deshpande, and V. Torchilin, "Immunoconjugates and long circulating systems: Origins, current state of the art and future directions," *Advanced Drug Delivery Reviews*, vol. 65. pp. 24–35, 2013.

[135] T. Lammers, F. Kiessling, W. E. Hennink, and G. Storm, "Drug targeting to tumors: Principles, pitfalls and (pre-) clinical progress," *Journal of Controlled Release*, vol. 161. pp. 175–187, 2012.

[136] S. Taurin, H. Nehoff, and K. Greish, "Anticancer nanomedicine and tumor vascular permeability; Where is the missing link?," in *Journal of Controlled Release*, 2012, vol. 164, pp. 265–275.

[137] K. F. Pirollo and E. H. Chang, "Does a targeting ligand influence nanoparticle tumor localization or uptake?," *Trends Biotechnol.*, vol. 26, pp. 552–558, 2008.

[138] D. B. Kirpotin, D. C. Drummond, Y. Shao, M. R. Shalaby, K. Hong, U. B. Nielsen, J. D. Marks, C. C. Benz, and J. W. Park, "Antibody targeting of long-circulating lipidic nanoparticles does not increase tumor localization but does increase internalization in animal models.," *Cancer Res.*, vol. 66, pp. 6732–6740, 2006.

[139] C. Mamot, D. C. Drummond, U. Greiser, K. Hong, D. B. Kirpotin, J. D. Marks, and J. W. Park, "Epidermal growth factor receptor (EGFR)-targeted immunoliposomes mediate specific and efficient drug delivery to EGFR- and EGFRvIII-overexpressing tumor cells.," *Cancer Res.*, vol. 63, no. 12, pp. 3154–61, Jun. 2003.

[140] X. Li, H. Zhou, L. Yang, G. Du, A. S. Pai-Panandiker, X. Huang, and B. Yan, "Enhancement of cell recognition in vitro by dual-ligand cancer targeting gold nanoparticles," *Biomaterials*, vol. 32, pp. 2540–2545, 2011.

[141] J. F. Stefanick, J. D. Ashley, T. Kiziltepe, and B. Bilgicer, "A systematic analysis of peptide linker length and liposomal polyethylene glycol coating on

cellular uptake of peptide-targeted liposomes," *ACS Nano*, vol. 7, pp. 2935–2947, 2013.

[142] M. Mammen, S.-K. Choi, and G. M. Whitesides, "Polyvalent Interactions in Biological Systems: Implications for Design and Use of Multivalent Ligands and Inhibitors," *Angew. Chemie Int. Ed.*, vol. 37, pp. 2754–2794, 1998.

[143] D. R. Elias, A. Poloukhtine, V. Popik, and A. Tsourkas, "Effect of ligand density, receptor density, and nanoparticle size on cell targeting," *Nanomedicine Nanotechnology, Biol. Med.*, vol. 9, pp. 194–201, 2013.

[144] D. E. Lopes de Menezes, L. M. Pilarski, and T. M. Allen, "In vitro and in vivo targeting of immunoliposomal doxorubicin to human B-cell lymphoma.," *Cancer Res.*, vol. 58, pp. 3320–3330, 1998.

[145] A. Béduneau, P. Saulnier, F. Hindré, A. Clavreul, J.-C. Leroux, and J.-P. Benoit, "Design of targeted lipid nanocapsules by conjugation of whole antibodies and antibody Fab' fragments.," *Biomaterials*, vol. 28, no. 33, pp. 4978–90, Nov. 2007.

[146] Y. Takakura, R. I. Mahato, and M. Hashida, "Extravasation of macromolecules," *Advanced Drug Delivery Reviews*, vol. 34. pp. 93–108, 1998.

[147] K. Maruyama, O. Ishida, T. Takizawa, and K. Moribe, "Possibility of active targeting to tumor tissues with liposomes," *Advanced Drug Delivery Reviews*, vol. 40. pp. 89–102, 1999.

[148] S. P. Egusquiaguirre, M. Igartua, R. M. Hernández, and J. L. Pedraz, "Nanoparticle delivery systems for cancer therapy: Advances in clinical and preclinical research," *Clinical and Translational Oncology*, vol. 14. pp. 83–93, 2012.

[149] A. L. Klibanov, K. Maruyama, V. P. Torchilin, and L. Huang, "Amphipathic polyethyleneglycols effectively prolong the circulation time of liposomes.," *FEBS Lett.*, vol. 268, pp. 235–237, 1990.

[150] G. Blume and G. Cevc, "Molecular mechanism of the lipid vesicle longevity in vivo.," *Biochim. Biophys. Acta*, vol. 1146, pp. 157–168, 1993.

[151] A. Salvati, A. S. Pitek, M. P. Monopoli, K. Prapainop, F. B. Bombelli, D. R. Hristov, P. M. Kelly, C. Åberg, E. Mahon, and K. a Dawson, "Transferrin-

functionalized nanoparticles lose their targeting capabilities when a biomolecule corona adsorbs on the surface.," *Nat. Nanotechnol.*, vol. 8, pp. 137–43, 2013.

[152] V. P. Torchilin, "Recent advances with liposomes as pharmaceutical carriers.," *Nat. Rev. Drug Discov.*, vol. 4, pp. 145–160, 2005.

[153] K. Mozafari, M. R. : Khosravi-Darani, "An overview of liposome-derived nanocarrier technologies," in *Nanomaterials and Nanosystems for Biomedical Applications*, New York: Springer, 2007, pp. 113–123.

[154] P. P. Deshpande, S. Biswas, and V. P. Torchilin, "Current trends in the use of liposomes for tumor targeting.," *Nanomedicine (Lond).*, vol. 8, pp. 1509–28, 2013.

[155] T. M. Allen and P. R. Cullis, "Liposomal drug delivery systems: From concept to clinical applications," *Advanced Drug Delivery Reviews*, vol. 65. pp. 36–48, 2013.

[156] M. E. R. O'Brien, N. Wigler, M. Inbar, R. Rosso, E. Grischke, A. Santoro, R. Catane, D. G. Kieback, P. Tomczak, S. P. Ackland, F. Orlandi, L. Mellars, L. Alland, and C. Tendler, "Reduced cardiotoxicity and comparable efficacy in a phase III trial of pegylated liposomal doxorubicin HCl (CAELYXTM/Doxil") versus conventional doxorubicin for first-line treatment of metastatic breast cancer," *Ann. Oncol.*, vol. 15, pp. 440–449, 2004.

[157] Avanti Polar Lipids, "Preparation of Liposomes." [Online]. Available: http://avantilipids.com/index.php?option=com_content&view=article&id=1384&Itemid= 72. [Accessed: 21-Aug-2014].

[158] Y.-L. Tseng, J.-J. Liu, and R.-L. Hong, "Translocation of liposomes into cancer cells by cell-penetrating peptides penetratin and tat: a kinetic and efficacy study.," *Mol. Pharmacol.*, vol. 62, no. 4, pp. 864–72, Oct. 2002.

[159] J. A. Silverman and S. R. Deitcher, "Marqibo?? (vincristine sulfate liposome injection) improves the pharmacokinetics and pharmacodynamics of vincristine," *Cancer Chemotherapy and Pharmacology*, vol. 71. pp. 555–564, 2013.

[160] V. P. Torchilin, T. S. Levchenko, A. N. Lukyanov, B. A. Khaw, A. L. Klibanov, R. Rammohan, G. P. Samokhin, and K. R. Whiteman, "p-nitrophenylcarbonyl-PEG-PE-liposomes: Fast and simple attachment of specific ligands, including monoclonal antibodies, to distal ends of PEG chains via p-nitrophenylcarbonyl groups," *Biochim. Biophys. Acta - Biomembr.*, vol. 1511, pp. 397–411, 2001.

[161] G. T. Noble, J. F. Stefanick, J. D. Ashley, T. Kiziltepe, and B. Bilgicer, "Ligand-targeted liposome design: challenges and fundamental considerations.," *Trends Biotechnol.*, vol. 32, no. 1, pp. 32–45, Jan. 2014.

[162] I. Canton and G. Battaglia, "Endocytosis at the nanoscale," *Chemical Society Reviews*, vol. 41. p. 2718, 2012.

[163] A. Albanese, P. S. Tang, and W. C. W. Chan, "The effect of nanoparticle size, shape, and surface chemistry on biological systems.," *Annu. Rev. Biomed. Eng.*, vol. 14, pp. 1–16, 2012.

[164] D. Needham, T. J. McIntosh, and D. D. Lasic, "Repulsive interactions and mechanical stability of polymer-grafted lipid membranes.," *Biochim. Biophys. Acta*, vol. 1108, pp. 40–48, 1992.

[165] A. S. Manjappa, K. R. Chaudhari, M. P. Venkataraju, P. Dantuluri, B. Nanda, C. Sidda, K. K. Sawant, and R. S. R. Murthy, "Antibody derivatization and conjugation strategies: application in preparation of stealth immunoliposome to target chemotherapeutics to tumor.," *J. Control. Release*, vol. 150, no. 1, pp. 2–22, Feb. 2011.

[166] D. Kirpotin, J. W. Park, K. Hong, S. Zalipsky, W. L. Li, P. Carter, C. C. Benz, and D. Papahadjopoulos, "Sterically stabilized anti-HER2 immunoliposomes: design and targeting to human breast cancer cells in vitro.," *Biochemistry*, vol. 36, pp. 66–75, 1997.

[167] E. Mastrobattista, G. A. Koning, and G. Storm, "Immunoliposomes for the targeted delivery of antitumor drugs," *Advanced Drug Delivery Reviews*, vol. 40. pp. 103–127, 1999.

[168] J. W. Park, K. Hong, D. B. Kirpotin, G. Colbern, R. Shalaby, J. Baselga, Y. Shao, U. B. Nielsen, J. D. Marks, D. Moore, D. Papahadjopoulos, and C. C.

Benz, “Anti-HER2 immunoliposomes: enhanced efficacy attributable to targeted delivery.,” *Clin. Cancer Res.*, vol. 8, pp. 1172–1181, 2002.

[169] J. W. Park, K. Hong, D. B. Kirpotin, O. Meyer, D. Papahadjopoulos, and C. C. Benz, “Anti-HER2 immunoliposomes for targeted therapy of human tumors.,” *Cancer Lett.*, vol. 118, pp. 153–160, 1997.

[170] C. Mamot, R. Ritschard, W. Küng, J. W. Park, R. Herrmann, and C. F. Rochlitz, “EGFR-targeted immunoliposomes derived from the monoclonal antibody EMD72000 mediate specific and efficient drug delivery to a variety of colorectal cancer cells.,” *J. Drug Target.*, vol. 14, pp. 215–223, 2006.

[171] W. W. K. Cheng and T. M. Allen, “Targeted delivery of anti-CD19 liposomal doxorubicin in B-cell lymphoma: A comparison of whole monoclonal antibody, Fab??? fragments and single chain Fv,” *J. Control. Release*, vol. 126, pp. 50–58, 2008.

[172] T. M. Allen, D. R. Mumbengegwi, and G. J. R. Charrois, “Anti-CD19-targeted liposomal doxorubicin improves the therapeutic efficacy in murine B-cell lymphoma and ameliorates the toxicity of liposomes with varying drug release rates.,” *Clin. Cancer Res.*, vol. 11, pp. 3567–3573, 2005.

[173] K. K. Jain, “Advances in the field of nanooncology.,” *BMC Med.*, vol. 8, p. 83, 2010.

[174] J. M. Nemunaitis and J. Nemunaitis, *Potential of Advexin: a p53 gene-replacement therapy in Li-Fraumeni syndrome.*, vol. 4. 2008, pp. 759–768.

[175] N. Senzer, J. Nemunaitis, D. Nemunaitis, C. Bedell, G. Edelman, M. Barve, R. Nunan, K. F. Pirollo, A. Rait, and E. H. Chang, “Phase I study of a systemically delivered p53 nanoparticle in advanced solid tumors.,” *Mol. Ther.*, vol. 21, no. 5, pp. 1096–103, May 2013.

[176] C. Mamot, R. Ritschard, A. Wicki, G. Stehle, T. Dieterle, L. Bubendorf, C. Hilker, S. Deuster, R. Herrmann, and C. Rochlitz, “Tolerability, safety, pharmacokinetics, and efficacy of doxorubicin-loaded anti-EGFR immunoliposomes in advanced solid tumours: a phase 1 dose-escalation study.,” *Lancet Oncol.*, vol. 13, no. 12, pp. 1234–41, Dec. 2012.

[177] A. Deniz, A. Sade, F. Severcan, D. Keskin, A. Tezcaner, and S. Banerjee, “Celecoxib-loaded liposomes: effect of cholesterol on encapsulation and in vitro release characteristics.,” *Biosci. Rep.*, vol. 30, no. 5, pp. 365–73, Oct. 2010.

[178] A. Erdoğ, Y. D. Putra Limasale, D. Keskin, A. Tezcaner, and S. Banerjee, “In vitro characterization of a liposomal formulation of celecoxib containing 1,2-distearoyl-sn-glycero-3-phosphocholine, cholesterol, and polyethylene glycol and its functional effects against colorectal cancer cell lines.,” *J. Pharm. Sci.*, vol. 102, no. 10, pp. 3666–77, Oct. 2013.

[179] H. Maeda, “Macromolecular therapeutics in cancer treatment: The EPR effect and beyond,” *Journal of Controlled Release*, vol. 164. pp. 138–144, 2012.

[180] Drug Bank, “Celecoxib,” 2008. [Online]. Available: http://www.drugbank.ca/drugs/DB00482.

[181] Avanti Polar Lipids, “Polymers & Polymerizable Lipids.” [Online]. Available: http://www.avantilipids.com/index.php?option=com_content&view=article&id=101&Itemid=109. [Accessed: 21-Aug-2014].

[182] A. D. Bangham, M. M. Standish, and J. C. Watkins, “Diffusion of univalent ions across the lamellae of swollen phospholipids.,” *J. Mol. Biol.*, vol. 13, pp. 238–252, 1965.

[183] Thermo Scientific, “Instructions 2-Mercaptoethylamine.HCl.” [Online]. Available: https://www.piercenet.com/instructions/2160131.pdf. [Accessed: 21-Jul-2014].

[184] D. Hayworth, “Sulfhydryl-reactive Crosslinker Chemistry,” *ThermoScientific*. [Online]. Available: http://www.piercenet.com/method/sulfhydryl-reactive-crosslinker-chemistry#maleimide. [Accessed: 24-Apr-2014].

[185] P. M. Dhabu and K. G. Akamanchi, “A stability-indicating HPLC method to determine Celecoxib in capsule formulations.,” *Drug Dev. Ind. Pharm.*, vol. 28, pp. 815–821, 2002.

[186] J. C. Stewart, “Colorimetric determination of phospholipids with ammonium ferrothiocyanate.,” *Anal. Biochem.*, vol. 104, pp. 10–14, 1980.

[187] K. Nishikawa, T. Asai, H. Shigematsu, K. Shimizu, H. Kato, Y. Asano, S. Takashima, E. Mekada, N. Oku, and T. Minamino, “Development of anti-HB-EGF immunoliposomes for the treatment of breast cancer,” *J. Control. Release*, vol. 160, pp. 274–280, 2012.

[188] B. Hinz, B. Renner, and K. Brune, “Drug insight: cyclo-oxygenase-2 inhibitors--a critical appraisal.,” *Nat. Clin. Pract. Rheumatol.*, vol. 3, pp. 552–560; quiz 1 p following 589, 2007.

[189] V. Perumal, S. Banerjee, S. Das, R. K. Sen, and M. Mandal, “Effect of liposomal celecoxib on proliferation of colon cancer cell and inhibition of DMBA-induced tumor in rat model,” *Cancer Nanotechnol.*, vol. 2, no. 1–6, pp. 67–79, Jul. 2011.

[190] R.-J. Ju, X.-T. Li, J.-F. Shi, X.-Y. Li, M.-G. Sun, F. Zeng, J. Zhou, L. Liu, C.-X. Zhang, W.-Y. Zhao, and W.-L. Lu, “Liposomes, modified with PTD(HIV-1) peptide, containing epirubicin and celecoxib, to target vasculogenic mimicry channels in invasive breast cancer.,” *Biomaterials*, vol. 35, no. 26, pp. 7610–21, Aug. 2014.

[191] J. Dong, D. Jiang, Z. Wang, G. Wu, L. Miao, and L. Huang, “Intra-articular delivery of liposomal celecoxib-hyaluronate combination for the treatment of osteoarthritis in rabbit model.,” *Int. J. Pharm.*, vol. 441, no. 1–2, pp. 285–90, Jan. 2013.

[192] D. Il Kang, S. Lee, J. T. Lee, B. J. Sung, J.-Y. Yoon, J.-K. Kim, J. Chung, and S.-J. Lim, “Preparation and in vitro evaluation of anti-VCAM-1-Fab’-conjugated liposomes for the targeted delivery of the poorly water-soluble drug celecoxib.,” *J. Microencapsul.*, vol. 28, no. 3, pp. 220–7, Jan. 2011.

[193] A. Sade, S. Banerjee, and F. Severcan, “Effects of the non-steroidal anti-inflammatory drug celecoxib on cholesterol containing distearoyl phosphatidylcholine membranes,” vol. 25, pp. 177–185, 2011.

[194] D. Lorusso, A. Di Stefano, V. Carone, A. Fagotti, S. Pisconti, and G. Scambia, “Pegylated liposomal doxorubicin-related palmar-plantar erythrodysesthesia (’hand-foot' syndrome),” *Annals of Oncology*, vol. 18. pp. 1159–1164, 2007.

[195] S. Karve, G. Bajagur Kempegowda, and S. Sofou, “Heterogeneous domains and membrane permeability in phosphatidylcholine-phosphatidic acid rigid vesicles as a function of pH and lipid chain mismatch.,” *Langmuir*, vol. 24, pp. 5679–5688, 2008.

[196] J. Damen, J. Regts, and G. Scherphof, “Transfer and exchange of phospholipid between small unilamellar liposomes and rat plasma high density lipoproteins. Dependence on cholesterol content and phospholipid composition.,” *Biochim. Biophys. Acta*, vol. 665, no. 3, pp. 538–45, Sep. 1981.

[197] J. A. Zhang, G. Anyarambhatla, L. Ma, S. Ugwu, T. Xuan, T. Sardone, and I. Ahmad, “Development and characterization of a novel Cremophor?? EL free liposome-based paclitaxel (LEP-ETU) formulation,” *Eur. J. Pharm. Biopharm.*, vol. 59, pp. 177–187, 2005.

[198] C. M. Dawidczyk, C. Kim, J. H. Park, L. M. Russell, K. H. Lee, M. G. Pomper, and P. C. Searson, “State-of-the-art in design rules for drug delivery platforms: Lessons learned from FDA-approved nanomedicines,” *J. Control. Release*, vol. 187, pp. 133–144, 2014.

[199] G. T. Hermanson, “Bioconjugation techniques,” *Acad. Press*, vol. 10, p. 0123705010, 2008.

[200] A. Palmer, J L : Nissonoff, “Reduction and reoxidation of a critical disulfide bond in the rabbit antibody molecule,” *J. Biol. Chememistry*, vol. 238, p. 2393, 1963.

[201] S. Yoshitake, Y. Yamada, E. Ishikawa, and R. Masseyeff, “Conjugation of glucose oxidase from Aspergillus niger and rabbit antibodies using N-hydroxysuccinimide ester of N-(4-carboxycyclohexylmethyl)-maleimide.,” *Eur. J. Biochem.*, vol. 101, pp. 395–399, 1979.

[202] J. Huwyler, D. Wu, and W. M. Pardridge, “Brain drug delivery of small molecules using immunoliposomes.,” *Proc. Natl. Acad. Sci. U. S. A.*, vol. 93, pp. 14164–14169, 1996.

[203] D. E. Koppel, “Analysis of Macromolecular Polydispersity in Intensity Correlation Spectroscopy: The Method of Cumulants,” *J. Chem. Phys.*, vol. 57, p. 4814, 1972.

[204] J. Y. Kim, J. K. Kim, J. S. Park, Y. Byun, and C. K. Kim, "The use of PEGylated liposomes to prolong circulation lifetimes of tissue plasminogen activator," *Biomaterials*, vol. 30, pp. 5751–5756, 2009.

[205] F. Olson, C. A. Hunt, F. C. Szoka, W. J. Vail, and D. Papahadjopoulos, "Preparation of liposomes of defined size distribution by extrusion through polycarbonate membranes.," *Biochim. Biophys. Acta*, vol. 557, pp. 9–23, 1979.

[206] M. Longmire, P. L. Choyke, and H. Kobayashi, "Clearance properties of nano-sized particles and molecules as imaging agents: considerations and caveats.," *Nanomedicine (Lond).*, vol. 3, pp. 703–717, 2008.

[207] D. Banerjee and S. Sengupta, "Nanoparticles in cancer chemotherapy," *Prog. Mol. Biol. Transl. Sci.*, vol. 104, pp. 489–507, 2011.

[208] R. A. Petros and J. M. DeSimone, "Strategies in the design of nanoparticles for therapeutic applications.," *Nat. Rev. Drug Discov.*, vol. 9, pp. 615–627, 2010.

[209] A. Z. Wang, R. Langer, and O. C. Farokhzad, "Nanoparticle Delivery of Cancer Drugs," *Annual Review of Medicine*, vol. 63. pp. 185–198, 2012.

[210] H. S. Choi, W. Liu, P. Misra, E. Tanaka, J. P. Zimmer, B. Itty Ipe, M. G. Bawendi, and J. V Frangioni, "Renal clearance of quantum dots.," *Nat. Biotechnol.*, vol. 25, pp. 1165–1170, 2007.

[211] D. Liu, A. Mori, and L. Huang, "Role of liposome size and RES blockade in controlling biodistribution and tumor uptake of GM1-containing liposomes.," *Biochim. Biophys. Acta*, vol. 1104, pp. 95–101, 1992.

[212] S. D. Li and L. Huang, "Pharmacokinetics and biodistribution of nanoparticles," in *Molecular Pharmaceutics*, 2008, vol. 5, pp. 496–504.

[213] O. Tirosh, Y. Barenholz, J. Katzhendler, and A. Priev, "Hydration of polyethylene glycol-grafted liposomes.," *Biophys. J.*, vol. 74, pp. 1371–1379, 1998.

[214] T. Nomura, N. Koreeda, F. Yamashita, Y. Takakura, and M. Hashida, "Effect of particle size and charge on the disposition of lipid carriers after intratumoral injection into tissue-isolated tumors," *Pharm. Res.*, vol. 15, pp. 128–132, 1998.

[215] T. Yang, F. De Cui, M. K. Choi, J. W. Cho, S. J. Chung, C. K. Shim, and D. D. Kim, “Enhanced solubility and stability of PEGylated liposomal paclitaxel: In vitro and in vivo evaluation,” *Int. J. Pharm.*, vol. 338, pp. 317–326, 2007.

[216] P. Crosasso, M. Ceruti, P. Brusa, S. Arpicco, F. Dosio, and L. Cattel, “Preparation, characterization and properties of sterically stabilized paclitaxel-containing liposomes,” *J. Control. Release*, vol. 63, pp. 19–30, 2000.

[217] G. Blume and G. Cevc, “Liposomes for the sustained drug release in vivo.,” *Biochim. Biophys. Acta*, vol. 1029, pp. 91–97, 1990.

[218] S. Loew, A. Fahr, and S. May, “Modeling the release kinetics of poorly water-soluble drug molecules from liposomal nanocarriers.,” *J. Drug Deliv.*, vol. 2011, p. 376548, 2011.

[219] A. Fahr, P. Van Hoogevest, S. May, N. Bergstrand, and M. L. S. Leigh, “Transfer of lipophilic drugs between liposomal membranes and biological interfaces: Consequences for drug delivery,” *European Journal of Pharmaceutical Sciences*, vol. 26. pp. 251–265, 2005.

[220] H. Xu, Y. Yu, and D. Marciniak, “Epidermal growth factor receptor (EGFR) − related protein inhibits multiple members of the EGFR family in colon and breast cancer cells Epidermal growth factor receptor (EGFR)– related protein inhibits multiple members of the EGFR family in colon and ,” pp. 435–442, 2005.

[221] M. Studenovsky, R. Pola, M. Pechar, T. Etrych, K. Ulbrich, L. Kovar, M. Kabesova, and B. Rihova, “Polymer Carriers for Anticancer Drugs Targeted to EGF Receptor,” *Macromol. Biosci.*, vol. 12, pp. 1714–1720, 2012.

[222] W. Leung and F. Mao, “Lipophilic sulfophenylcarbocyanine dyes: synthesis of a new class of fluorescent cell membrane probes,” *Bioorganic Med. ...*, vol. 6, no. 13, pp. 1479–1482, 1996.

[223] Life technologies, “DiI Derivatives for Long-Term Cellular Labeling,” vol. 18, no. 3, pp. 6999–7001, 2005.

[224] J. W. Nichols and R. E. Pagano, “Use of resonance energy transfer to study the kinetics of amphiphile transfer between vesicles,” *Biochemistry*, vol. 21, no. 8, pp. 1720–1726, Apr. 1982.

[225] C. Mamot, D. C. Drummond, C. O. Noble, V. Kallab, Z. Guo, K. Hong, D. B. Kirpotin, and J. W. Park, "Epidermal growth factor receptor-targeted immunoliposomes significantly enhance the efficacy of multiple anticancer drugs in vivo.," *Cancer Res.*, vol. 65, pp. 11631–11638, 2005.

[226] K. Subbaramaiah and A. J. Dannenberg, "Cyclooxygenase 2: a molecular target for cancer prevention and treatment," *Trends Pharmacol Sci*, vol. 24, pp. 96–102, 2003.

[227] C. E. Eberhart, R. J. Coffey, A. Radhika, F. M. Giardiello, S. Ferrenbach, and R. N. DuBois, "Up-regulation of cyclooxygenase 2 gene expression in human colorectal adenomas and adenocarcinomas.," *Gastroenterology*, vol. 107, pp. 1183–1188, 1994.

[228] A. Ristimaki, N. Honkanen, H. Jankala, P. Sipponen, and M. Harkonen, "Expression of cyclooxygenase-2 in human gastric carcinoma," *Cancer Res*, vol. 57, pp. 1276–1280, 1997.

[229] M. Parrett, R. Harris, F. Joarder, M. Ross, K. Clausen, and F. Robertson, "Cyclooxygenase-2 gene expression in human breast cancer.," *Int. J. Oncol.*, vol. 10, pp. 503–507, 1997.

[230] R. E. Harris, G. A. Alshafie, H. Abou-Issa, and K. Seibert, "Chemoprevention of breast cancer in rats by celecoxib, a cyclooxygenase 2 inhibitor.," *Cancer Res.*, vol. 60, pp. 2101–2103, 2000.

[231] X. H. Liu, A. Kirschenbaum, S. Yao, R. Lee, J. F. Holland, and A. C. Levine, "Inhibition of cyclooxygenase-2 suppresses angiogenesis and the growth of prostate cancer in vivo.," *J. Urol.*, vol. 164, pp. 820–825, 2000.

[232] M. Yao, S. Kargman, E. C. Lam, C. R. Kelly, Y. Zheng, P. Luk, E. Kwong, J. F. Evans, and M. M. Wolfe, "Inhibition of cyclooxygenase-2 by rofecoxib attenuates the growth and metastatic potential of colorectal carcinoma in mice.," *Cancer Res.*, vol. 63, pp. 586–592, 2003.

[233] G. Steinbach, P. M. Lynch, R. K. Phillips, M. H. Wallace, E. Hawk, G. B. Gordon, N. Wakabayashi, B. Saunders, Y. Shen, T. Fujimura, L. K. Su, and B. Levin, "The effect of celecoxib, a cyclooxygenase-2 inhibitor, in familial adenomatous polyposis.," 2000.

[234] R. D. Brandão, J. Veeck, K. K. Van de Vijver, P. Lindsey, B. de Vries, C. H. van Elssen, M. J. Blok, K. Keymeulen, T. Ayoubi, H. J. Smeets, V. C. Tjan-Heijnen, and P. S. Hupperets, "A randomised controlled phase II trial of pre-operative celecoxib treatment reveals anti-tumour transcriptional response in primary breast cancer.," *Breast Cancer Res.*, vol. 15, p. R29, 2013.

[235] D. Dhawan, A. B. Jeffreys, R. Zheng, J. C. Stewart, and D. W. Knapp, "Cyclooxygenase-2 dependent and independent antitumor effects induced by celecoxib in urinary bladder cancer cells.," *Mol. Cancer Ther.*, vol. 7, pp. 897–904, 2008.

[236] B. Buecher, D. Bouancheau, A. Broquet, S. Bezieau, M. G. Denis, C. Bonnet, M.-F. Heymann, A. Jarry, J.-P. Galmiche, and H. M. Blottière, "Growth inhibitory effect of celecoxib and rofecoxib on human colorectal carcinoma cell lines.," *Anticancer Res.*, vol. 25, pp. 225–33, 2005.

[237] G. D. Basu, L. B. Pathangey, T. L. Tinder, S. J. Gendler, and P. Mukherjee, "Mechanisms underlying the growth inhibitory effects of the cyclo-oxygenase-2 inhibitor celecoxib in human breast cancer cells.," *Breast Cancer Res.*, vol. 7, pp. R422–R435, 2005.

[238] H.-C. Chuang, A. Kardosh, K. J. Gaffney, N. A. Petasis, and A. H. Schönthal, "COX-2 inhibition is neither necessary nor sufficient for celecoxib to suppress tumor cell proliferation and focus formation in vitro.," *Mol. Cancer*, vol. 7, p. 38, 2008.

[239] M. I. Patel, K. Subbaramaiah, B. Du, M. Chang, P. Yang, R. A. Newman, C. Cordon-Cardo, H. T. Thaler, and A. J. Dannenberg, "Celecoxib inhibits prostate cancer growth: evidence of a cyclooxygenase-2-independent mechanism.," *Clin. Cancer Res.*, vol. 11, pp. 1999–2007, 2005.

[240] H. Safran, M. Suntharalingam, T. Dipetrillo, T. Ng, L. A. Doyle, M. Krasna, A. Plette, D. Evans, H. Wanebo, P. Akerman, J. Spector, N. Kennedy, and T. Kennedy, "Cetuximab With Concurrent Chemoradiation for Esophagogastric Cancer: Assessment of Toxicity," *Int. J. Radiat. Oncol. Biol. Phys.*, vol. 70, pp. 391–395, 2008.

[241] S.-W. Han, D.-Y. Oh, S.-A. Im, S. R. Park, K.-W. Lee, H. S. Song, N.-S. Lee, K. H. Lee, I. S. Choi, M. H. Lee, M. A. Kim, W. H. Kim, Y.-J. Bang, and T.-Y. Kim, "Phase II study and biomarker analysis of cetuximab combined with modified FOLFOX6 in advanced gastric cancer.," 2009.

[242] F. Kullmann, S. Hollerbach, M. M. Dollinger, J. Harder, M. Fuchs, H. Messmann, J. Trojan, E. Gäbele, A. Hinke, C. Hollerbach, and E. Endlicher, "Cetuximab plus gemcitabine/oxaliplatin (GEMOXCET) in first-line metastatic pancreatic cancer: a multicentre phase II study.," 2009.

[243] P. Sapra and B. Shor, "Monoclonal antibody-based therapies in cancer: Advances and challenges," *Pharmacology and Therapeutics*, vol. 138. pp. 452–469, 2013.

APPENDIX A

STANDARD CALIBRATION CURVES

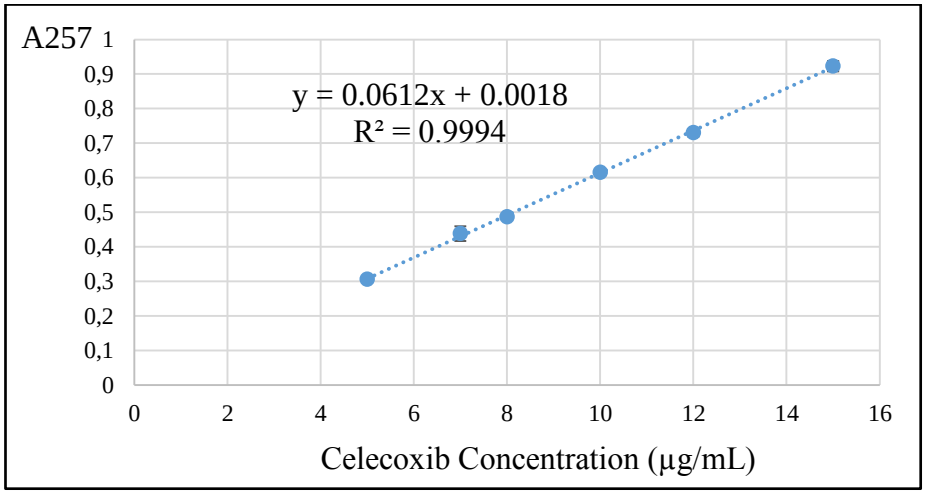

Figure A. 1 Standard calibration curve of CLX.

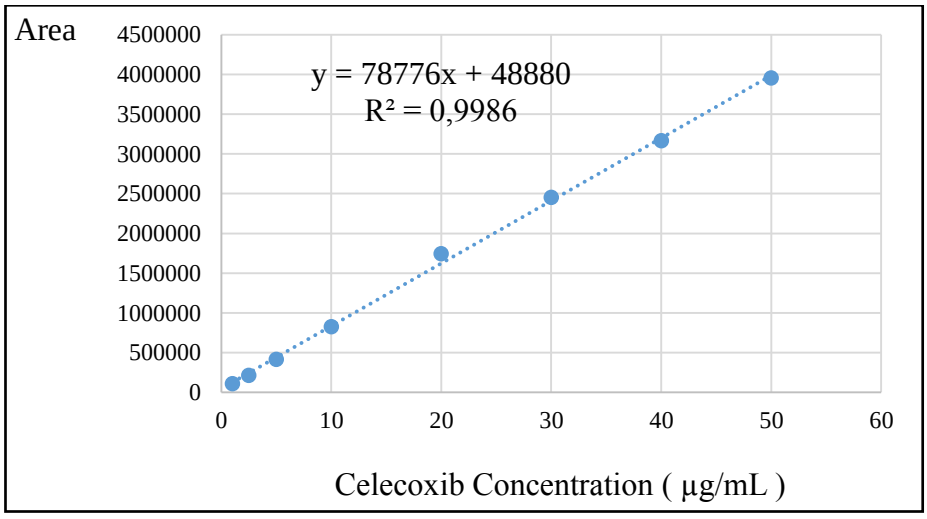

Figure A.2 Standard calibration curve of CLX for HPLC.

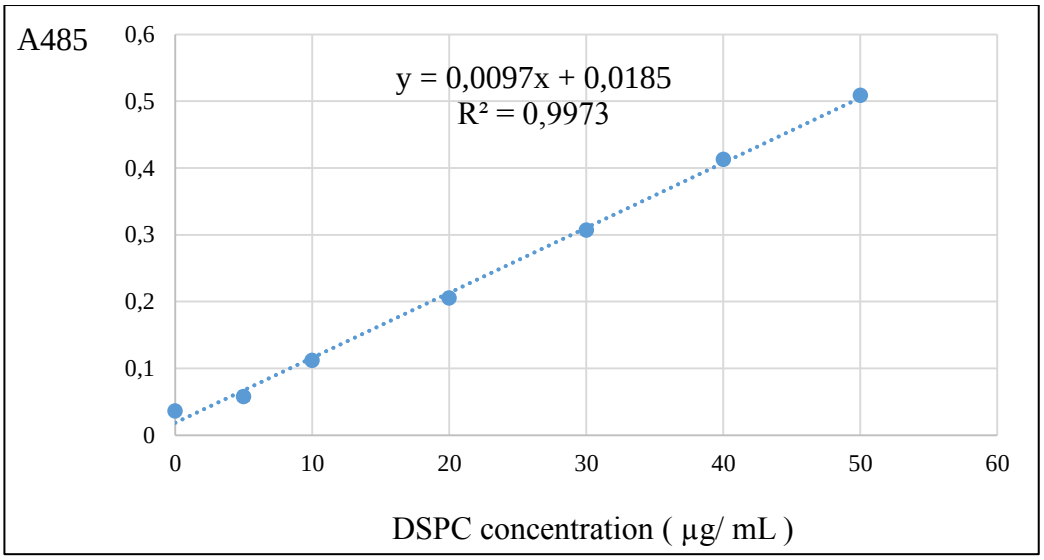

Figure A.3 Standard calibration curve of DSPC.

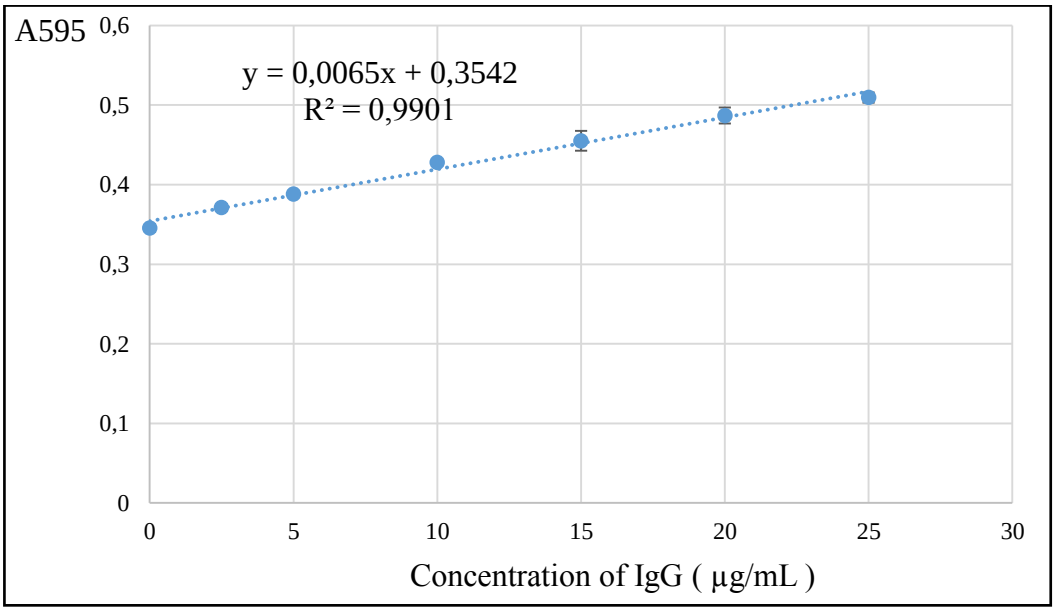

Figure A.4 Standard calibration curve of IgG.

APPENDIX B

CHARACTERISTICS OF HUMAN COLORECTAL AND BREAST CANCER CELL LINES

Table A. 1 Characteristics of human cancer cell lines HCT-116, HT-29, SW620, and MDA-468

Cell Lines	**HCT-116 (ATCC CCL-247)**	**HT-29 (ATCC HTB-38)**	**SW620 (ATCC CCL-227)**	**MDA-468**
Origin	*Homo sapiens*, human	*Homo sapiens*, human	*Homo sapiens*, human	*Homo sapiens*, human
Tissue	colon	colon	colon; derived from metastatic site: lymph node	mammary gland/breast; derived from metastatic site: pleural effusion
Morphology	epithelial	epithelial	epithelial	epithelial
Disease	colorectal carcinoma	colorectal adenocarcinoma	Dukes' type C, colorectal adenocarcinoma	Adenocarcino-ma
Mutations	RAS mutation in codon 13 PIK3CA mutation	myc +; ras +; myb +; fos +; sis +; p53 +; abl -; ros -; src -	myc +; myb + ; ras +; fos +; sis +; p53 +; abl -; ros -; src -	PTEN, RB1, SMAD4,TP53
Population Doubling Time	21 h	23 h	26 h	47 h